W-PM-Sym1 BIOPHYSICS OF DEVELOPMENT OF STRUCTURAL PATTERNS IN ORGANISMS.
Scott Fraser, Hans Meinhardt, Jay Mittenthal, George Oster.

This symposium will address the issue of how the cells of an embryo order themselves during development. The embryo initially appears homogeneous and patternless, but then elaborates patterns as development proceeds. These patterns become evident in the types of cells produced, the positions of these cells within the tissue, and the overall shape of the tissue. While a great deal is known about the developmental timetable for the appearance of patterns, little is known about the underlying mechanisms responsible for their establishment.

The symposium will describe the use of a biophysical approach to develop models of how the cells of the embryo might interact with one another. Although our present knowledge of developmental phenomena is too incomplete for a full biophysical description of the processes responsible for the organization of the embryo, it is clear that a biophysical approach can help to guide research in developmental biology. Simulations of models can be used to test the feasibility of ideas and to design experiments that better address the proposed cell interactions. Such experiments can help to build the needed data base for a more complete treatment of the problem.

The speakers in this symposium will address several types of interactions between cells and the patterns these interactions can generate. The topics are: 1. the morphogenesis of epithelia made possible by electrical and adhesive interactions between cells (Jay Mittenthal); 2. the patterning of epithelia and mesenchyme made possible by the tractional forces among cells and between the cells and their substrata (George Oster); 3. the patterning of developing tissues made possible by the exchange of chemical messengers between cells (Hans Meinhardt); 4. the patterning of neural interconnections made possible by adhesive interactions between neurons and their target tissue (Scott Fraser). Each of these topics shows the power of simple biophysical mechanisms in the generation of structures in developing organisms.

W-PM-Sym2 PROBLEMS AND PROSPECTS IN THE BIOPHYSICS OF EPITHELIAL MORPHOGENESIS. Jay E. Mittenthal, Dept. of Anatomical Sciences, University of Illinois College of Medicine, Urbana, IL 61801

Two models suggest physiological processes underlying morphogenesis in a chick embryo. During gastrulation cells emigrate from the epiblast at the primitive streak. Transport of ions through the epiblast may cause emigration of cells.[1] Basolateral pumps transport sodium and water into a cavity between epiblast and hypoblast. Transport increases the electrochemical and hydrostatic potential differences across the epiblast. When these differences exceed a threshold, sodium pumping stops. Apical influx of sodium raises $[Na]_{in}$, releasing calcium from intracellular pools and stimulating contraction of the cytoskeleton. At the resulting foci of contraction, cells descend into the cavity.

During development epithelia thicken and fold. In one model[2] for the biomechanics of these deformations, an epithelium is a fluid elastic shell. It is fluid-like in that cells in a small multicellular element can exchange neighbors to relieve shear stress. The element responds to bending or isotropic stretching elastically; its stiffness is associated with the cytoskeleton and with intercellular junctions. Interfacial tensions between lateral surfaces of cells which differ in their adhesive affinities, and elasticity of the epithelium, support external forces and moments acting on the element. This model interprets the elongation of a chick embryo as a result of cell rearrangement to reduce interfacial tensions. Thickening of the neural plate may result from the insertion of neural cell adhesion molecules into plate cell membranes. Transport by epithelial cells, differential adhesion among them, and deformation generated by the cytoskeleton may contribute to epithelial morphogenesis. (Supported by P.H.S. grant HD 16577.)

[1]Stern CD 1984 J Theor Biol 107:229; [2]Mittenthal JE, Mazo RM 1983 JTB 100:443.

W-PM-Sym3 MECHANOCHEMICAL ASPECTS OF MORPHOGENESIS. George Oster

W-PM-Sym4 MODELS OF BIOLOGICAL PATTERN FORMATION IN THE DEVELOPMENT OF HIGHER ORGANISMS.
HANS MEINHARDT,Max-Planck-Institut für Entwicklungsbiologie,
Spemannstr. 35, D 74 Tübingen, W.-Germany

The development of a fertilized egg into a higher organisms with its complex arrangement of differentiated cells is one of the most striking examples of self-organization. We have formulated molecular feasable interactions in a mathematically precise way which account for essential steps in this process. Computer simulations (movie) demonstrate that the regulatory features of our (yet hypothetical) interactions agree well with those experimentally observed. The proposed main steps in embryonic pattern formation are: (i) By local autocatalysis and long-ranging inhibition, graded concentration profiles are generated. (ii) This "positional information" is used to obtain in the early embryo an ordered activation of feedback loops (genes). In this way, the embryo becomes subdivided into a few cardinal regions. (iii) The borders between these cardinal regions act as frames for the further subdivision of the embryo. (iv) Legs and wings are formed at the intersection of two borders, i.e. at a point where four quadrants or three sectors are close to each other. Further, a mechanism will be presented which allows the generation of net-like structures such as the blood vessels, the tracheae or the veins of leaves. The linkage of these steps and the explanatory power of these models will be illustrated by a comparison with experimental observations obtained in insect development.

Reference: H.Meinhardt, Models of biological pattern formation. Academic Press (1982)

W-PM-Sym5 THE PATTERNING OF NEURAL CONNECTIONS: A MODEL BASED ON ADHESIVE INTERACTIONS BETWEEN CELLS.
Scott E. Fraser, Department of Physiology and Biophysics, University of California, Irvine, CA 92717.

Neural connections are highly ordered such that a map of one neural center is conveyed intact to the next neural center. The visual system of lower vertebrates is one of the most striking examples of this patterning. The optic nerve axons exit from the eye, grow to the opposite optic tectum, and form a "map" of the visual field of the eye over the surface of the tectum. This topographic retinotectal projection has been the subject of many different experimental approaches. These experiments demonstrate both the regularity of the projection and its response to experimental perturbation.

In order to explore the cell interactions that might underlie the patterning of neural connections, we have used computer simulations to develop a model based on simple interactions between the cells. The model proposes a dominant adhesion of all optic nerve fibers to the tectum, an activity-modulated competition between synapses, and a position dependent adhesion between the cells that gives subsets of optic nerve fibers a best-fit site on the tectal surface. Computer simulations of this simple set of interactions show that the model can generate the patterned connections characteristic of the retinotectal projection and its response to surgical manipulation. Interestingly, the model demonstrates metastable states that correspond to the mixed results obtained from some experiments on the system. In addition, due to the activity-modulated competition between synapses, the model is able to generate the ocular dominance columns observed when two eyes are forced to coinnervate the same tectum. Experiments are now underway to test for some of the interaction proposed in the model.

(supported by NSF 80-23638 and a McKnight Scholar Award)

W-PM-A1 PLASMA MEMBRANE CA FLUXES IN INTACT RODS ARE INCONSISTENT WITH THE 'CA HYPOTHESIS'. Geoffrey H. Gold, Dept. Physiology, Yale U. School of Medicine, New Haven, CT (Intro. by L. M. Masukawa).

Plasma membrane Ca fluxes in intact bullfrog rods are compared with the extracellular rod photovoltage. Ca fluxes are derived from high resolution Ca_o measurements. Flash illumination initially causes a net Ca efflux, which is followed by a net influx, during which all of the released Ca is taken back up. The dark adapted Ca release stoichiometry for flash illumination is $\sim 6 \times 10^4$ Ca/rod. The maximum Ca release produced by either flash or continuous illumination is $\sim 3 \times 10^7$ Ca/rod. At subsaturating intensities, the Ca flux and photovoltage waveforms are nearly identical during the efflux phase. However, the Ca flux reverses from efflux to influx before the photovoltage returns to baseline. As stimulus intensity increases, the Ca flux and photovoltage traces begin to diverge at earlier times. At suprasaturating intensities, the Ca efflux reaches an initial peak of $\sim 3 \times 10^6$ Ca/rod·sec simultaneously with the photovoltage, but declines rapidly ($t_{1/2} \sim 4$ sec). In contrast, at the same intensity the photovoltage exhibits a plateau lasting more than 10 sec. These dissimilarities between the Ca flux and photovoltage waveforms are inconsistent with Ca_i controlling the light regulated conductance (g_{Na}), unless further ad hoc assumptions are made. Because the Ca efflux and photovoltage saturate at about the same intensity, the efflux could be due to reduced influx through g_{Na}. Following a period of photovoltage saturation, the Ca influx phase begins simultaneously with the recovery of g_{Na}, further suggesting that modulation of the inward leak through g_{Na} could account for the observed Ca fluxes. If so, the Ca leak would constitute ~5% of the total dark current. Supported by EY03955 & Sloan Research Fellowship.

W-PM-A2 LIGHT REDUCES CYTOPLASMIC FREE CALCIUM IN RETINAL ROD OUTER SEGMENT. K.-W. Yau and K. Nakatani, Dept. Physiol. Biophys., Univ. of Texas Medical Branch, Galveston, TX 77550.

Membrane current was recorded from an isolated toad rod with a suction pipet while its outer segment was perfused. In response to a bright flash or step of light the dark inward current at the outer segment declined with a rapid and a slow phase. The slow phase disappeared if Li replaced Na externally, indicating that it represented Ca extrusion via a Na-Ca exchanger. This Ca extrusion was stereotyped in magnitude and time course, and was independent of light intensity and duration once the light response reached saturation. The exchange current had a peak amplitude of $\sim$ 1.5 pA and it declined roughly exponentially (time constant $\sim$ 0.4 sec) to a basal level of either 0 or at any rate < 0.1 pA, the limit of our recording resolution. We have also estimated the dark Ca influx through the light-sensitive conductance, by trapping the influx within the outer segment using 0-Na solution and then estimating this influx from the subsequently reactivated efflux in Ringer. We estimated that the dark Ca influx in Ringer was $\sim$ 3 pA; in steady state this influx should be balanced by an equal efflux via the Na-Ca exchanger which, with its 3Na:1Ca stoichiometry, would produce an inward exchange current of $\sim$ 1.5 pA, same as the peak amplitude of the slow phase mentioned above. We have interpreted these results to mean that the light-triggered Ca efflux observed by others simply reflected a reduction in Ca influx, and not a novel efflux caused by light. This idea predicts that the net efflux caused by a photon should be $\sim 10^5$ Ca ions, more than enough to account for what others have measured using Ca-sensitive electrodes. The observation that the Ca extrusion declines immediately at the turning on of light suggests that intracellular free Ca actually declines in the light. This means that internal Ca does not mediate visual transduction but most probably contributes to light adaptation.

W-PM-A3 cGMP OPENS THE LIGHT-SENSITIVE CONDUCTANCE IN RETINAL RODS. K. Nakatani and K.-W. Yau (Intr. by R. Baker), University of Texas Medical Branch, Galveston, Texas 77550.

A cell-free, "inside-out" membrane patch from the plasma membrane of a light-adapted toad rod outer segment was recorded by a suction pipet using the gigohm patch-clamp technique. The pipet contained Ringer's solution while the bath contained an artificial intracellular solution with low Na and high K. Without cGMP, the I-V relation measured across the membrane patch was ohmic, reflecting the leakage resistance at the seal between pipette wall and membrane (typically 5 GΩ); this relation was unchanged with bath Ca at 1 μM or 1 mM. With cGMP in the bath, however, the membrane current increased significantly; the new I-V relation had a reversal potential near 0 mV and exhibited prominent outward rectification, similar to that observed for the light-sensitive conductance in the intact rod. This suggested that the cGMP-sensitive conductance was the light-sensitive conductance. The cGMP-sensitive current also showed little dependence on bath Ca between 1 μM and 1 mM. The dependence of the current on cGMP concentration was sigmoidal, suggesting positive cooperativity among cGMP molecules in opening the conductance (Hill coefficient > 1). The current was half-maximal at 50-75 μM cGMP and saturated at $\sim$ 1 mM. The recorded membrane patch had an area $\sim$ 0.1 μm^2, which in the intact rod would have a dark current of $\sim 3 \times 10^{-3}$ pA. By extrapolating the current-cGMP concentration relation obtained at -40 mV to this current level we estimated that in darkness the free cGMP concentration in the intact outer segment would be roughly 0.1 - 1.0 μM. We conclude that cGMP is most likely the internal messenger mediating visual transduction. Moreover, since cGMP can open the conductance in a cell-free environment, it either interacts with the conductance site directly or activates a membrane-bound kinase that opens the conductance by phosphorylation.

W-PM-A4 A DISSOCIATED INVERTEBRATE PHOTORECEPTOR PREPARATION SUITABLE FOR PATCH-CLAMP RECORDING. Enrico Nasi and Carter Cornwall, Department of Physiology, Boston University School of Medicine, Boston, MA 02118.

A physiologically viable isolated photoreceptor preparation has been developed by enzymatically dissociating the eye of the file clam Lima Scabra. The resulting cells are 25-35 μm in length and display a striking morphological differentiation into three distinct lobes. The surface of the membrane appears to be free of coating or glia, and high resistance seals (10-150 Gigaohms) are established with great ease when the tip of a fire-polished micropipette is brought in contact with a patch of membrane. By filling the patch electrode with a solution compatible with the intracellular ionic environment and rupturing the patch of membrane after a tight seal is formed, the basic electrophysiological properties of these cells were investigated using conventional voltage recording and current clamp methods. The primary depolarizing light response is greatly attenuated by removal of either Na or Ca from the extracellular bath, while a later hyperpolarizing phase appears to be mediated by K ions and is also sensitive to manipulations of Ca in the bath. The photoreceptors could be voltage-clamped with the whole-cell patch clamp technique, and a brief flash of light was shown to induce a transient inward current, followed by a slower outward current. Voltage-clamp steps administered in the dark revealed voltage-activated conductances that can account for the spiking behavior that is observed in response to bright lights. Extracellular patch clamp was also attempted, and the high resistance seals obtained permitted recording single ionic channel currents with a high resolution. Supported by NIH Grant EY01157.

W-PM-A5 TRANSDUCTION BY CONES IN THE RETINA OF MACACA FASCICULARIS. D.A. Baylor, J.L. Schnapf and B.J. Nunn. Neurobiology Department, Stanford Medical School, Stanford, CA, 94305.

Membrane current has been recorded from the outer segments of single red-, green-, and blue-sensitive cones in chopped pieces of retina maintained in flowing Locke's solution near 37°C. Brief flashes evoked graded outward photocurrents with a time to peak of 50-75 msec and with a pronounced underswing on the recovery phase. Responses from all three classes of cone had similar time scales. The kinetics of transduction in the cones may explain the resonant peak near 10 Hz in the flicker sensitivity of human cone vision. From the sensitivity to dim flashes a single photoisomerization is estimated to give a peak response of the order of 10 fA.

A current noise present in darkness was suppressed by saturating light; this noise may limit the detection of dim lights. In some recordings dim light increased the current noise.

Spectral sensitivities showed peaks near 430, 540, or 570 nm. In wavenumber plots the spectra broadened as the peak sensitivity moved to higher wavenumber. Associated with the broadening was a gentler descent of the log sensitivity at low wavenumber.

(Supported by USPHS grant EY01543.)

W-PM-A6 ELECTRICAL PROPERTIES OF THE LIGHT-SENSITIVE CONDUCTANCE OF SALAMANDER RETINAL RODS. A.L. Zimmerman and D.A. Baylor, Neurobiology Department, Stanford Medical School, Stanford, CA, 94305.

Isolated rods from the retina of Ambystoma tigrinum were studied by voltage clamp and noise analysis methods. Membrane current was collected from the outer segment with a suction electrode while the internal potential was controlled with a patch clamp electrode sealed on the inner segment (patch ruptured).

Current-voltage relations of the light-sensitive conductance showed a pronounced outward-going rectification and a reversal potential of about +15 mV. There was no evidence that the rectification resulted from a rapid voltage-dependent relaxation of the conductance (time resolution 3 msec).

Power spectra of the whole cell current noise that was suppressed by saturating light showed a lobe at very low frequency, as well as a higher frequency component of Lorentzian form. The Lorentzian rolled off at roughly 100 Hz, as reported by Bodoia and Detwiler (1984) and Attwell and Gray (1984). Assuming that the noise results from random independent openings of light-sensitive channels, the underlying event is estimated to have an amplitude of 2 fA and a mean duration of 1.6 msec. Assuming that the channel is closed about 95% of the time in darkness, the density of light-sensitive channels would be about 200 μm^{-2}.

References: Attwell, D. and Gray, P. (J. Physiol. 351: 9P).
Bodoia, R.D. and Detwiler, P.B. (Biophys. J. 45: 337a).

(Supported by USPHS grant EY01543.)

W-PM-A7 RHODOPSIN, ISORHODOPSIN AND BATHORHODOPSIN HAVE C=N TRANS CHROMOPHORES.

Ilona Palings and Richard A. Mathies, Dept. of Chemistry, University of California, Berkeley, CA 94720, and Johannes A. Pardoen, Chris Winkel and Johan Lugtenburg, Dept. of Chemistry, Leiden University, The Netherlands.

The configuration of the protonated Schiff base linkage between the retinal chromophore and the protein in visual pigments is an important element in determining the orientation and environment of the C=NH moiety. We have recently shown that the configuration about the C=N bond can be determined from the sensitivity of the C_{14}-C_{15} stretching frequency to deuteration of the Schiff base nitrogen: N-deuteration of a C=N *cis* linkage results in a large increase in frequency of the C_{14}-C_{15} stretch (>50 cm^{-1}), while in a C=N *trans* linkage only a small shift is observed [Smith *et al.* (1984) PNAS 81, 2055]. The C_{14}-C_{15} stretch in bathorhodopsin, the primary visual photoproduct, is found to be localized in a normal mode at 1210 cm^{-1} based on resonance Raman spectra of the 14,15-di[^{13}C] pigment analogue. The corresponding vibrations of rhodopsin and isorhodopsin have similarly been assigned at 1195 and 1207 cm^{-1}, respectively. Deuteration of the Schiff base nitrogen has no effect on the C_{14}-C_{15} stretching frequencies in any of these pigments. Therefore, rhodopsin, isorhodopsin and bathorhodopsin each contains a *trans* C=N linkage. The primary photochemistry, then, involves isomerization of only the C_{11}=C_{12} bond. This argues that the Schiff base N-H bond changes its orientation when bathorhodopsin is formed. If this reorientation is accompanied by a displacement of the Schiff base moiety into a different protein environment, then altered vibrational properties for the Schiff base normal mode in bathorhodopsin would be expected, as is observed in K, bacteriorhodopsin's primary photoproduct. However, the Schiff base vibrations in rhodopsin and bathorhodopsin exhibit very similar frequencies and isotopic shifts.

W-PM-A8 DOUBLE-QUANTUM COHERENCE AND TRIPLE RESONANCE NMR OF DOUBLE LABELED RETINALS: A NEW AVENUE FOR UNAMBIGUOUS ASSIGNMENTS IN RHODOPSIN AND BACTERIORHODOPSIN. G.D. Mateescu, M. Iqbal and Christine Wheeler, Department of Chemistry, Case Western Reserve University, Cleveland, Ohio 44106

Important C-13 signals from labeled retinals incorporated in rhodopsin and bacteriorhodopsin may overlap with natural abundance apoprotein absorptions. This inconvenience can entirely be avoided employing double-quantum pulse sequences on double labeled retinal preparations. For example, if such a sequence is applied to a sample containing [14,15-$^{13}C_2$]retinal and lysozyme (Figure b), only the signals of the two enriched, coupled carbons(14-15) are observed, in contrast with the conventional FT NMR measurement (Figure a) which yields a huge number of absorptions, including those particularly overlapping with the 14 resonance (if retinal were bound to the protein the 15 signal would also fall in a crowded region). Key triple resonance experiments such as ^{13}C-[^{1}H,^{13}C] and ^{13}C-[^{1}H,^{15}N] are also feasible. In frozen solution valuable dipolar coupling information can be obtained. We are now preparing rhodopsin and bacteriorhodopsin regenerated with double labeled retinals in order to obtain the much needed "fingerprint" of these pigments and their photointermediates (Mateescu et al., in Spectroscopy of Biological Molecules, Sandorfy&Theophanides, Eds., Reidel: Boston, 1984, pp 250-283). Supported by NIH, EY02998.

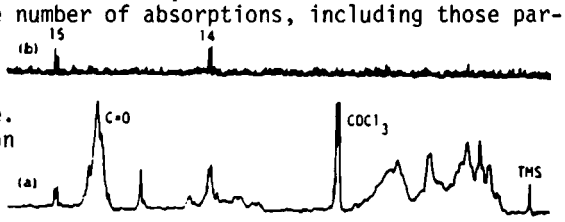

W-PM-A9 TWO-DIMENSIONAL CRYSTALS OF BOVINE RHODOPSIN, Darrell R. McCaslin and Joseph M. Corless, Dept. Anatomy. Duke Univ. Med. Cntr., Durham, NC 27710.

There is an extensive literature on the chemical and physical properties of rhodopsin and most of these data are derived from studies on bovine rhodopsin. Therefore, the rigorous determination of the three-dimensional structure of bovine rhodopsin will be of considerable use in integrating these data into a comprehensive view of the structure and function of the visual pigment.

We have been systematically investigating the use of the nonionic detergent, Tween 80, for the induction of two-dimensional crystals of bovine rhodopsin. The crystalline specimens are examined by electron microscopy after negative staining with uranyl acetate. The results of these studies will be presented as well as further characterization of rhodopsin solubilized in Tween 80.

In the course of these investigations several crystalline forms have been observed. One form presents a projected shape for rhodopsin dimers similar to our earlier crystals of frog rhodopsin (Corless et al, PNAS 79, 1116). The lattice parameters are somewhat variable: a*=1/(55-60 Å) and b*=1/(145-150 Å); the included angle is 90-93°. The resolution is ~35 Å; projection symmetry is slightly distorted pmg; the 2-sided plane group would be $p222_1$. In highly delipidated preparations, a second form is observed: unit cell dimensions ~53 x 58 Å, included angle 89-90.5°; resolution ~26 Å. We are currently investigating the relationships among the varied crystalline forms and hope to use these data to define the perimeter of the rhodopsin monomer.

W-PM-A10 A NEW METHOD FOR TISSUE DISSOCIATION OF THE BUFO RETINA. K. N. Leibovic. State University of New York at Buffalo, Buffalo, NY 14214.

Techniques for tissue dissociation in cell cultures are generally based on enzymatic dissociation or the mechanical teasing apart of fresh tissue followed by incubation in a variety of maintenance media. We have worked with the Bufo isolated retina using a number of different enzymes, both singly and in combination, and we have compared the quality of the dissociations with those obtained on fresh tissue by mechanical methods. We have also used several different culture media to study the viability of the dissociated cells based on morphological observations and dye exclusion. As a result we have developed a new technique for tissue dissociation and a medium which gives the best results so far in the overall dissociation and viability of the cells, especially of photoreceptors. Our method consists of the following steps: the retina is peeled off the eye cup and incubated in our medium for up to 24 hours. The medium is based on toad Ringer solution with the addition of essential and non-essential amino acids, vitamins, BFS, BSA, insulin and antibiotics. After incubation the retinal pieces are triturated with Pasteur pipettes into Petri dishes containing fresh medium. A good dissociation is obtained. The dishes are stored in the refrigerator and inspected daily under the microscope. The medium is renewed every two days. As judged by morphological observation, the photoreceptors survive for more than a week. It is clearly an advantage to dissociate the cells in a medium which promotes cell viability, and to avoid enzymes which may cause unknown damage. Moreover, by pre-incubation in the medium the dissociation yield is improved to the point where it is comparable to enzymatic dissociation.

W-PM-B1 NMR STRUCTURAL ANALYSIS OF A MEMBRANE PROTEIN: BACTERIORHODOPSIN PEPTIDE BACKBONE ORIENTATION IN DMPC VESICLES. B.A. Lewis*#, G.S. Harbison**, J. Herzfeld**, and R. G. Griffin*
*Francis Bitter Magnet Lab., M.I.T., Cambridge MA 02139; **Dept. of Physiology & Biophysics, Harvard Medical School, Boston MA 02115; #Present address: Oak Ridge National Laboratory, Biology Division, Oak Ridge TN 37830.

The ^{13}C NMR powder lineshape of the leucine peptide carbonyls in bacteriorhodopsin (BR) is motionally narrowed in reconstituted DMPC vesicles at 30 °C due to rotational diffusion about an axis normal to the membrane plane. Using this motionally averaged lineshape, the range of Euler angles of the peptide groups relative to the diffusion axis has been calculated. This range is inconsistent with those expected for either alpha helix or beta sheet perpendicular to the membrane, or for beta sheet tilted at angles up to about 70 degrees from the membrane normal. However, alpha helices tilted at 10 to 20 degrees give a lineshape very similar to that which is experimentally observed. From the lineshape alone we cannot rule out the presence of beta sheet oriented close to parallel to the membrane plane, but this seems unlikely in the case of BR. Thus these NMR results lend strong support to models which place most of BR in transmembrane helices, and are inconsistent with models in which more than ~10% of the BR secondary structure is transmembrane beta sheet.

These experiments suggest a new approach, using solid state NMR methods, for structural studies on transmembrane proteins in fluid membrane environments (natural or reconstituted). Analysis of NMR lineshapes narrowed by anisotropic rotational motion provides information on secondary structure, or more generally on the orientation of labelled groups relative to the membrane plane. For many membrane proteins such information is unobtainable by more traditional structural methods.

W-PM-B2 GAP JUNCTION DYNAMICS: STRUCTURAL TRANSITION DEPENDENT UPON WATER ACTIVITY. Thomas T. Tibbitts, D.L.D. Caspar, Walter C. Phillips and D.A. Goodenough, Rosenstiel Center, Brandeis University, Waltham, MA 02254.

We have discovered that treatments which vary the water content of rat liver gap junction membrane pellets effect connexon packing and conformation. Our specimens show a graded, reversible compaction of the hexagonal lattice (typically going from 88 to 75 Å) upon slow dehydration. This change is correlated with a decrease in membrane stacking period associated with the removal of interstitial water. These observations were made possible by the production of reproducible, well-oriented unfixed specimens and by a new method of mounting these centrifuged membrane pellets for X-ray study. This new method involves partial drying of the pellets, gently coaxing them out of their BEEM capsules, then wedging them into 1.5 mm glass capillary tubes. Slow, stepwise dehydration is effected by equilibration against a series of saturated salt solutions of progressively smaller relative humidities. As the specimens lose water, an overall increase of the equatorial diffraction relative to the meridional intensities is observed. This arises from more orderly connexon lattice packing in the drier states. Under very dry conditions, diffraction from a separated lipid phase appears on the meridian with a repeat period of 60 Å. Disappearance of these reflections upon rehydration suggests that lipids excluded from the hexagonal lattice during compaction will reintegrate if the specimens are not too severely dried. Intensities of equatorial and off-equatorial reflections also change relative to one another as the specimen dries, an indication that a conformational change occurs within the connexon pair. This lateral compaction and conformational change illustrate the variable, dynamic character of the connexon lattice.

W-PM-B3 ANTIGEN LOCALIZATION, DIFFUSION AND MIGRATION ON SPERM CELL SURFACES. Dennis E. Koppel*, Paul Primakoff‡, and Diana Gold Myles‡, Departments of Biochemistry* and Physiology‡, University of Connecticut Health Center, Farmington, CT 06032.

We are using measurements of fluorescence redistribution after photobleaching on guinea pig sperm cells to study the mechanisms that control the regional distributions of cell surface molecules. The guinea pig sperm surface has been mapped with monoclonal antibodies and shown to be a mosaic of distinct regions with different compositions (Myles et al., 1981, Cell 23, 433; Primakoff and Myles, 1983, Develop. Biol. 98, 417). Prior to sperm capacitation, the surface protein recognized by antibody PT-1 is confined to the posterior tail, but exhibits free diffusion ($D = 2.5 \times 10^{-9}$ cm^2/sec) within its domain (Myles, Primakoff and Koppel, 1984, J. Cell Biol. 98, 1905). During capacitation, in a process requiring active cell swimming, the PT-1 antigen migrates and concentrates onto the anterior tail (Myles and Primakoff, 1984, J. Cell Biol. 99, in press). Preliminary photobleaching experiments on cells immobilized in agar after a period of migration indicate that PT-1 antigen can move between the anterior and posterior tail regions. However, a partial barrier to diffusion still exists at the boundary, and the major part (~ 70%) of antigen on the anterior tail is immobile. These results are consistent with a model of diffusion-mediated antigen migration.

W-PM-B4 DIFFUSION AND REGIONALIZATION OF A SURFACE GLYCOLIPID OF EJACULATED RAM SPERMATOZOA. **Wolf, D.E., Hagopian, S.S., Lewis, R.G., Voglmayr, J. and Fairbanks, G. Worcester Foundation for Experimental Biology, Shrewsbury, Mass. 01545.**

We have used fluorescence recovery after photobleaching (FRAP) to study the physical state of a mobile surface antigen of ejaculated ram spermatozoa. A mouse monoclonal IgG antibody, ESA152, was used to label the surface. Hybridoma ESA152 was selected from survivors of a fusion of NS1 myeloma cells with spleen cells from a mouse immunized with intact ejaculated spermatozoa. The corresponding antigen is maturation dependent (present at much lower density on rete testis spermatozoa). Because it is extracted by detergents and by chloroform-methanol, it is thought to be a glycolipid. Two surface labeling regimens were used: (i) Indirect--intact, bivalent ESA152 antibody followed by rhodamine-conjugated monovalent Fab of anti-(mouse IgG). (ii) Direct--monovalent Fab of fluorescein-conjugated ESA152 IgG. The results of the fluorescence studies were as follows: (i) When visualized with monovalent antibody or with bivalent antibody after aldehyde fixation, the antigen distribution is regionally restricted with a relative concentration on the posterior head. (ii) Exposure to bivalent antibody induces a reorganization excluding the probe from the posterior head. (iii) The diffusion coefficient of the antigen is lipid-like, but both diffusion constant and mobile fraction vary significantly over the surface. (iv) The redistribution induced by bivalent antibody is associated with striking and distinct shifts in the diffusibilities of the antigen on the midpiece and head.

W-PM-B5 CHARACTERIZATION OF REACTIVE -SH GROUPS IN THE BAND 4.5 PROTEIN OF THE HUMAN ERYTHROCYTE MEMBRANE. Mark R. Deziel and Aser Rothstein. Research Institute, The Hospital for Sick Children, Toronto, Ontario, Canada. M5G 1X8

Cysteine residues of Band 4.5, the putative hexose transport protein of the human erythrocyte membrane, were quantified by alkylation of the -SH groups with [^{14}C] N-Ethylmaleimide (NEM), followed by monitoring the radioactivity present in electrophoretograms of Band 4.5 and its tryptic fragments. Band 4.5 contained five (5.22 ± 0.11) -SH groups that were alkylated in SDS-denatured preparations. Limited proteolytic digestion of the protein yielded two fragments, a glycosylated peptide (MW~30,000 daltons, 30K) that contained three (2.83 ± 0.15) -SH groups and a carbohydrate-free peptide (MW~19,000 daltons, 19K) that appeared to contain the remaining two (2.42 ± 0.08) -SH groups. Alklyation of native band 4.5 resulted in modification of three (2.74 ± 0.15) of the five -SH groups. Two (1.81 ± 0.20) of these residues were located on the 30K fragment, and one (0.93 ± 0.02) was found on the 19K fragment. When the native protein was modified in the presence of cytochalasin B, a potent inhibitor of hexose transport that protects the transporter against inactivation by NEM, the reactivity of -SH groups on both the 30K and 19K fragments was diminished. These results suggest that the environments surrounding the single reactive -SH on the 19K peptide and at least one of the two reactive groups on the 30K peptide are altered when cytochalasin B is bound to the transporter, and that these groups may play a role in hexose transport. (This work supported by Grant MT4665 from the Medical Research Council of Canada.)

W-PM-B6 THE β PHASES OF MEMBRANE LIPIDS - A CRYSTAL STRUCTURE ANALYSIS OF THE "ROTATOR" CHAIN PACKING OF ACYL GROUPS. Douglas L. Dorset, Electron Diffraction Department, Medical Foundation of Buffalo, 73 High Street, Buffalo, N.Y. 14203

Although the gel or β phases of membrane phospholipids are often described as crystalline, the acyl moieties are disordered and aggregate in the so-called chain- "rotator" hexagonal packing originally found for the high temperature pre-melt phase of n-paraffins. Since electron and/or X-ray diffraction data from crystalline projections along the chain axes can not distinguish among several suggested models for this rotator phase, the employment of epitaxial crystal growth to provide a projection onto the chain axes has enabled a first crystallographic verification of a kink defect structure using 0kℓ electron diffraction data from n-hexatriacontane heated near its pre-melt transition (see Dorset, Moss, Wittmann and Lotz (1984) PNAS 81, 1913). The kink model, *via* production of chain end voids, explains the marked attenuation of 00ℓ intensities due to lamellar disorder, but much less change of intensities which represent the transform of the chain zig-zag. More recent analysis of the salient continuous diffuse scattering in these patterns further supports this structural model since the diffuse scattering persists below 16°K, and a thermal diffuse scattering calculation does not explain the observed data as adequately as the defect structural model. Experiments on odd chain paraffins, moreover, give similar results (in support of earlier spectroscopic measurements by Maroncelli, *et al.* (1982) J. Amer Chem Soc 104, 6237) as do those on even chain n-paraffins ≥ $nC_{40}H_{82}$ which do not form a separate pre-melt hexagonal phase. Incorporation of kink defects is therefore a gradual process such that the phase transitions are not strictly first order. Research supported by NIH Grant GM-21047.

W-PM-B7 REVERSIBILITY OF THE THERMAL TRANSITIONS OF CHLOROPLAST THYLAKOID MEMBRANES. Leland P. Vickers and William G. Nolan. Laboratory for Microbial and Biochemical Sciences, Georgia State University, Atlanta, GA 30303.

High sensitivity differential scanning calorimetry was used to examine the reversibility of the thermal transitions in thylakoid membranes. Chloroplast thylakoids were isolated by standard procedures from pea and cucumber seedlings. These studies were performed using a Hart Scientific DSC. A scan rate of 30 deg C/hr was used in both the heating and cooling scans. The temperature range covered was -20°C to 100°C. The low temperature work was done in buffers containing 50% ethylene glycol. Ionic strength was varied so that thylakoids could be studied both stacked and unstacked.

Thylakoids isolated from pea seedlings had six thermal transitions in the region studied. Three to five of these transitions were at least partially reversible, depending on buffer conditions. No prominent transitions were observed below 30°C. Thylakoids from cucumber seedlings were characterized by very low reversibility. The only peak visible in the cooling scans was a small exotherm starting at about 20°C. Subsequent heating scans did not show any of the 3 or 4 peaks between 40° and 100°C observed in the first heating scan. The largest peak, at 67°C in peas and 62°C in cucumbers, was reversible in peas but not in cucumbers. With pea thylakoids, additional peaks were observed in the cooling scans in low ionic strength buffers (unstacked) compared to high ionic strength buffers (stacked). Changes in ionic strength altered the peak temperatures for cucumbers, but did not alter the irreversibility of the transitions.

W-PM-B8 AN INFRARED SPECTROSCOPIC STUDY OF THE GEL TO LIQUID CRYSTAL PHASE TRANSITION IN LIVE ACHOLEPLASMA LAIDLAWII.

Henry H. Mantsch, Adèle Martin and David G. Cameron.
National Research Council of Canada, Ottawa, K1A 0R6, Canada.

A comparative study of the temperature dependence of the infrared spectra of live Acholeplasma laidlawii and of intact plasma membranes isolated from Acholeplasma laidlawii demonstrates that the profiles of the gel to liquid crystal phase transitions are quite different. The live mycoplasma is able to keep the fluidity of its plasma membrane around the temperature of growth at a much higher value compared to that found in the isolated plasma membrane at the same temperature.Thus, live Acholeplasma laidlawii grown at 37°C on a fatty acid depleted medium supplemented with myristic acid (14:0), pentadecanoic acid (15:0) or palmitic acid (16:0), are entirely fluid, i.e., the fractional population of the liquid crystalline phase is 100% at 37°C, whereas in the case of the isolated plasma membranes the fractional population of the liquid crystalline phase is only 57% (14:0), 39% (15:0) or 38% (16:0) at a temperature of 37°C.

W-PM-B9 CORRELATIONS OF HYPERTHERMIC SENSITIVITY, MEMBRANE FATTY ACIDS, MICROVISCOSITY AND GROWTH STAGE IN *E. COLI*. M.B. Yatvin, J.J. Gipp, D.R. Klessig, and W.H. Dennis (Introduced by P. Kaesberg) Depts. of Human Oncology and Physiology, University of Wisconsin, Madison, WI 53792

In two strains of *E. coli*, B/r and B_{s-1}, hyperthermic sensitivity was determined on mid-log (ML) and stationery phase (SP) cells. Bacteria are grown in nutrient broth medium and aliquots heated in PBS for 4 hrs at 47, 48 or 49°. Surviving fractions are based on average colony counts from at least three agar plates of samples taken hourly. Data are averages from two to six experiments. ML were strikingly more sensitive to heat than SP. At 48°, ML cells were 100 fold more sensitive than SP. Survival curves of early phase cells were between the ML and SP curves. As the differences between strains were small compared to the differences between growth stages, all composition data is averaged. The major fatty acid composition for the ML were 18% - 16:1, 29% - 18:1, 6% - cis-9,10-methylene-hexadecanoic (Δ17) and 3% - lactobacillic (Δ19). In contrast, the SP compositions were 1% - 16:1, 5% - 18:1, 21% - Δ17 and 25% - Δ19. Total membrane microviscosity by 1,6-diphenyl-1,3,5,-hexatriene fluorescence polarization was positively correlated with cell survival and membrane Δ17 and Δ19 fatty acid composition. These data support the hypothesis that membrane microviscosity and lipid composition play a critical role in hyperthermic cell killing. (Supported by NIH grant CA-24872-05)

W-PM-B10 DIRECT DETERMINATION OF THE SUBSTITUTION DISORDER PARAMETER IN MEMBRANE DIFFRACTION.
C.R. Worthington and Mita Gupta, Depts. of Biological Sciences and Physics, Carnegie-Mellon University, Pittsburgh, PA.
We treat the case when the membrane assemblies contain a membrane pair within the unit cell. The assemblies may contain both lattice disorder and substitution disorder. Lattice disorder is associated with the broadening of the X-ray reflections and does not pose any restrictive problems for the X-ray analysis. Substitution disorder can occur when the separation distance between membranes within the membrane pair follows some probability function that is peaked at some average width. This variation in the average width gives rise to diffuse scattering which is superimposed on the X-ray data. While it is possible to derive formulas for the diffuse scattering based on preconcieved models the actual magnitude of the diffuse scattering in a membrane diffraction experiment remains a guess. We have developed an approach for directly estimating the substitution disorder parameter. The basis for the method is that the calculated Fourier profiles contain this disorder and Fourier transformation about the centers of the individual membranes therefore contain information of the substitution disorder.

W-PM-B11 INSERTION AND TRANSPORT OF DIPHTHERIA TOXIN ACROSS LIPID BILAYER MEMBRANES DEPENDS UPON MEMBRANE LIPID COMPOSITION.
James J. Donovan and Kelly M. Standifer. Department of Pharmacology, University of Florida, Gainesville, FL 32610

Diphtheria toxin (DT) enters the cytoplasm of a target cell through receptor-mediated endocytosis followed by insertion into the membrane of an endocytic vesicle and transport across the membrane in response to the acidic environment. This lab has already shown that DT forms channels under similar conditions, and that channel formation depends upon the lipid composition of teh membrane. We report here that the transport step also depends upon membrane lipid composition. The appearance inside vesicles of the enzymatic activity of the A fragment of DT was measured by entrapping elongation factor-2 (EF-2) and labeled NAD inside vesicles and treating the vesicles with toxin at low pH. Transfer of label from acid-soluble to acid-insoluble fractions indicates an attack on EF-2 by fragment A after entry into the vesicles. DT can enter asolectin vesicles and attack the EF-2 inside, but the ability of the toxin to attack trapped EF-2 disappears when the vesicles are made with 20% phosphatidylserine (PS) and 80% phosphatidylcholine (PC). With vesicles of 20% phosphatidylinositol (PI) and 80% PC, the ability of the toxin to enter the vesicles returns, but the extent of attack is less than for asolectin. The concentration of toxin needed to achieve a 50% maximal attack on EF-2 is 0.3 uM for asolectin and PI/PC, and is not measurable for PS/PC.

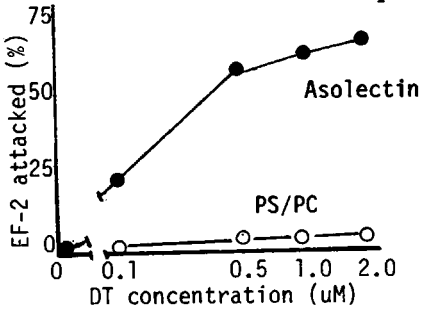

This work supported by NIH grant # CA37100.

W-PM-C1 SURFACE PLASTICITY (YIELD AND FLOW) OF GIANT DMPC VESICLE BILAYERS BELOW THE ACYL CHAIN CRYSTALLIZATION TEMPERATURE. E. Evans, D. Needham, Pathology, M. Bloom, Physics, Univ. of British Columbia, Vancouver, B.C. V6T 1W5

Micropipet aspiration of giant (2 x 10^{-3}cm diameter) dimyristoylphosphatidylcholine (DMPC) bilayer vesicles was used to study the mechanical properties of a frozen bilayer for temperatures from 5°- 24°C which range up to the acyl chain crystallization temperature, T_m, for DMPC. It was observed (as reported in the companion abstract) that freezing a vesicle from above T_m produced submicroscopic surface irregularities after rupture of the vesicle at the phase transition. Also, these irregularities (presumed to be ripples) could be avoided if the vesicle was slightly stressed but reduced in volume so that the area could condense without vesicle rupture. Below T_m, the vesicle could be expelled from the micropipet as a frozen replica of the aspirated geometry. The orientation of this frozen capsule was then reversed and reaspirated into the micropipet. For this and subsequent aspirations, the vesicle bilayer exhibited a classic plastic solid behaviour characterized by a surface yield shear, T_s, and surface shear viscosity, η_m. These properties were derived from analysis of the mechanics of deformation of the entire vesicle body in response to the aspiration pressure. The surface yield and viscosity represent the kinetics of crystal formation and dissolution along the perimeter of crystal microdomains in the surface. Both properties were found to increase with reduced temperature below T_m which indicated an increase in domain size. At fixed temperature, the yield shear and surface viscosity decreased with the number of aspiration cycles with an apparent approach to limiting values; this result indicated that the domains were homogenized and reduced in size. Yield values ranged from 10^{-2} dyn/cm to 10^{-1} dyn/cm. The surface viscosity ranged from 10^{-3} dyn-sec/cm to 1 dyn-sec/cm.

W-PM-C2 MOLECULAR DYNAMICS AT MEMBRANE SURFACES PROBED BY SPIN EXCHANGE. T.P. Silverstein and W.L. Hubbell, Department of Chemistry, University of California, Berkeley, CA 94720.

Spin exchange in solutions of nitroxide radicals is the result of radical-radical encounters and hence can be used to estimate local concentrations of one radical in the vicinity of another. Since the local concentration of charged radicals is a function of the local electrical potential (and hence of ionic strength), the degree to which a central radical spin exchanges can be used to estimate its its location and potential. Accordingly, spin exchange frequency in solutions of charged nitroxide radicals is dependent on radical concentration and ionic strength in a manner well accounted for by Debye-Hückel theory. On the other hand, the exchange frequency between a nitroxide radical tethered to the surface of a phospholipid bilayer and transition metal ion complexes in solution [$(C_6H_6)_2Cr^+$, $Fe(CN)_6^{3-}$] is not the expected function of concentration, even in neutral bilayers. This suggests a general phenomenon in which some sub-population of the tethered radicals is protected from collisions with free radicals in solution. A similar interpretation was recently proposed (Petrossian and Owicki, 1984, Biochim. Biophys. Acta 776, 212) based on the binding of soluble antibody to fluorescent lipid haptens incorporated into bilayers. We applied the spin exchange method (at low concentrations) to qualitatively examine surface potentials on spin labeled rhodopsin. Using both anionic and cationic radicals, the presence of a negative charge near the bound nitroxide on rhodopsin was confirmed.

W-PM-C3 ACYL CHAIN MODULATION OF PHASE TRANSITIONS IN GLYCEROL ESTERS. Elliott Berlin and Eduardo Sainz, Lipid Nutrition Laboratory, BHNRC, U.S. Dept. of Agriculture, Beltsville, MD 20705 Residual order was observed fluorometrically when sonicated dispersions of cis unsaturated triacylglycerols were held at temperatures above their DSC-determined fusion points, t_f (Berlin, E. and Sainz, E., Biochim. Biophys. Acta 794(1984)49). Temperatures, $t_{0.08}$, for transitions to an isotropic liquid state were noted when DPH fluorescence anisotropy equaled 0.08, corresponding to a zero value order parameter; thus $\Delta t = t_{0.08} - t_f$ may be taken as a measure of residual order in the liquid state. The reduced fluidity was attributed to restrictions imposed by the bonding of adjacent cis fatty acids onto the glycerol molecule. In contrast, adjacent binding of saturated and trans fatty acyl moieties, with their Z-shaped structure of zigzagging methylene groups, should not impose such order in the liquid state. This concept is tested now by comparing various isomeric glycerides. Triolein, 1,2-diolein, and 1,3 diolein Δt values were 75, 60.9, and 13.6°C, respectively. Similarly, trilinolein, 1,3 dilinolein, and monolinolein t values were 86, 30, and 41°C, respectively. Clearly, the restrictions in mobility, when observed, can be attributed at least in part to interactions between adjacent fatty acyl chains. Appropriately the trans series trielaidin, 1,3 dielaiden, and monoelaidin Δt values were -0.5, -9.0, and 7.0°C, respectively, and the saturated series tripalmitin, 1,2-dipalmitin, and 1,3, dipalmitin Δt values were -5.0, -1.0, and -14.0°C, respectively. Double bond location within the fatty acyl residue also affects ordering in the liquid state as simple triacylglycerol esters of cis 18:1 $\Delta 6$, trans 18:1 $\Delta 6$, and cis 24:1 $\Delta 15$ acids exhibited Δt = 37, 14, and 13°C, respectively.

W-PM-C4 PROSTAGLANDIN EFFECTS ON MODEL MEMBRANES

Ray M. Price, Dept. Microbiology, SUNY at Buffalo, Buffalo, NY, 14214

Prostaglandins are uniquely configurated molecules derived from arachidonic acid. Their conformation suggests that they might affect the physical state of membrane lipids. Bioactive prostaglandins, e.g., PGE_2, decrease the fluorescent anisotropy of diphenylhexatriene incorporated into egg lecithin unilamellar vesicles. This effect was dependent on pH when the prostaglandins were in the aqueous phase but not when the prostaglandins were directly incorporated into egg lecithin liposomes. The presence of 33 mol% cholesterol in the vesicles completely abolished the effects of the prostaglandins. These results are consistent with the suggestion that prostaglandins affect membrane fluidity. I will present the results from studies concerning the physical effects of prostaglandins on model membranes.

W-PM-C5 BINDING OF BACTERIAL LIPOPOLYSACCHARIDE TO UNILAMELLAR VESICLES

Ray M. Price and Diane M. Jacobs, Dept. Microbiology, SUNY at Buffalo, Buffalo, NY,14214

The details of the interaction of bacterial lipopolysaccharide (LPS) with biological membranes are unknown. It is thought that the biological activity of LPS is dependent on the insertion of the lipid A component into the cell membrane. We have found that the fluorescence anisotropy of diphenylhextriene in unilamellar egg lecithin vesicles is increased when those vesicles are incubated with LPS (from E. coli 055:B5). This is consistent with the hypothesis that some component of LPS, most likely the hydrophobic lipid A, interacts with the hydrophobic region of membranes and can affect the fluidity of these membranes. We will present the results of our studies on the interaction of LPS, or its lipid A and saccharide components, with some models of biological membranes.

W-PM-C6 TEMPERATURE DEPENDENCE OF TRANS-BILAYER PROTON/HYDROXYLATE PERMEATION

Ron DeGuzman & John Bramhall; Microbiology and Immunology Department, UCLA School of Medicine and UCLA Cancer Center, Los Angeles, California 90024.

We have previously introduced the amphiphilic fluorescent dye dansyl-glycine as a probe suitable for monitoring the magnitude and stability of trans-membrane proton gradients [Biophys. J. 45,332A (1984)]. For work with small unilamellar lipid vesicles dansyl-glycine offers several advantages over the more widely used 9-aminoacridine. When the internal trapped aqueous volume of a vesicle system is extremely small, as is the case with our system, the small amount of concentration quenching of 9-aminoacridine becomes very hard to detect. In contrast, the membrane associated dansyl glycine shows little dependence on vesicle diameter. Using this novel probe we have been able to monitor the decay of pH gradients established across the boundary bilayer of small lecithin [DPPC] vesicles. By determining the rate constant for pH gradient decay over a range of temperatures we have been able to detect a marked discontinuity in proton/hydroxylate flux occuring at Tc, the temperature of the major gel-liquid crystalline phase transition. The discontinuity is unlike those seen for the permeation of electrically neutral amphiphilic solutes across identical bilayers, and is dramatically different from the permeation behavior of hydrated ions such as sodium and potassium. The implication is that the mechanism of permeation of protons/hydroxylate ions across homogeneous phospholipid bilayers is fundamentally different from that of metal ions. [Supported by NIH grants CA 12800 and CA 16042 and by grants from the UCLA Academic Senate and California Institute for Cancer Research].

W-PM-C7 A "MILLING CROWD" MODEL FOR THE LATERAL MOBILITY OF MEMBRANE PROBES, J. Eisinger, J. Flores, and W. P. Petersen, AT&T Bell Laboratories, Murray Hill, New Jersey 07974

The long range (~1μm) mobility of probes in membranes and model systems is usually measured by fluorescence photo-bleaching recovery (FPR) experiments and represents an average over a displacement in the membrane plane which includes many membrane proteins. The "milling crowd" model (MC) simulates the mobility of the probe molecule by an algorithm in which the phospholipid matrix forms a regular trigonal array with a fraction, x, of lattice points occupied by probes. The probes exchange positions at random with one of their six nearest neighbor lipids at an exchange frequency ν. It is shown that if half the area of the membrane is occupied by a stationary random distribution of small proteins (diameter ~1.5nm), the probe's diffusibility is greatly decreased. If the same area fraction is occupied by larger proteins, the effect on the probe's mobility is smaller. The local (1-10nm) lateral mobility of membrane probes cannot be measured by FPR but can be determined from the excimer production rate of excimeric membrane probes. The MC model is used to obtain the average number of spatial exchanges, $n(p_E,x)$, which leads to an excimer, where p_E is the probability of excimer formation between nearest neighbor probes. From the experimental excimeric/monomeric yield ratio, $\rho(x)$, and its limiting value ρ^*, obtained with high-x excimeric and low-x monomeric yields, one may determine ν from: $\rho(x) = \rho^*\tau_M\nu/n(p_E,x)$, where τ_M is the monomer lifetime. This equation is derived from excimer formation kinetics. Experimental data for $\rho(x)$, obtained with the excimeric probe 1-pyrenehexadecanoic acid in lecithin vesicles, intact erythrocyte membranes and in ghosts were analyzed by means of the MC model. The local diffusibilities are found to be several times larger than the corresponding results for long range diffusion as measured by FPR and will be discussed in terms of the membrane's dynamical structure.

W-PM-C8 STRUCTURAL EFFECTS ON TB^{3+} BOUND TO SMALL UNILAMELLAR VESICLES (SUVs). Everett C. Schreiber, Jr. and Arnold Wishnia, SUNY at Stony Brook.

The lifetime of the excited $^5D_4$ state of Tb^{3+} is sensitive to deexcitation via vibrational modes of its environment, especially those of (^{1}H) H_2O in the hydration sphere: in simple systems replacement of H_2O by other ligands or by D_2O increases the lifetime 4-5 fold, to about the intrinsic emission lifetime (see, e.g., Horrocks and Sudnick, J. Am. Chem. Soc., 101, 334-340 (1979)). For uncharged phosphatidyl choline vesicles, in 1mM Tb^{3+}, 30mM phospholipid P, the Tb^{3+} is almost completely bound to the SUV outer surface (data below and related NMR work). The Tb^{3+} emission decay rate is strictly exponential, over 5 half times, under all conditions, but the actual rates depend on both the nature and the concentration of the counter anion (added as NaX), and the H_2O/D_2O rates are strikingly atypical. Considering only the differences in rates in H_2O and D_2O, hydration of bound Tb^{3+} shifts up from 2.5 to 4.2 (vs. 9 in the aquo ion) with NO_3^- but falls smoothly from 7 to 4, with Cl^- over 0-500mM NaX. The actual rates in both H_2O and D_2O are quite high (e.g., 2.37 vs. 1.78, x10^3 sec^{-1}, in 3mM NO_3^-), indicating that the non-H_2O vesicle head group matrix has a major role in relaxing Tb^{3+}. Changes upon adding X^- must involve not only direct anion binding and changes in hydration number, but also structural modifications that change the matrix vibrational - Tb^{3+} energy gap coupling. Comparative studies with Eu^{3+} are being carried out, to help sort out these factors. Binding to the SUV inner surface is under study. (NIH GM27176).

W-PM-C9 THE USE OF Co^{2+} AS A COLLISIONAL QUENCHER TO PROBE SURFACE CHARGE AND DEFECTS IN LIPID VESICLES. S.J. Morris, D. Bradley and R. Blumenthal. Neurotoxicology Section, NINCDS and Membrane Structure and Function Section, NCI, NIH, Bethesda, Md.

The effect of Co^{2+} on the fluorescence of the lipid probes NBD-PE and N-Rh-PE, incorporated into lipid vesicles, was studied in order to probe surface charge and barrier properties of the lipid bilayer. The results were consistent with a collisional quenching mechanism in agreement with the Stern-Volmer law. The quenching coefficient (Q) for NBD-PE, incorporated into uncharged PC vesicles was 13.8 M^{-1}. This value was similar to the quenching coefficient of a water-soluble derivative NBD-taurine, indicating that Co^{2+} was readily accessible to the outer surface of PC vesicles. In PS:PE (1:1) vesicles, Q was 8000x lower. Calculation of the effective Co^{2+} at the membrane surface using the Gouy-Chapman-Stern model with a binding constant of 28 M^{-1} for the Co-PS complex (Mclaughlin et al, 1981), indicated that this value is consistent with the Q measured for NBD-PE in uncharged vesicles. In Small Unilamellar Vesicles (SUV), at about 100 μM concentration, Co^{2+} rapidly quenched NBD-PE in both outer and inner surfaces of PS:PE (1:1), indicating rapid permeation of the ions into the SUV. Since there was no change in optical density of the sample under those conditions, we concluded that this phenomenon was not related to possible aggregation or fusion of the vesicles. Large unilamellar vesicles formed by reverse phase evaporation were not permeable to Co^{2+}. Using stopped-flow kinetics we measured the rate constant for influx of Co^{2+}, and correcting for surface potential using the Gouy-Chapman-Stern model, we calculated a permeability coefficient of 10^{-9} cm/sec in PS/PE. In SUV made of PS/PC, the permeability coefficient was much lower. The higher permeability in PS/PE suggests defects in the packing of the SUV, and this might be related to its ability to undergo membrane fusion.

W-PM-C10 FLUORESCENT PROPERTIES OF BIOACTIVE FLAVONOIDS IN MODEL MEMBRANE SYSTEMS
Ray M. Price, Greg Smutzer, and Elliott Middleton, Jr., Depts. Microbiology and Biochemistry, SUNY at Buffalo, Buffalo, NY, 14214 and Allergy Research Lab, Buffalo General Hospital, Buffalo, NY, 14203

Flavonoids are low molecular weight compounds that are ingested as a part of the mammalian diet from plants. They have been shown to affect many membrane enzyme activities in vitro. Since the bioactive flavonoids are planar molecules, we thought their effects on membrane activities might be mediated through their physical interaction with the membrane. Therefore, we sought to determine the physical effects of flavonoids on model membrane phase transitions. However, measurements of diphenylhexatriene fluorescent anisotropy were unsuccessful in the presence of flavonoids. The emission peak of diphenylhexatriene at 430 nm was completely quenched and a new peak appeared on the DPH emission spectrum at 530 nm. Some of the flavonoids that we used seem to be fluorophores. We will present the results from our studies on the fluorescent properties of bioactive flavonoids and their use as fluorescent probes in model membrane systems.

W-PM-C11 FLUORESCENCE STUDIES OF EXCIMER FORMATION IN SINGLE BILAYER LIPOSOMES USING A PYRENE-METHYL CHOLESTEROL ADDUCT. Lesley Davenport and Ludwig Brand, Biology Department, The Johns Hopkins University, Baltimore, Maryland 21218.

1-Pyrenemethyl 3-β-hydroxy-22,23-bisnor-5-cholenate (PMC), a fluorescent cholesterol analogue may be incorporated into DML vesicles by co-sonication. The broad structureless excimer fluorescence (λ_{max} 480nm) is readily distinguished from the highly structured monomer fluorescence (PMC to phospholipid > 1:100). On incorporation of cholesterol (up to 33 mole%), the dimer to monomer fluorescence intensity ratio (D/M) for PMC, at any given temperature, shows an increase. A decrease in this ratio is found for pyrene under the same conditions. Nanosecond time-dependent studies of PMC labeled vesicles (1:50) below the phase transition, reveal a multi-exponential decay. From decay-associated spectra of this system, the inferred kinetic mechanism for formation of excimer differs significantly from that of the closely related pyrene molecule. The data suggests ground-state heterogeneity with one class of PMC molecules closely aligned in the ground-state. On excitation, these molecules rapidly form excimer species, as evidenced by a relatively fast rise time. A second population of molecules form excimer by a slower diffusion process occuring on a longer time-scale, as proposed for pyrene. That a non-random distribution of PMC molecules exist under these conditions, is further supported by spectral differences in excitation spectra recorded at emission wavelengths for either the monomer or excimer species. Interpretations of this data in terms of cholesterol microheterogeneity will be presented.
(Supported by NIH grant No. GM 11632).

W-PM-C12 FLUORESCENCE MICROSCOPE STUDIES OF ANTIBODIES BOUND SPECIFICALLY TO PLANAR SUPPORTED BILAYERS CONTAINING LIPID HAPTENS. Sriram Subramaniam, Nancy L. Thompson, Lukas K. Tamm and Harden M. McConnell. Department of Chemistry, Stanford University, Stanford, CA 94305

There is much current interest in the development of suitable model membrane systems for immunological studies. Our specific objective has been the preparation of phospholipid bilayers containing lipid haptens supported on macroscopic planar substrates coated with controlled numbers of specific antibodies. We have successfully achieved this objective.

Phospholipid bilayer membranes were supported on clean quartz slides or silicon wafers by sequential transfer of two monolayers from an air-water interface. The membranes contained varying mole fractions of a nitroxide lipid hapten (NLH) in the host lipid DMPC. Our principal conclusions are: (1) Binding of fluoresceinated anti-NLH antibodies to these membranes is highly specific to the presence of the lipid hapten. (2) This binding, as monitored by fluorescent emission from the labeled antibodies, increases with increasing hapten concentration in the range of 1 to 25 mol %. (3) Their lateral diffusion coefficient as measured by fluorescence photobleaching recovery decreases from 2×10^{-8} cm^2/sec at 0.5 mol % hapten to 1.5×10^{-10} cm^2/sec at 25 mol % hapten. (4) At a given hapten mol %, the diffusion coefficient decreases with increasing amounts of added antibodies.

We are actively pursuing studies to: (a) Explore the binding and triggering of cells of the immune system to these antibody coated target membranes, and (b) understand in molecular detail physical processes such as phase separation and two-dimensional crystallization in these membranes.
(This work was supported by NIH Grant UC-SC-32072 and Damon Runyon-Walter Winchell Cancer Fund Fellowship DRG 593 to N.L.T.)

W-PM-D1 N-ACETYLASPARTATE AS AN INTRINSIC THERMOMETER FOR ^{1}H NMR OF BRAIN.
Carlos Arús, Yen-Chung Chang, and Michael Bárány. Dept. of Biochemistry, College of Medicine, University of Illinois, Chicago, IL 60612

We recorded ^{1}H NMR spectra of excised rat brain at 360 MHz with the JR water suppression pulse sequence (J. Am. Chem. Soc., 104, 7310, 1982). A strong temperature dependence was observed for the chemical shift of the amido proton of N-acetylaspartate (N-AcAsp), a common metabolite of the brain. This observation suggested the use of N-AcAsp as a brain thermometer. The temperature dependence of the chemical shift of the amido proton of N-AcAsp, using the $N-CH_3$ resonance of creatine at 3.022 ppm as the internal chemical shift standard, was determined in the following systems: 1) A solution containing 20 mM N-AcAsp, 20 mM creatine, 150 mM NaCl, pH 7.18; 2) Brain cytosol (200,000 x g supernatant); 3) Intact brain. The variable temperature unit reading of the Nicolet instrument was calibrated with ethylene glycol. The slope of the temperature dependence curves was the same for the 3 systems: 0.00846 ppm/°C. The chemical shift of the N-AcAsp amido proton in the brain cytosol was found to be independent from the pH, between 6.05 - 8.31, 37°C. Therefore, tissue acidosis will not affect the measurements. Accordingly, the brain temperature was calculated by substituting δ_{obs}, the observed chemical shift of the amido proton, in the following formula: $T\ (°C) = (8.142 - \delta_{obs})/0.00846$. The accuracy of our temperature determination, due to the digital resolution used, is ± 0.4°C. As far as we know this is the first application of an intrinsic NMR thermometer to a tissue. (Supported by MDA Postdoctoral Fellowship to C.A., and grants from MDA and Shriners Hospitals).

W-PM-D2 NATURAL ABUNDANCE ^{13}C NMR OF BRAIN, MOBILIZATION OF PHOSPHOLIPIDS BY HALOTHANE.
Michael Bárány, Yen-Chung Chang, Carlos Arús, and Alice M. Wyrwicz. Departments of Biological Chemistry and Chemistry, University of Illinois at Chicago, IL 60612

Natural abundance ^{13}C NMR spectra (90.8 MHz) of brain excised from rats, rabbits, pigs, and from human bodies 7-36 hours after death revealed a very similar ^{13}C pattern. With rat brain 55 resonances were resolved, 52 of them were assigned, including the carbons of myo-inositol. The unsaturated carbons of the rat brain showed a well defined resonance at 128.9 ppm (relative to dioxane at 67.4 ppm), however, the saturated aliphatic carbons were buried in a broad envelope, 25-35 ppm region of the spectrum. All these phospholipid resonances were clearly visible in the chloroform-methanol extract of the same brain, suggesting that the saturated fatty acyl carbons are immobilized in the structure of the native brain. These carbon resonances remained immobilized upon raising the temperature of the brain to 37°C, or by treatment of the brain with deoxycholate, verapamil, or trifluoperazine. However, upon a 10-min treatment of the intact excised brain with halothane ($CF_3CHBrCl$), a general anesthetic agent, the saturated fatty acyl carbons were mobilized. Under the same conditions, halothane had no effect on the phospholipid carbons of excised rat liver or kidney. Furthermore, the saturated fatty acyl carbons were also found to be mobilized in brain of live rats anesthetized with halothane. Pure (99%) linoleic, linolenic, and arachidonic acids were mixed with halothane in chloroform. Changes in the intensity and chemical shift in resonances of several fatty acyl chain carbons occurred upon interaction with halothane. These data suggest that halothane interacts with the phospholipid moiety of brain membranes. (Supported by MDA, Shriners Hospital for Crippled Children, and MDA Postdoctoral Fellowship to C.A.).

W-PM-D3 USE OF ^{19}F NMR TO MEASURE INTRACELLULAR pH. C. Deutsch and J. Taylor, Department of Physiology, University of Pennsylvania, Philadelphia, Pa. 19104

We have developed a repertoire of ^{19}F NMR indicator molecules whose chemical shifts are strongly pH-dependent. These include the alanine derivatives, mono-, di-, and tri- fluoro-α methylalanines. The pK_as are approximately 8.5, 7.3, and 5.9, respectively. The resonances of these three are separated from each other by more than 50 ppm compounds, so that mono- and di-, or di- and trifluoro-α-methylalanines can be used in tandem in the same cell suspension, in order to cover a wide range of pH. These compounds are nonmetabolizable and noncytotoxic by virtue of the α-methyl group. The methyl esters of these fluorinated amino acids were used in order to enhance the uptake of the indicator. The less polar esters diffuse rapidly across cell membranes and are cleaved by endogenous esterases to generate the desired indicator molecule, the free amino acid. While the fluorinated methyl esters are hydrolyzed by several mammalian cells (human lymphocytes, rat hepatocytes, rabbit colon) they are not hydrolyzed by Paracoccus denitrificans, E. coli or insulinoma cells. However, we have evidence that cells lacking methyl esterase activity with respect to fluorinated methylalanine methyl esters are still capable of cleaving esters with aromatic or larger aliphatic groups esterified to the carboxyl group. We have also investigated the use of dipeptides, specifically fluorinated α-methylalanylalanines, as precursors for fluorinated pH indicators in methyl esterase-deficient cells.

W-PM-D4 SPATIAL LOCALIZATION OF SODIUM IONS AND LONGITUDINAL RELAXATION TIMES (T_1) IN THE BOVINE EYE BY NMR ROTATING FRAME ZEUGMATOGRAPHY. T. Schleich, M. Garwood, M.E. Moseley[+], and W. Chew[+], (Dept. of Chemistry, Univ. of California, Santa Cruz, CA 95064, and [+]Dept. of Pharmaceutical Chemistry, Univ. of California, San Francisco, CA 94143

NMR surface coils are used to generate one- and two-dimensional topographical distribution maps of the Na-23 ion levels present in the enucleated bovine eye. The one-dimensional spatial localization experiment, which is based upon the rotating frame zeugmatography method, depends on the B_1 field gradient produced by a surface coil. Application of equally incremented evolution pulses produce nutation of the magnetization away from the z-axis in the rotating frame. The frequencies of nutation are invariant along curved surfaces of constant B_1 strength which define one dimension of the Na-23 distribution map directed along the axis of the surface coil. Application of a read-out gradient along the z-axis during signal acquisition provides spatial discrimination in the longitudinal direction as well, and two-dimensional Fourier transformation of the data results in a two-dimensional Na-23 distribution map. The introduction of a phase cycling saturation preparation pulse sequence along with a variable delay time between the preparation pulse and evolution pulse allows spatially resolved T_1 relaxation times to be obtained for Na-23 ion in the aqueous humor, the lens, and the vitreous in an intact bovine eye. Slice selection in the two-dimensional experiment can also be achieved by utilizing an amplitude modulated evolution pulse (i.e. a sin(t)/t shaped B_1 pulse envelope). The computer calculated frequency-selectivity of various pulse shapes as predicted by the Bloch equations will be presented, along with the two-dimensional Na-23 distribution and T_1 maps of the bovine eye.

W-PM-D5 NONINVASIVE ANALYSIS OF TISSUE HETEROGENEITY: NUCLEAR MAGNETIC RESONANCE STUDY OF THE RAT KIDNEY IN VIVO. M. Garwood, T. Schleich, R.T. Bogusky[+], G. Acosta, L. Cowgill[++], and G.B. Matson[+++] (Dept. of Chemistry, Univ. of California, Santa Cruz, CA 95064, [+]Dept. of Internal Medicine, School of Medicine, [++]Dept. of Medicine, School of Veterinary Medicine, and [+++]NMR Facility, Univ. of California, Davis, CA 95616)

NMR spatial localization techniques have been developed to noninvasively measure levels of tissue Na-23 ion and P-31 containing metabolites in different regions of rat kidney. The one-dimensional metabolite mapping experiment depends on the B_1 field gradient produced by a surface coil in the presence of a homogeneous B_0 field. Equally incremented RF pulse durations are applied to the sample, producing nutation of the magnetization away from the z-axis in the rotating frame. The nutation frequencies are invariant along curved surfaces of constant B_1 strength which define the mapping dimension. Two-dimensional Fourier transformation of the data results in a suite of chemical shift spectra displayed as a function of mapping distance. The method distinguishes metabolite level differences between tissue regions with a resolution greater than 2mm. The left kidney of a 350g anesthetized rat was exposed through a flank incision and was supported by copper shielding that also separated the exposed kidney from the abdominal wall. A two-turn surface coil was placed over the kidney, and the NMR probe restraining the rat was placed in a wide-bore 4.7 Tesla magnet of Nicolet spectrometer. In the normal kidney the cortex has the highest content of ATP and the medulla the least. Sodium is concentrated to the highest levels in the outer-medulla. The metabolite maps acquired from rat kidneys made acidotic with NH_4Cl or hypokalemic with DOCA injections reveal striking changes in the ATP distributions in the kidney.

W-PM-D6 NMR MEASUREMENTS OF MYOCARDIAL CREATINE KINASE RATES BY MULTIPLE SATURATION TRANSFER. K. Ugurbil, M. Petein, R.R. Maidan, S.P. Michurski, J.N. Cohn, and A.H. L. From. University of Minnesota, Navarre, MN.

Forward (creatine phosphate (CP) → ATP) and reverse (ATP → CP) fluxes of myocardial creatine kinase (CK) measured using ^{31}P NMR and conventional saturation transfer (CST) methods are unequal; this is a paradoxical result since during steady-state, fluxes into and out of the CP pool must be equal. These measurements, however, treat the CK reaction as a two-site exchange problem and ignore the $ATP_\gamma \rightleftarrows P_i$ exchange involving the ATPases. We have developed a method involving saturation of multiple resonances by which a single unidirectional rate constant can be measured unequivocally in the presence of multiple exchanges. We have applied this method to the measurement of CK fluxes in isovolumic rat hearts perfused with pyruvate + glucose, consuming O_2 at 46 ± 2.2 μmoles/min. g dry weight, and developing a rate-pressure product of 46580 ± 3769; the ratio of the reverse to the forward CK flux was measured by CST to be 0.56 ± 0.04 (24 measurements). In contrast, when $ATP_\gamma \rightleftarrows P_i$ exchange was eliminated, multiple saturation transfer (MST) measurements on the same hearts yielded the expected ratio of 1.03 ± .07; the rate constant for the ATP_γ → CP conversion measured by MST was ~ 60% larger than the value obtained by the conventional methodology whereas both methods gave the same rate constant in the CP → ATP direction. These results demonstrate that the cause of the paradoxical data obtained by CST measurements of CK kinetics is the $ATP_\gamma \rightleftarrows P_i$ exchange, and that CK rates when determined rigorously are consistent with CK reaction being in equilibrium.

W-PM-D7 ANALYSIS OF COMPARTMENTATION OF ATP IN SKELETAL AND CARDIAC MUSCLE USING P-31 NMR SATURATION TRANSFER. Raphael Zahler, John A. Bittl, and Joanne S. Ingwall, Harvard Medical School NMR Laboratory, Boston, MA 02115.

In striated muscle, cellular ATP is distributed in at least two compartments, the mitochondria and the cytosol. We have developed a simple model for the analysis of the creatine kinase (CK) reaction [CrP + ADP $\rightleftharpoons$ Cr + ATP] in heart and skeletal muscle measured by NMR saturation transfer. This model allows for the existence of two ATP pools, one which is NMR-visible and saturable (ATP-VIS) and another which is NMR-invisible and non-saturable (ATP-INVIS). The model is consistent with the double-exponential behavior seen in some experimental results. We have applied the method to experimental data obtained for cardiac and quadriceps muscles of the rat and have defined the dependence of the resulting rate constants and fluxes on work load. The model suggests that 1. The ATP-INVIS pool in stimulated skeletal muscle lies wholly or partly at the mitochondrion. 2. Flux from ATP-INVIS to ATP-VIS is increased in stimulated muscle, mainly because of activation of the cytosolic reaction CrP $\rightarrow$ATP-VIS. In heart, there is a similar, graded increase in flux from ATP-INVIS to ATP-VIS with increasing work load, mediated by increases in both CrP $\rightarrow$ATP-VIS and ATP-INVIS $\rightarrow$CrP. 3. In skeletal muscle, but not in heart, total flux from CrP to ATP is independent of work load. 4. In heart the rate constants from CrP to ATP-VIS and from ATP-INVIS to CrP increase by a factor of 6 with increasing work load from K-arrest to maximal work. In skeletal muscle, however, only the constant for ATP-VIS $\rightarrow$CrP shows a large increase with increased work load. 5. Regardless of load, flux from CrP to ATP-INVIS is negligible in heart but significant in skeletal muscle.

W-PM-D8 DEVELOPMENTAL CHANGES OF CREATINE KINASE AND PHOSPHOMONOESTERS IN N1E-115 NEUROBLASTOMA, DISSOCIATED RAT BRAIN CELLS, AND WHOLE ANIMAL RAT BRAINS SEEN WITH 31P NMR. P.Glynn, S.Ogawa, T.M. Lee, AT&T Bell Laboratories, R. Chappell, Hunter College, NY (intro by W.E.Blumberg)

There are dramatic developmental changes in creatine kinase kinetics and in the concentrations of phosphomonoesters (PME) in neuronal cell systems as measured by 31P NMR. We have looked at N1E-115 neuroblastoma (NB) undifferentiated cells, NB cells induced to differentiate with DMSO, and dissociated fetal rat brain cells from 16 through 21 day fetuses. Brains of living neonates and adult rats were looked at. We find the PME associated with peaks at 4.37 ppm, identified as phosphatidylethanolamine (PEt) and 3.86 ppm, tentatively assigned as phosphocholine (chemical shifts are relative to phosphocreatine assigned -2.53 ppm). There peaks are about the level of ATP in differentiated NB cells and are too small to be observed above noise in the undifferentiated NB.The observable peaks have been seen in very large concentrations (> 10mM) presumably in the cytosol, as judged by their chemical shifts. In the dissociated fetal rat brain cells, 70% neuronal in nature, the PEt concentration is also equal to the ATP concentration. In contrast, the one day old neonate has a very large PEt concentration, which decreases as the animal matures. The difference in PEt content between the 21 day old fetus cultured for one day and the one day old neonate suggest either the neuronal content of PEt is small in comparison to other brain cells, i.e. glia, or there is a loss of PEt in the cultured cells as an artifact of the dissociation and culture procedure.The rate constant k_1 of the creatine kinase reaction in the direction of dephosphorelation of phosphocreatine was found to be zero in undifferentiated NB cells, very small in dissociated rat brain cells and one day old neonates, and increased threefold in the 21 day old animal. We conclude that a large pool of PEt and a change in the activity of creatine kinase is associated with development.

W-PM-D9 CYTOSOLIC PHOSPHATE ESTIMATED BY (PCr + ATP) AND BY "CRYO"^{31} P-NMR: A DIRECT COMPARISON IN QUICK FROZEN SAMPLES OF WORKING DOG GRACILIS MUSCLE. Jeff Olgin, Richard Connett and Britton Chance. Department of Biochemistry Biophysics, University of Pennyslvania, Philadelphia, PA and Department of Physiology, University of Rochester, Rochester, NY.

Vascularly isolated autoperfused dog gracilis muscles were stimulated via the obturator nerve to generate maximal isometric twitch contractions at a frequency of 4/s. Fast frozen samples of the stimulated muscle were obtained by applying a copper heat sink at specific times after the conset of contraction. Samples of the frozen tissue were extracted in perchloric acid and assayed for PCr and ATP by standard enzymatic techniques. Parallel samples of the same muscle were assayed for PCr/P_i by application of the "cyro-NMR" technique (Chance et al., Proc. Nat. Acad. Sci., USA 95: 4925-4929, 1978). Tissue phosphate (P_i) levels were calculated from chemical assays: $P_i=(PCr+ATP)_T-(PCr+ATP)_{rest}$ and compared with values calculated from the PCr/P_i using measured PCr. The agreement is well within the error of the assays for all times.

	Chemical Assay			NMR	
Treatment	ATP	PCr	Pi	PCr/Pi	Pi
Rest	3.43	10.83	-	15.52	.70
5 sec	3.85	10.28	.833	10.76	.96
10 sec	3.40	9.90	1.66	10.86	.91
15 sec	3.60	10.25	1.11	9.88	1.04
30 sec	3.03	6.88	4.35	0.83	8.29
60 sec	2.68	4.77	7.51	0.70	6.81
180 sec	3.35	5.84	5.77	0.63	9.27

(Supported by USPHS AM22124)

W-PM-D10 IN VIVO DEPHOSPHORYLATION OF WR-2721 EXAMINED BY ^{31}P NMR. S. Knizner, A. Jacobs, Armed Forces Radiobiology Research Institute, Bethesda, MD, R. Lyon, National Cancer Institute, NIH, Bethesda, MD, and C.E. Swenberg, Armed Forces Radiobiology Research Institute, Bethesda, MD.

Phosphorous NMR is presently being used to study a wide variety of biochemical, physiological, and medical problems. WR-2721 (2-(3-Amino-propyl)aminoethyl phosphorothoic acid) is a phosphorothioate which has been shown to exert a radioprotective effect in several animal species. Presumably this drug is dephosphorylated in vivo to yield the active thiol form of the drug (WR-1065), and inorganic phosphate. In this study we report on the in vivo dephosphorylation of WR-2721 in mice monitored by ^{31}P NMR. The ^{31}P NMR spectra of the abdomen and hind quarters region of the mouse are characteristic of muscle tissue, exhibiting seven distinct resonances. These can be assigned to sugar phosphates, inorganic phosphate (P_i), phosphodiesters, phosphocreatine (PCr), and the α, β, and γ phosphates of ATP. The intracellular pH prior to drug treatment was estimated from the position of the P_i resonance to be 7.1 ± 0.1. Upon injection of WR-2721 (600 mg/Kg i.p.) the signal due to this drug is immediately detected at 19 ppm downfield (higher frequency) from PCr. Dephosphorylation of WR-2721 commences immediately after it is injected, as evidenced by the increase in P_i over control value. Also, the P_i peak is now split, indicating P_i is found in two different pH environments, corresponding to pH 7.1 ± 0.1 and pH 6.6 ± 0.1. Thirty minutes post injection approximately half of the WR-2721 is dephosphorylated. P_i continues to be elevated, and now is split into two clearly distinct peaks corresponding to pH 7.1 and pH 6.2. The more acidic P_i is a sharp resonance and represents phosphate in the urine. Sixty minutes post injection most of the drug is dephosphorylated, and urinary P_i continues to be more acidic (pH 6.1) than cellular phosphate (pH 7.1). Twenty four hours following injection ^{31}P spectra were again obtained, and the levels of phosphorous compounds had returned to control values.

W-PM-D11 EXPLORATION OF THE BIOCHEMICAL RESPONSES RELEVANT TO STRESSED, INTACT CORN ROOT TISSUE VIA ^{31}P NMR SPECTROSCOPY. P. E. Pfeffer, S. Tu, W. V. Gerasimowicz, and J. R. Cavanaugh. (Intr. by Leo D. Kahn), Eastern Regional Research Center, U. S. Department of Agriculture, Philadelphia, PA 19118.

In vivo ^{31}P NMR spectroscopy has been established as a useful tool for defining the biochemical status and viability of corn root meristerm tissue. In the present study introduction of certain perturbants responsible for inducing stressed conditions have been examined to evaluate alternate processes by which the root cells may adapt for survival. Perfusion of root tissue with a relatively high concentration of Mn^{+2} led to a sequential broadening of the ^{31}P resonances associated with ATP, P_i in the cyctoplasm and ultimately P_i within the vacuole. The inability to remove Mn^{+2} associated with the vacuole compartment clearly demonstrated the vacuole's metal trapping function in the root cells. In addition, preloading of the root tissue with Mg^{+2} caused the vacuole P_i to be insensitive to broadening by Mn^{+2}. Final washing of the Mn^{+2} treated cells showed that Mg^{+2} was also irreversibly trapped in the vacuole. Results obtained when oxygen supply to the roots is cut off in the presence of excess ADP suggest that the cells utilize adenylate kinase activity for the production of ATP and AMP. Although the observed ATP level in these experiments decreased by 70% (AMP increased by 50%), the integrity of the cell compartmentation was clearly maintained. Apparently, the lower level of ATP did not significantly affect the transmembranous proton pumping of the subcellular organelles. However, the production of glucose-6-phosphate was severely reduced. Upon aeration, ATP is regenerated in contrast to results of previous studies on the effects of anaerobic fermentation in roots.

W-PM-D12 A NOVEL SPIN LABEL METHOD FOR MONITORING DISSOLVED OXYGEN IN THE PERFLUOROCHEMICAL BLOOD SUBSTITUTE, FC-43 EMULSION

C.-S. Lai, W. Froncisz and J. S. Hyde

National Biomedical ESR Center, Department of Radiology, Medical College of Wisconsin, Milwaukee, Wisconsin 53226

Perfluorochemicals are excellent solvent of O_2 and CO_2 gases. These compounds have received great attention in recent years because of their potential usefulness in the development of artificial blood substitutes. FC-43 emulsion, consisting mainly of perfluorotributylamine (PFT) emulsified in a saline solution, has been used in numerous experiments on animals and demonstrated to be an effective oxygen-transporting substance in vivo. We report here that TEMPO-laurate, a lipid spin probe, partitions favorably into PFT, either in pure form or in the emulsified preparation, FC-43 emulsion. The signal amplitude of the ESR spectrum of TEMPO-laurate was shown to be sensitive to the levels of oxygen in perfluorochemical preparations. The spin probe dissolved into pure PFT gave rise to a single component ESR spectrum. Partition of the probe into the micelles of FC-43 emulsion, however, revealed a two-component ESR spectrum; a major component attributed to the probe inside the micelles and a minor component probably due to the probe associated with the surface of the micelles. The results suggest that the ESR signal of TEMPO-laurate may be a useful parameter for determining the uptake and release of oxygen in perfluorochemical blood substitutes.

W-PM-E1 ELECTROSTATIC AND DYNAMIC EFFECTS OF SEMISYNTHETIC ALIPHATIC SUBSTITUTIONS AT THE AMINO TERMINUS OF MYOGLOBIN. Mark R. Busch, George W. Neireiter, David E. Harris and Frank R. N. Gurd, Department of Chemistry, Indiana University, Bloomington, Indiana 47405.

A series of semisynthetic variants of sperm whale myoglobin having ^{13}C enriched aliphatic amino acids at the amino terminus has been prepared and extensively characterized (Busch et al., Biophysical J. 45, 248a, 1984). The replacement of the native valine with enriched glycine, alanine, valine, isoleucine, and leucine resulted in proteins indistinguishable from native in characterization by visible and ultraviolet spectroscopy, electrophoretic mobility, acid stability, and ^{13}C NMR spectroscopy of the underlying natural abundance spectra. The pK values of the amino terminus of each variant have been determined using ^{13}C NMR spectroscopy, and the observed decrease in the pK value from 7.72 for [Gly^1]myoglobin to 7.15 for [Leu^1]myoglobin can be correlated with increasing hydrophobicity of the side chain. Analysis of ^{13}C NMR relaxation data using the model free approach of Lipari and Szabo (JACS 104, 4546, 1982) with subsequent application to specific models of molecular motion shows the range of motion of the amino terminal alpha carbon in [Gly^1]myoglobin decreasing with protonation, whereas the more hydrophobic terminal side chains are more rigidly held with little apparent effect of pH. The extent of interaction of the amino terminal side chain with the hydrophobic nucleus formed with the side chains of invariant residues leucine-2 and leucine-137 and the resultant effects on the self energy at this charge site are considered as potential explanations for the electrostatic and dynamic phenomena observed in this series of variants.

(Supported by U.S. Public Health Service Research Grants HL-05556 and HL-14680.)

W-PM-E2 A COMPARISON OF THE INTRINSIC FLUORESCENCE OF RED KANGAROO, HORSE, AND SPERM WHALE MET-MYOGLOBINS. Rhoda Elison Hirsch, Division of Hematology, Department of Medicine, Albert Einstein College of Medicine, Bronx, N.Y. 10461.

Several met-myoglobin variants (red kangaroo, horse, and sperm whale), containing different numbers of tyrosine and invariant tryptophan residues (7, 14), exhibit intrinsic fluorescence when studied by steady-state front face fluorometry. The increasing tyrosine content of these myoglobins correlates with an emission maximum to shorter wavelengths with excitation light of 280 nm: red kangaroo, tyr 146 (335 nm); horse, tyr 103, 146 (333 nm); sperm whale IV, tyr 103, 146, 151 (331 nm). The possibility that apoprotein significantly contributes to the emission signal is ruled out by insignificant fluorescence of 1-anilinonapthlalene-8-sulfonate in the presence of these protein preparations. The pH-dependence of the fluorescence emission was studied. Upon titration to pH 12.5, there is a reversible shift of the emission maximum to longer wavelengths with a large increase in fluorescence. This spectral change monitors the reversible unfolding of the molecule, previously suggested by tyrosine difference spectroscopy (Uyeda & Peisach, Biochem. (1981) 20:2028). These studies suggest: (1) intact myoglobins exhibit intrinsic fluorescence; (2) tyrosine residues contribute to the observed emission of these tryptophan-containing proteins ("Class B proteins"); (3) a general unfolding is observed upon titration since the emission maximum shifts with either 280 nm or 296 nm excitation (the latter excites tryptophan only).

(Supported in part by the New York Heart Association J. Fred Weintz Investigatorship for Research and NIH Grant #HL-21016.)

W-PM-E3 THE STRUCTURES OF THE FERRYL ION COMPLEXES OF MYOGLOBIN AND PEROXIDASE HIGHLIGHT SOME OF THEIR FUNCTIONAL DIFFERENCES, Chance,M.(1),Powers,L.(2),Kumar, C.(1),& Chance,B.(1), 1)Dept. of Biochem. and Biophy.,Univ. of Penn. & ISFS, Phila. Pa., 2)ATT Bell Laboratories,Murray Hill, N.J.

Although all hemeproteins have peroxidase activity, myoglobin forms a stable intermediate upon reaction with H_2O_2. Chance and Powers et.al.,in a recent paper (Arch, Biochem.&Biophy.,in press),have proposed specific structures for the intermediates of the horse radish peroxidase reaction. We have studied myoglobin peroxide by X-ray absorption spectroscopy,in order to compare its structure with those of the hrp intermediates. Both hrp and myoglobin form ferryl ion type intermediates with a short Fe-O bond upon reaction with H_2O_2 however, the iron-pyrrole nitrogen(Fe-Np) and the proximal histidine(Fe-Ne)distances are quite different. Myoglobin peroxide has a contracted Fe-Np compared to Compound I of hrp while its Fe-Ne distance is longer. Examination of other chemically similar peroxidase and myoglobin compounds reveals structural classes,called aquo,peroxy, and oxy. Each have similar spin states,Fe-Np distances,and axial ligands. But, each,with the exception of Com. II of hrp,have Fe-Ne distances characteristic of peroxidases or myoglobins. The myoglobin compounds have a Fe-Ne distance of 2.10 +/- .04Å while the peroxidase compounds have a shorter bond at 1.93 +/-.05Å. The differences in the structures of myoglobin and the peroxidase compounds reflects some of the functional differences between oxygen carriers and heme enzymes.

W-PM-E4 PEROXIDE COMPOUNDS OF CYTOCHROME OXIDASE AND PEROXIDASES B. Chance. Naqui. A., Kumar. C., Inst. Struc. & Functional Studies, Univ. City Sci. Ctr., and Dept. Biochem. Biophys., Univ. of Penna., Phila., PA 19104; L. Powers, Y. Ching AT&T Bell Labs, Murray Hill, NJ 07974

X-ray absorption spectroscopy of the intermediate compounds of peroxidase and H_2O_2 has revealed structural features which are characteristic of the π cation radical combined with the ferryl ion (Compound I) and the ferryl ion only (Compound II) in the case of horseradish peroxidase. The optical and structural properties of these compounds can be compared with three peroxide compounds of cytochrome oxidase: a) the reaction product of the unbridged or pulsed form with H_2O_2 (absorption maximum at 428 nm) (pulsed oxidase peroxide); b) Compound B_2 as formed from the reaction of reduced cytochrome oxidase CO with oxygen in a photolysis procedure at low temperatures (triple trapping), and c) Compound C, similar to B_2 but formed from the mixed valence state. The diagnostic criterion employed here is the X-ray (EXAFS) evidence for an oxygen atom in the second shell, characteristic of the Compounds I and II and found there to be at a distance of 1.64 and 1.93 Å ± 0.02 Å, respectively (1). In the case of the pulsed peroxide compound, X-ray absorption spectroscopy indicate that the iron oxygen bond length is 1.70 Å (2). In the case of Compound C, the copper edge data is identical to that of (b) while the Cu edge data of Compounds B, differs (2). Optical data indicate that (a) is red shifted 8 nm with respect to the unligated form (420 nm). These data would classify the compound (a) in the general category of lacking a π cation radical but having a ferryl ion configuration (2). (1) Chance, B. et al(1984) Arch.Biochem.Biophys.235:In press. (2) Powers,L. & Chance, B, 3rd Intl.EXASF (1984). Partial support by NIH Grants HL 31909, GM 33165, GM 31992 & RR 01633 and SSRL Proj. 632B supported by NSF through DMR & NIH through Biotech.Res.Prog. in DRR DOE.

W-PM-E5 "HEME-PROTEIN DYNAMICS IN CYTOCHROME OXIDASE: A TRANSIENT RAMAN STUDY OF CARBONMONOXIDE PHOTOLYSIS FROM CYTOCHROME $\underline{a_3}$". E. W. Findsen and M. R. Ondrias, Department of Chemistry, University of New Mexico, Albuquerque, NM 87131.

Transient resonance Raman spectroscopy provides a highly specific probe of the dynamic interactions between the heme active site and the protein matrix in heme proteins and has recently been applied to hemoglobins and myoglobins. In this study we extend the application of this technique to mammalian cytochrome oxidase. The dynamics of the cytochrome $\underline{a_3}$ site subsequent to carbonmonoxide photolysis by 10 nsec wide blue laser pulses have been probed. We find that the Fe-His mode of the transient species is dramatically shifted from its steady-state value (213 cm^{-1}) to higher frequency (222 cm^{-1}). This is analogous to the behavior of photolytic transients of hemoglobin and myoglobin and may represent a generic response of the proximal heme pocket in heme proteins. In contrast to hemoglobin and myoglobin, cytochrome oxidase transients display only negligible shifts (<1 cm^{-1}) in the electron density sensitive mode, ν_4. The dynamic behavior of the heme $\underline{a_3}$ pocket was found to be dependent upon both pH and the redox state of cytochrome $\underline{a}$. These results will be discussed in the context of the relationship between functional and dynamic behavior of the ligand binding sites in hemoglobins and cytochrome oxidase.

W-PM-E6 CYTOCHROME OXIDASE FROM BEEF HEART AND THERMOPHILIC BACTERIUM PS3: A COMPARISON OF LOW TEMPERATURE INTERMEDIATES AND RESTING TO PULSED TRANSITION. A. Naqui, N. Sone, C. Kumar & B. Chance; Dept. of Biochem. & Biophys., Univ. of Penna. & Inst. Struc. Functional Studies, Phila., PA 19104 & Dept. Biochem., Jichi Medical School Japan 329-04.

Recent interest in bacterial terminal oxidases of aa_3 type has been triggered by the fact that the bacterial cytochrome oxidases have remarkable resemblance to mammalian oxidase but appear to have much simpler subunit composition. We have studied the reactions of O_2 and CO with terminal oxidase from thermophilic bacterium PS3 using the triple trapping method of Chance et al. (1975). The CO recombination at the temperature range studied (-50°C to -80°C) followed first order kinetics with an activation energy of 7 kcal/mole. In the presence of O_2, at -113°C, the photolyzed reduced form binds O_2 to form an "oxy" intermediate similar to compound A. At a higher temperature (-97°C) another intermediate similar to compound B is formed as a result of electron transfer from the enzyme to liganded O_2. The PS3 oxidase also showed resting to pulsed transition. Upon pulsing the cytochrome c oxidation rate increased over 10 fold. Small changes in the optical spectrum were observed for resting to pulsed transition and for H_2O_2 ligation to the pulsed enzyme. The EPR spectra of the resting PS3 oxidase was very similar to mitochondrial enzyme. But the transient g=5, 1.78, 1.69 EPR signal associated with the pulsed beef heart oxidase was not observed in the case of pulsed PS3 oxidase. (1) Chance, B., Saronio, C. & Leigh. J.S. (1975) J. Biol. Chem. 250, 9226-9237. Supported by Grants HL 31909, GM 31992 and RR 01633.

W-PM-E7 RESONANCE RAMAN STUDIES OF HORSERADISH PEROXIDASE, OBSERVATION OF THE Fe(IV)=O GROUP OF COMPOUND II. Catherine M. Reczek, Andrew J. Sitter, and James Terner, Dept. of Chemistry, Virginia Commonwealth University, Richmond, VA 23284

Horseradish peroxidase is a member of an important class of heme proteins which undergo oxidation of the heme to states above iron(III). Upon reaction with peroxide and substrate, the enzyme forms two sequential intermediates known as compounds I and II which are respectively two and one oxidation equivalents above the resting enzyme. We have recently investigated the heme stucture of compound II. Though compound II is photolabile we have been able to obtain high quality resonance Raman spectra. We have found a resonance Raman band at 779 cm^{-1} in the resonance Raman spectrum of horseradish peroxidase isoenzyme A-1 which shifts to 743 cm^{-1} upon oxygen-18 substitution. We find the same band at 775 cm^{-1} shifting to 745 cm^{-1} upon oxygen-18 substitution for horseradish peroxidase isoenzymes B and C. Since these bands are very weak and overlap with other bands, the small differences in frequencies observed for the two sets of isoenzymes can not be said to be significant. This frequency is too high for a single bond iron-oxygen frequency and is in the region expected for oxygen-metal double bonds. Thus we have made a direct observation of the Fe(IV)=O group of horseradish peroxidase compound II. Compound X (Shahangian and Hager, J. Biol. Chem. 257, 11529-11553 (1982)) has also been suggested to contain an Fe(IV) heme. A band at 787 cm^{-1} appears in the resonance Raman spectrum of compound X and is a strong candidate for an Fe(IV)=O vibration.

Support is acknowledged from Research Corporation, the Petroleum Research Fund as administered by the American Chemical Society, and the Jeffress Memorial Trust.

W-PM-E8 OBSERVATION OF THE Fe(IV)=O VIBRATION OF THE MYOGLOBIN-HYDROGEN PEROXIDE COMPLEX BY RESONANCE RAMAN SPECTROSCOPY. Andrew J. Sitter, Catherine M. Reczek, and James Terner, Dept. of Chemistry, Virginia Commonwealth University, Richmond, VA 23284

Ferric myoglobin is known to react with hydrogen peroxide to form a heme with the iron in the +4 oxidation state, similar to what is found in compound II of various peroxidases. Several proposals have been made regarding the coordination of the iron in this state. These include Fe(IV)=O, Fe(IV)-OH, and Fe(IV)-OOH. We have formed the myoglobin-hydrogen peroxide complex with both hydrogen peroxide of natural isotopic abundance, and oxygen-18 labelled hydrogen peroxide. A band at 797 cm^{-1} appears which is not evident in the resonance Raman spectrum of ferric myoglobin. This band is found to shift upon oxygen-18 substitution to 771 cm^{-1}. These frequencies are only slightly higher than what we have previously observed for the Fe(IV)=O group of horseradish peroxidase compound II. Thus we have been able to directly identify the Fe(IV)=O group in the myoglobin-hydrogen peroxide complex. The resonance Raman frequencies of the myoglobin-hydrogen peroxide complex in the region above 1300 cm^{-1} are systematically higher than the corresponding frequencies of horseradish peroxidase compound II. From these frequencies a porphyrin center to nitrogen distance can be calculated to be 0.199 nm which is significantly less than the center to nitrogen distance of 0.201 nm calculated for horseradish peroxidase compound II.

Support for this work is acknowledged from Research Corporation, the Petroleum Research Fund as administered by the American Chemical Society, and the Jeffress Memorial Trust.

W-PM-E9 CARBON MONOXIDE BINDING TO RHODOSPIRILLUM MOLISCHIANUM CYTOCHROME C'. M.L. Doyle and S.J. Gill, Department of Chemistry, University of Colorado, Boulder, CO 80309.

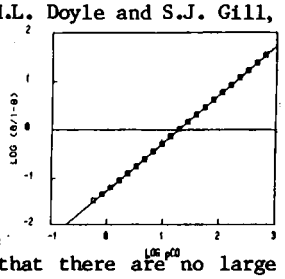

The cytochromes c' are a class of bacterial heme proteins whose biological functions are not known. The crystal structure of R. molischianum cytochrome c' has been solved (Weber, P.C., Biochemistry (1982) 21, 5116.) and was found to be a symmetrical dimer. The dimeric form may exist to allow allosteric communication between subunits. We have made high precision carbon monoxide binding measurements to this molecule and find that it binds CO with a complete lack of cooperativity (see adjacent Hill plot). A Bohr effect is observed and a basic group is involved which has a shift in pK from 8.3 to 7.8 upon ligation with CO. There is also a small change in CO affinity at neutral pH in the presence of phosphate. Overall, we conclude that there are no large changes in quarternary structure associated with CO ligation for this molecule. Earlier studies on the CO binding reaction of other cytochromes c' indicated an unusual stoichiometry of two moles CO per mole heme (Gusanovich and Gibson, J. Biol. Chem. (1973) 248, 822.) with only one of the two eliciting a spectral response. A van't Hoff enthalpy from the temperature dependence of the binding constant, measured by spectrophotometry, is compared with the enthalpy measured by direct calorimetry. Calorimetry yields the enthalpy per mole of heme reacted with CO. The spectrophotometric procedure yields the enthalpy per mole of CO. If the two procedures yield the same value of enthalpy, then the stoichiometry of the reaction is one CO per heme. The enthalpy change determined by the van't Hoff method (-11 kcal/mole CO(aq)) agrees within experimental error with the enthalpy change measured calorimetrically (-9 kcal/mol heme). Thus, the stoichiometry of binding CO to R. molischianum cytochrome c' is one mole CO per mole heme. (Supported by NIH grant HL 22325.)

W-PM-E10 CYTOCHROME b-561 CATALYZED ELECTRON TRANSFER REACTIONS IN CHROMAFFIN VESICLES. Patrick M. Kelley and David Njus (Intr. by R.S.Stephenson). Dept. of Biological Sciences, Wayne State Univ. Detroit, MI 48202

Cytochrome b-561, a membrane protein found in both adrenal medullary chromaffin vesicles and posterior pituitary secretory vesicles, may be responsible for maintaining intravesicular ascorbate by transferring electrons from a cytosolic donor to intravesicular semidehydroascorbate. Semidehydroascorbate, formed because intravesicular enzymes use ascorbate as a one-electron donor, is thus reduced back to ascorbate. A good assay for electron transfer across these vesicle membranes is the reduction of an externally added oxidant, such as ferricyanide or ferricytochrome c, by ascorbate-loaded vesicles. Although this outward electron transfer is in the opposite direction as the in vivo electron flow, it provides an important functional assay for a physiologically significant activity. To fully characterize this assay in chromaffin-vesicle ghosts, we have analyzed the kinetics of cytochrome b-561-dependent cytochrome c reduction at a variety of internal ascorbate and external cytochrome c concentrations. The rate constant for the reaction between internal ascorbate and cytochrome b-561, k_0, is 1.4×10^{-3} mg/ml min. regardless of the internal ascorbate concentration. The rate constant for the reaction between cytochrome b-561 and cytochrome c, k_1, is 0.8 mg/ml min. Ascorbate-loaded chromaffin-vesicle ghosts reduce ferricyanide much more rapidly than they reduce ferricytochrome c. As expected, if ferricyanide is used as the electron acceptor, k_0 is unchanged but k_1 is larger. Supported by NIH grant GM-30500.

W-PM-E11 EFFECT OF VINYLS OF PROTOPORPHYRIN ON FRONTIER ORBITAL ENERGIES AND ELECTRON-ELECTRON REPULSION* J. A. Shelnutt, Sandia National Laboratories Albuquerque, NM 87185

The influence of peripheral substituents on the porphyrin ring is investigated by comparing MO energies and electron-electron repulsion (configuration interaction) energies for metal protoporphyrin IX (ProtoP^{2-}), -porphine (P), -meso-tetraphenylporphyrin, -octaethylporphyrin, and -uroporphyrin I. The MO energies and CI energy for each porphyrin are obtained by using a new theoretical method to evaluate systematic differences in the uv-visible absorption spectra. Level shifts and CI energies found characterize each porphyrin's interaction with its substituents. The main effect of alkyl substituents is to destabilize top-filled π orbitals; the effect on the lowest empty π^* orbital is less. Destabilization of the π orbitals depends on the substituents' inductive ability. Destabilization is caused by conjugation with a filled p orbital of the substituent α carbons. Further, conjugation delocalizes charge from frontier MO's onto the α-carbons. Because the electrons occupy increased volume with increasing electron withdrawing ability, the CI energy is predicted to, and does, decrease as the π level increases. Vinyls are mildly electron withdrawing, and, consequently, ProtoP^{2-} shows a larger than predicted π orbital shift and a small CI energy. Both findings are consistent with slightly enhanced conjugation with the unsaturated vinyls compared with other alkyl substituents. Porphine is anomalous because it lacks substituent carbons and their conjugating orbitals. The CI energy for P is high and the MO energies are low. Metal conjugation also lowers the CI energy via delocalization of ring charge onto the metal.

*This work was performed at Sandia National Laboratories, Albuquerque, NM, supported by the U.S. Dept. of Energy under Contract No. DE-AC04-76DP00789.

W-PM-E12 HYDROGEN PEROXIDE INTERACTIONS WITH THE BINUCLEAR COPPER SITE OF *LIMULUS POLYPHEMUS* HEMOCYANIN. Celia Bonaventura and Joseph Bonaventura, Duke University Marine Laboratory, Beaufort, North Carolina, 28516.

One feature shared by all hemocyanins is the binuclear copper active site where oxygen is reversibly bound. We have undertaken studies of hydrogen peroxide interactions with subunits of varied hemocyanins in order to clarify the extent and significance of active-site heterogeneity between subunits. The hemocyanins of arthropods and molluscs, while similar in physiological function, have long been recognized as differing in regard to their interactions with hydrogen peroxide. We have now found that the ability of hydrogen peroxide to regenerate oxyhemocyanin from the oxidized state varies appreciably between the isolated subunits of *Limulus* hemocyanin. Subunits III and IV are diametrically opposed. Subunit III exhibits "mollusc-like" character while Subunit IV more closely resembles the "typical" arthropod hemocyanin that becomes completely oxidized in the presence of hydrogen peroxide. These results carry interesting implications with regard to active-site heterogeneity among the hemocyanins and may provide an explanation for a number of previously perplexing observations such as the incomplete removal of copper from a number of hemocyanins that accompanies treatment with mercury.

W-PM-F1 ELECTRICAL ACTIVITY OF TWO TYPES OF MULTIPLY INNERVATED FIBERS IN RAT EXTRAOCULAR MUSCLES. J. Jacoby, E. Stefani[§] and D.J. Chiarandini, Depts. Ophth. and Physiol. and Biophys., NYU Medical Ctr., New York, NY 10016 and [§]Dept. Physiol., Ctr. for Adv. Studies, I.P.N., Mexico D.F. 14

Mammalian extraocular muscles are composed of singly and multiply innervated muscle fibers (SIFs and MIFs) intermingled in two layers: global and orbital. Global MIFs (GMIFs, diam. 15-25 μ) generate tonic tension and lack action potentials (APs). On nerve stimulation they give graded responses or slow peak potentials (SPPs). The contractile properties of orbital MIFs (OMIFs, diam. 3-15 μ) are unknown. In the inferior rectus muscle of the rat the nerve threshold of OMIFs, 0.15-3V ($\bar{x}$=0.6V), falls within the same range as that of SIFs. In contrast, the threshold of GMIFs is higher, range 3-10V. The mean membrane time constant for OMIFs is 10 msec, shorter than in GMIFs (80 msec), but longer than in SIFs (4 msec). Input resistance also differs. The mean in OMIFs is 14.5 MΩ (range 9-26) lower than in GMIFs (21.5 MΩ, range 11-36) and higher than in SIFs (7.3 MΩ, range 0.5-17). Nerve stimulation of OMIFs evokes compound epps and small amplitude spiking responses whose presence and features depend on the location of the recording electrode. These spiking responses are accompanied by a complex right-hand shoulder consisting of a large fast rising epp with a small peak. APs were also recorded in some OMIFs, primarily near the endplate zone. In GMIFs, nerve stimulation evokes SPPs but not APs. Small amplitude spiking responses of OMIFs are faster than SPPs (10-30 V/S vs 1-8 V/S), and they exhibit to a limited degree the graded characteristics of the SPP. These differences indicate that GMIFs and OMIFs constitute two functionally distinct classes of MIFs and that OMIFs appear to have properties intermediate between those of SIFs and GMIFs. Supported by USPHS EY01297, EY07009, NSF INT 7920212 and CONACyT 790022.

W-PM-F2 EXTRACELLULAR CALCIUM TRANSIENTS AT SINGLE EXCITATIONS IN RABBIT ATRIUM. Donald W. Hilgemann, Department of Physiology, UCLA, Los Angeles, CA, 90025.

Tetramethylmurexide (2 mM) was applied extracellularly in superfused left rabbit atrial strips (0.4 to 0.7 mm) selected for homogeneity. Fiber optics were used to illuminate a 2 mm patch of muscle, collect and split transmitted light for simultaneous measurement of 3 wavelengths (usually 680, 470 and 580 nm). With 100 to 200 μM total calcium (60 to 120 μM Ca^{2+}) the extracellular calcium transient could be resolved routinely from the motion artifact signal component after signal averaging. In order to test for wavelength-dependence of the motion signals and validity of scaling procedures, the dye-containing bath solution was buffered to the same pCa with 25 mM citrate, markedly reducing the calcium-dependent signal but preserving inherent optical complexities. The figure shows typical Ca-transient, Ca-independent motion artifact (680 nm) and action potential during 0.4 Hz stimulation. Ca depletion reaches maximum rate within 4 ms of upstroke; maximum depletion is achieved within 20 ms and is about 0.3% of total Ca; replenishment begins early during rising contraction. The rapid repolarization of this preparation at low frequencies is followed by a late low-level AP phase, which correlates with net calcium efflux, being enhanced at potentiated post-stimulatory excitations and being abolished by 0.1 μM ryanodine. After ryanodine, depletion continues undiminished for 200 ms if repolarization is prevented by 4-aminopyrydine.

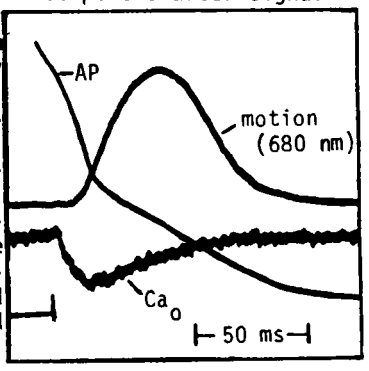

W-PM-F3 TENSION-VOLTAGE RELATIONSHIPS OF SINGLE FROG CARDIAC CELLS. M. Tarr, J.W. Trank, and K.K. Goertz.* Physiology Dept., Univ. of Kansas College of Health Sciences and Hospital, Kansas City, KS 66103.

Voltage clamp experiments were performed on single isolated frog atrial cells to determine the dependency of the contractile response on membrane potential. Preliminary experiments indicate that the contractile response associated with a stepwise change in membrane potential depends on the membrane potential stepped to. At membrane potentials negative to about +20 mv, the contractile response activates rapidly; full activation occurs with a pulse duration of about 500 msec. In this voltage region the tension response is phasic in nature in that the tension is not maintained when the potential is held at the depolarized potential. The magnitude of this phasic tension response correlates with the magnitude of the slow inward current. In contrast, at potentials positive to +20 mv the tension response activates slowly with the onset of tension development beginning after a delay of several hundred milliseconds. In this voltage region the tension response is more tonic in nature with the tension continuing for the duration of the membrane depolarizations. The magnitude of the tonic tension response increases with membrane depolarizations above +20 mv and is not correlated with the magnitude of the slow inward current. The phasic and tonic tension components of the tension response of the single cardiac cell are in some respect similar to those which have been reported from studies on multicellular frog atrial preparations. However, the voltage dependency of the tonic tension component in the isolated cell appears to be shifted significantly to more depolarized potentials than that found in multicellular preparations. (Supported by a Grant-in-Aid from the American Heart Association.)

W-PM-F4 CONTRACTILE INACTIVATION WITHOUT ACTIVATION. Carlo Caputo and Pura Bolaños. Laboratorio de Biofísica del Músculo. Centro de Biofísica y Bioquímica. IVIC Apartado 1827 CARACAS VENEZUELA.
Short muscle fibers (≤1.5 mm) of Rana pipiens can be voltage clamped with a two microelectrodes technique (holding potential = -100 mV), in the presence of TTX (300 nM).
Subthreshold conditioning depolarizing prepulses affect the contractile responses to prolonged test depolarization to -0 mV. Depending on the magnitude and duration of the conditioning pulse, the response is affected showing first a marked reduction of its time course, followed by a decrease in its peak tension. Occasionally the response to the test depolarization can be almost totally abolished; however it is difficult to abolish it completely without tension development in response to the conditioning pulse. When conditioning depolarizing ramps are used, with slopes greater than 0.2 mV/sec, partially inactivated contractile responses can be obtained, when a threshold value between -50 to -30 mV is reached. Using conditioning depolarizing ramps, with slopes $\leq$ 0.1 mV/sec it is possible to inactivate contraction without ever activating it, in a reversible way. When the fibre membrane potential is brought slowly to values of -30 to -20 mV, test pulses which bring the membrane potential to values up to + 100 mV, are ineffective in eliciting contractile responses. In the presence of D-600, 50 μM, ramps with slopes between 0.4 to 1 mV/sec are also effective in producing complete inactivation showing that this drug facilitates contractile inactivation.
(Supported by CONICIT, Fund S1-1148)

W-PM-F5 SKELETAL MUSCLE EXCITATION-CONTRACTION COUPLING: EVIDENCE FOR Ca^{2+}-DEPENDENCE IN TT:SR TRANSDUCTION. Sue K. Donaldson and Daniel A. Huetteman. Dept. of Physiology, School of Medicine; School of Nursing; University of Minnesota, Minneapolis, Minnesota, 55455.

The peeled mammalian skeletal muscle fiber preparation (sarcolemma mechanically removed) was used to distinguish and manipulate various steps in the excitation-contraction coupling process. Single rabbit adductor magnus fibers were peeled in a solution mimicking sarcoplasmic ionic conditions of relaxed muscle except that 70 mM Na^+ plus 60 mM imidazole$^+$ replaced K^+, propionate was the major anion, and 50 μM EGTA was added to reduce calcium activity. Fibers peeled under these conditions appear to have sealed, polarized tranverse tubules (TT's) which can be stimulated via ionic depolarization (with Cl^-) to trigger Ca^{2+} release from sarcoplasmic reticulum (SR); SR depolarization does not appear to be involved in Cl^--induced Ca^{2+} release. Ionic depolarization was accomplished by abrupt substitution of choline$^+$ for K^+, and Cl^- for propionate$^-$, at constant $[K^+]x[Cl^-]$ in the bathing solutions. In this study we found that when peeled fibers were loaded with Ca^{2+} in a solution containing pCa 5.6 and 4 mM total EGTA, they released Ca^{2+} in response to both ionic depolarization (Cl^--induced) and 10 mM caffeine (Ca^{2+}-induced). However, when the same fibers were loaded with Sr^{2+} at pSr 5.6 and 4 mM total EGTA, they released Sr^{2+} only in response to caffeine stimulation. Sr^{2+} substitution for Ca^{2+} in the caffeine contracture was verified by demonstrating a decline in ^{45}Ca release during maintained caffeine contractures with Sr^{2+} loading. Thus, under the fiber loading conditions used in this study, Sr^{2+} replaced Ca^{2+} in the Ca^{2+}-induced but not the Cl^--induced mechanism of SR release, demonstrating a specific role for Ca^{2+} in TT:SR transduction. Supported by NIH grant AM 35132.

W-PM-F6 PERMEANT CATION DISTRIBUTION IN SKINNED MUSCLE FIBERS. Elizabeth W. Stephenson, Dept. of Physiology, UMDNJ-NJ Medical School, Newark, NJ 07103

Stimulation of Ca^{2+}-dependent ^{45}Ca efflux from skinned fibers by negative diffusion potentials (choline Cl replacement of K methanesulfonate (KMes) at constant KxCl) has a small Ca^{2+}-insensitive component (Biophys. J. 41:231a, 1983). The voltage change responsible for this component was explored by comparing ^{86}Rb accumulation under resting and stimulatory conditions, and after detergent treatment to collapse transmembrane gradients. The stimulatory gradients, Cl 120:2.5, should permit detection of appreciable SR potentials with a 48-fold permeant cation ratio at the maximum diffusion potential. Simultaneous uptake of ^{14}C-urea (U) + ^{3}H-deoxyglucose (DOG) or ^{14}C-U + ^{86}Rb was measured in segments of bullfrog semitendinosus fiber skinned by the Natori method in mineral oil. ^{14}C-U served as total solvent marker and ^{3}H-DOG as myofilament space solvent marker (Biophys. J. 33:152a, 1981). Isometrically mounted segments were loaded under oil in 10 ul droplets with 120 mM primary salt, imidazole, Mg, Na_2ATP, EGTA, and 40 uC ^{14}C/ml + either 80 uC ^{3}H/ml or 15-25 uC ^{86}Rb/ml and then eluted. After solvent markers alone, fibers were exposed to ^{14}C-U + ^{86}Rb in KMes or choline Cl for 2-4 min/cycle; some fibers were recycled in choline Cl after Triton-X100 treatment. The ratio (R) ^{86}Rb:^{14}C-U rose significantly from 1.12 in KMes (n=7) to 1.34 in choline Cl (n=18), but R_{Cl} remained 1.34 (n=6) after Triton treatment and thus did not reflect membrane-bounded accumulation. Triton did not decrease R_{Cl} in the same segment (Δ = +0.012 ± 0.023 (4)), even in extra studies with valinomycin to ensure ^{86}Rb equilibration (Δ = +0.002 ± 0.020 (5)). These results imply that negative diffusion potentials do not generate a substantial SR voltage gradient, and are more likely to stimulate ^{45}Ca efflux primarily by depolarization of sealed repolarized T-tubules. Supported by NIH Grant AM 30420.

W-PM-F7 USE OF AEQUORIN TO DEMONSTRATE DEPENDENCE OF CALCIUM-INDUCED RELEASE OF CALCIUM FROM THE SARCOPLASMIC RETICULUM OF A SKINNED CARDIAC CELL ON ACTIVE SARCOMERE LENGTH. A. Fabiato, Department of Physiology, Medical College of Virginia, Richmond, VA 23298.

Skinned cardiac cells from the dog ventricle were prepared by microdissection. The tension-pCa curve obtained in the presence of 10 mM total ethyleneglycol-bis(β-aminoethyl ether)-*N,N'*-tetraacetic acid (EGTA) showed an increase of sensitivity of the myofilaments to Ca^{2+} when the sarcomere length (SL) at the plateau of tonic tension was increased from 1.6 to 2.2 μm, as reported for rat ventricular skinned cells (J.Gen.Physiol. 76:15a, 1980). There was no hysteresis when step changes of [free Ca^{2+}] were applied in an increasing or decreasing manner. Simultaneous recordings of tension and aequorin bioluminescence were used to detect Ca^{2+} release from the sarcoplasmic reticulum (SR) induced by a rapid increase of [free Ca^{2+}] with a microprocessor-controlled system of microinjection-aspirations. Ca^{2+}-induced release of Ca^{2+} was elicited by an increase of [free Ca^{2+}] at the outer surface of the SR, wrapped around individual myofibrils, from pCa 7.30 to pCa 6.60 or 6.30 in the presence of 0.80 mM total EGTA, pMg 2.50, pMgATP 2.50, pH 7.10 at 22°C in ∿1 ms. Increase of SL, measured at the peak of the tension transient from 1.6 to 2.2 μm, resulted in: (1) an immediate and significant increase of the Ca^{2+} transient, which was attributed to a direct effect on the Ca^{2+}-induced release of Ca^{2+} from the SR; and (2) a slow further increase of the Ca^{2+} transient over 5 to 10 min during repeated stimulations by transient increases of [free Ca^{2+}] at regular intervals of 25 s, which was attributed to an enhancement of Ca^{2+} accumulation into the SR. Rapid release of SL during the Ca^{2+} transient failed to produce an additional Ca^{2+} release or even to slow down the descending phase of the Ca^{2+} transient. (Supported by N.I.H. grant HL19138 and A.H.A. grant 83-667)

W-PM-F8 THE INFLUENCE OF INWARD CURRENT & DEPOLARIZATION ON CONTRACTION IN INTERNALLY PERFUSED CARDIAC MUSCLE CELLS. Barry London & John Krueger, Albert Einstein Col.of Med., Bronx N.Y.

Single, enzymatically isolated guinea pig heart cells were voltage clamped using a suction micropipet technic and internally perfused with a weakly buffered pCa=7, ATP-containing solution. Contractile shortening was measured by projecting the image of one free end of the cell onto a linear photodiode array. 300 msec step depolarizations from -50 to 0 mv at 30/min caused uniform and synchronous shortening in the unattached parts of the cell. Smaller depolarizing steps only partially activated the slow inward current (I_{si}) and immediately reduced the peak velocity of shortening (V_{peak}). Larger depolarizing steps also immediately decreased both I_{si} and V_{peak}. Shortening during depolarization was nearly eliminated when depolarization exceeded +75 mv, the apparent reversal potential for Ca^{2+}; in these cases, shortening was often associated with repolarization and tail currents. Altering depolarization also caused a slower change over the course of 4-5 contractions, during which time the inward currents did not change. V_{peak} was gradually increased by depolarizations of large amplitude and/or long duration, and vice versa. This occurred even with depolarizations near the Ca^{2+} equilibrium potential (i.e., >50 mv), where inward currents are small. It is unlikely that these adjustments reflect phosphorylation or ATP availability in the internally perfused cell. These results indicate that (1) the transmembrane Ca^{2+} current, and not depolarization, triggers a graded release of intracellular Ca^{2+}, and (2) over the time course of several contractions a process related to the amplitude and duration of depolarization, and not Ca^{2+} currents, grades contraction--presumably by modulating the amount of Ca^{2+} available for release.
Supported by HL-21325, NIH T32-GM-7288, and the NYHA.

W-PM-F9 THE INCREASE IN METABOLIC RATE ASSOCIATED WITH STRETCHING IN SKELETAL MUSCLE MIGHT BE RELATED TO AN INCREMENT IN FREE $[Ca^{2+}]_i$. López, J.R., Alamo, L. and Caputo, C. Centro Biofísica y Bioquímica, IVIC, Apartado 1827, Caracas 1010A, Venezuela.

It is well known that stretching frog skeletal muscle cause a rise in its metabolic rate: Feng Effect (Feng 1932). We have measured the changes in myoplasmic free calcium concentration that occur when the muscle fibers were stretched along the descending limb of the length-tension diagram. The experiments were carried out in small bundle of semitendinosus muscle, isolated from Rana pipiens, using calcium selective micro-electrodes, containing the neutral ligand sensor resin (ETH 1001). The microelectrodes were prepared and calibrated as described previously (López et. al. Biophys. J. 43: 1-4, 1983). The striation spacing at rest was determined by the Laser diffraction technique described by Cleworth and Edman (1972). A length dependent increase of $[Ca]_i$ was found: At 2.1 μm (slack length) the $[Ca^{2+}]_i$ was 0.12 μM; elongation of the muscle to 2.4 μm, 2.6 μm, 2.8 μm, 3.0 μm, 3.2 μm, 3.4 μm and 3.6 μm induced an increase in the cytosolic free calcium concentration to 0.14 μM, 0.21 μM, 0.27 μM, 0.34 μM, 0.49 μM, and 0.86 μM respectively. Such changes were completely reversed when the muscle fibers were returned to their initial slack lengths. This results offers a direct demonstration that the increase in metabolic rate associated with stretching may be linked to an increase in intracellular free calcium concentration. Partially supported by CONICIT S1-1277, S1-1148 and the MDA of America.)

W-PM-F10 THE EFFECTS OF IODOACETATE ON MUSCLE CONTRACTION STUDIED IN SKINNED RAT FAST-TWITCH MUSCLE FIBERS. R.L. Ruff. Department of Neurology, Case Western Reserve University and Cleveland Veterans Administration Medical Center, Cleveland Ohio 44106

The study of disorders of muscle glycogenolysis and glycolysis may provide valuable insights into the interactions between the metabolic and contractile properties of skeletal muscle. The human diseases are rare, and human tissue is difficult to study physiologically, therefore a valid experimental model would be a valuable tool. Brumback et al. (Muscle & Nerve 6:52, 1983) proposed that intra-aortic injection of iodoacetate, which blocks the glycolytic enzyme glyceralde-3-phosphate dehydrogenase as an animal model for defective muscle glycolysis. This treatment produces exercise-induced, electrically silent muscle contraction and rhabdomyolysis. To determine if the effect of iodoacteate was due to altered cellular metabolism or a direct effect on the contractile proteins or sarcoplasmic reticulum, the actions of iodoacetate were studied in individual skinned fast-twitch rat muscle fibers. Iodoacetate did not cause contraction of skinned muscle fibers in relaxing solution, or alter the pCa-tension relationship. The maximum normalized tension was also not changed by iodoacetate treatment. In addition, iodoacetate did not appear to cause calcium release from the sarcoplasmic reticulum or prevent calcium accumulation by the sarcoplasmic reticulum. Consequently, iodoacetate does not appear to act directly on the myofibrillar proteins or the sarcoplasmic reticulum, and it appears that the exercise-ischemic contractures produced by iodoacetate result from an iodoacetate-induced block of muscle glycolysis which has been shown to result in depletion of intracellular ATP.

W-PM-F11 THE EFFECT OF SARCOPLASMIC RETICULUM INHIBITORS ON THE RESPONSE OF VENTRICULAR MUSCLE TO ACIDOSIS. C.H.Orchard, NIH, Baltimore, Md.

Increasing superfusate $[CO_2]$ produces a rapid decrease of developed tension in heart muscle, followed by a slow partial recovery. The initial decrease of tension is independent of changes in intracellular $[Ca^{2+}]$ while the recovery is accompanied by an increase in $[Ca^{2+}]$ (J.Physiol. (1983). 335, 555-567). The mechanisms underlying these changes have been investigated in rat papillary muscles.

Increasing superfusate $[CO_2]$ from 5 to 20% caused a monotonic decrease of intracellular pH (pH_i), monitored using H^+-selective microelectrodes. The half time of this decrease (27±4 sec, mean±S.E.M, n=6) was not significantly different from the half time of the decrease of developed tension (21± 2 sec). In the presence of the sarcoplasmic reticulum inhibitor caffeine (10 mM), increasing $[CO_2]$ still caused a monotonic decrease of pH_i, however the partial recovery of tension was abolished. Ryanodine (10 μM) also abolished the recovery of tension.

These results suggest that: i) the initial decrease of developed tension may be due to a direct effect of pH_i on the myofilaments. ii) the partial recovery of tension is due to increased Ca^{2+} release from the sarcoplasmic reticulum. Since the direct effect of acidosis on the sarcoplasmic reticulum is to decrease Ca^{2+} uptake and release (J.Physiol. (1978). 276, 233-255), it seems likely that the cell becomes Ca^{2+} loaded during acidosis. Decreasing the rate of stimulation from 0.33 to 0.2 Hz did not affect the initial decrease of tension, but slowed the rate of recovery, suggesting that at least some of the Ca^{2+} loading is due to Ca^{2+} entry due to activity.

W-PM-G1 CONFORMATION OF SPIN-LABELED MYOSIN IN THE PRESENCE OF NUCLEOTIDES AND NUCLEOTIDE ANALOGS AS DETECTED BY ELECTRON PARAMAGNETIC RESONANCE.

Vincent A. Barnett and David D. Thomas, Dept. of Biochemistry, University of Minnesota Medical School, Minneapolis, MN 55455.

We have used two nitroxide spin probes attached specifically to SH_1, the fast-reacting sulfhydryl of myosin, to monitor changes in the conformation of the myosin head in the presence and absence of nucleotides in purified myosin and in glycerinated rabbit psoas fibers. EPR spectra in the absence of nucleotides indicate that both IASL (an iodoacetamide derivative) and MSL (a maleimide derivative) are rigidly attached to the myosin head. However, the EPR spectra of IASL-labeled myosin have been shown to be sensitive to local conformational effects induced by nucleotide binding to the active site of myosin (Seidel et al., (1970), Biochemistry 9: 3265-3572) while the spectrum of MSL-labeled myosin is sensitive only to whether myosin heads are bound to or detached from actin (Thomas & Cooke, (1980), Biophys. J. 32: 873-889). At 20°C, the conventional and saturation-transfer EPR spectra of MSL-labeled fibers indicate that all myosin heads are detached from actin. Conventional EPR spectra of IASL-myosin during steady-state ATP hydrolysis indicate the presence of at least two distinct conformations in both purified myosin and in relaxed muscle fibers. Spectra taken under equilibrium conditions with ATP analogs (such as ADP $\pm$ V_i and AMP-PNP) permit the analysis of steady-state spectra in terms of individual conformational states (e.g., M*ATP, M**ADP.P_i, and M*ADP) and their relative concentrations.

W-PM-G2 ADP DOES NOT INDUCE RIGID AXIAL ROTATION OF MYOSIN HEADS IN RIGOR MUSCLE FIBERS.

David D. Thomas, Eric C. Svensson, and Carl F. Polnaszek, Dept. of Biochemistry, University of Minnesota Medical School, Minneapolis, MN 55455.

EPR spectra of nitroxide spin labels report highly resolved information about the orientation of probe axes in space. Previous studies, in collaboration with R. Cooke and M. Crowder, have shown that spin labels bound specifically to the SH1 groups on myosin heads in rabbit psoas muscle fibers in rigor have their principal axes uniformly oriented with respect to the fiber axis, and that those probes having a preferred orientation in other attached states (e.g., during force generation, or in the presence of AMPPNP or PPi or ADP) have precisely the same spectrum. This type of observation has been confirmed by a number of other probes, both spin and fluorescent. However, the preferred orientation of another SH1 probe, IATR, changes significantly when a fiber passes from rigor into force generation, and a similar change is caused by the addition of ADP to rigor (Burghardt & Boreijdo, 1984). Thus the question arises whether an unfavorable orientation of the spin label (and other probes) relative to the myosin head might have prevented their detection of a large-scale rigid head rotation in response to ADP. However, a quantitative analysis of EPR spectra, taking into account the nonaxial components of the magnetic tensors, shows that the probability is negligible that any axis of the spin label rotates by more than 10 degrees relative to the fiber axis upon the addition of ADP. Thus the myosin head does not undergo any large (10%) ADP-induced rotations as a rigid body, and evidence for the axial rotation of any other probe implies either independent rotation of the probe itself (most probable) or internal segmental rotations within myosin.

W-PM-G3 EPR STUDIES OF MUSCLE CONTRACTION AT LOW IONIC STRENGTH (IS). P. Fajer, E. Fajer, E. Svensson, N. Brunsvold, C. Wendt and D. Thomas, Dept. of Biochem., Univ. of Minnesota, Minneapolis, MN 55455, Introduced by E. Ackerman.

Characterization of the orientation and motional freedom of myosin heads in the particular states of contraction cycle is required for a full elucidation of the contraction mechanism. Under low IS (30 mM) and low temperature (T=5°C) conditions, biochemical and physiological evidence indicates that a large fraction of the myosin heads are attached to thin filaments without force generation [Yanagida et. al., J. Biochem., 90, 407-, 1982; Brenner et. al., PNAS, 79, 7288-, 1982]. This probably corresponds to the early stages of crossbridge attachment ("weakly bound crossbridges"). EPR measurments under these conditions reveal that 15-30% of the myosin heads are oriented at the same angle as in rigor, but with more disorder, consistent with weaker binding than that in the absence of ATP. Stiffness and X-ray diffraction measurements on the same fibers (in collaboration with Dr. B. Brenner) also support the above findings. The addition of Ca^{++} at low IS and low T, reveals the presence of similar crossbridges during contraction. At 20°C (low IS, no Ca^{++}) muscle tension is developed, but shortening is inhibited. EPR spectra indicate the same orientation of the myosin heads but with less disorder. Similar spectra were obtained during contraction at 24°C at physiological IS consistent with results of Cooke et. al., Nature, 300, 776-, 1982. The lack of any major reorientation of the spin-labeled region of myosin heads under conditions corresponding to different states in the contraction cycle undermines any model invoking large scale, rigid head rotation by 45° as a source of tension generation.

W-PM-G4 THE BINDING AND ORIENTATION OF A SPIN LABELED NUCLEOTIDE IN GLYCERINATED MUSCLE FIBERS. M. Crowder, M. Wilkie, and R. Cooke. Department of Biochemistry & Biophysics, and the CVRI, University of California, San Francisco, CA 94143 and IBM Instruments Inc., San Jose, CA 95110.

A spin label analogue of adenosine 5'-triphosphate (BBA 601:34,1980) has been used to probe the nucleotide site of myosin in fibers from rabbit psoas, rabbit soleus and insect flight muscle. In the rigor state, the EPR spectrum shows that bound SL-ADP is ordered with respect to the fiber axis, with a mean angle of 55° and a spread of 25°. This orientation distribution is independent of muscle types showing that the structure of the nucleotide site is highly conserved during evolution. The association constant of SL-ADP is higher for soleus muscle fibers, 1 X 10^4/M, than for insect or psoas muscle, 7 X 10^3/M. When psoas muscles are stretched beyond filament overlap, the EPR spectrum shows that bound SL-ADP has a random distribution of orientations, and the association constant is increased to 2 X 10^4/M. Addition of sodium vanadate (1mM), caused rigor muscles to relax and the EPR spectrum of bound SL-ADP underwent a transition from highly ordered to randomly distributed. These findings support the interpretation that SL-ADP is strongly immobilized on the myosin head, and that the heads are ordered when attached to actin and disordered when not attached to actin. The above results are similar to those obtained using spin labels attached to a reactive sulfhydryl on the myosin head. Preliminary experiments on soleus muscle suggest that no new angles are detected for myosin bound nucleotide during isometric contraction. Supported by a grant from the USPHS: AM30868.

W-PM-G5 THE CONFORMATION OF THE RIGOR CROSS-BRIDGE IS NOT ALTERED BY STRESS APPLICATION TO MUSCLE FIBERS AT LOW FILAMENT OVERLAP. A.J. BAKER and R. COOKE. Department of Biochemistry & Biophysics, and the CVRI, University of California, San Francisco, San Francisco, CA 94143.

Contraction of muscle is thought to involve a conformational change of cross-bridges when attached to actin. Several previous studies have looked for and failed to find alterations in the configuration of rigor cross-bridges due to a torque generated between the thick and thin filaments when stress is applied to fibers. However, in rigor most of the cross-bridges are attached and therefore the load per bridge during stress application will be smaller than during contraction where fewer attached bridges support the isometric force. In the present experiments the orientation of spin probes attached to rigor cross-bridges in glycerinated rabbit psoas muscle at low filament overlap has been monitored with EPR spectroscopy before and during stress application. The reduced filament overlap ensured that the loads supported by the cross-bridges remaining attached were more comparable to those experienced during contraction. The spectra of a spin labeled derivative of Maleimide which rigidly attaches to a specific site (SH_1) on the cross-bridge were unchanged by stress application to such fibers. Similar preliminary results were found using a spin labeled analogue of ATP as a probe of the nucleotide binding site region. One explanation of these results is that the domains of the cross-bridge which contain these probes is immobilized by the rigor bond whilst the more proximal portions of the myosin molecule are capable of the configurational changes which present theory envisages during contraction. A.J.B. is a California Heart Association Research Fellow. Supported by Grants from USPHS AM30868.

W-PM-G6 FORCE GENERATION IN RIGOR MUSCLE FIBERS

Brian Collett and Richard J. Podolsky, NIADDK, NIH, Bethesda, MD 20205.

Skinned muscle fibers in the rigor (ATP-free) state swell radially and generate axial force when the pH of the bathing solution is raised or the ionic strength reduced. For a given condition, at a sarcomere length of 2.4μm, the increase in fiber diameter is greater than the increase in lattice spacing, and this difference is most pronounced at large swellings (Yu et. al. in CONTRACTILE MECHANISMS IN MUSCLE Pollack & Sugi eds., Plenum, 1984). Isolated myofibrils show the same swelling behavior as whole fibers (Arata,unpublished work). It was suggested that the overlap region of the sarcomere, which produces the X-ray pattern, might expand less than other parts of the sarcomere. In that case the actin and myosin filaments would be curved rather than straight and the force would be born by cross-bridge strain. Our computer simulation of the diffraction from bent filaments showed that the amount of bending needed to explain the swelling (up to 30°) should give a large (more than 3 fold) increase in the axial width of the [1,1] equatorial reflection. We therefore used two-dimensional X-ray diffraction with a point focussed beam to look for such an increase in rabbit psoas bundles at 25°C. We found no change (0±10%) in the axial width of the [1,1] reflection even under the most extreme swelling conditions (pH8.5, 5mM total ionic strength). This suggests that expansion is homogeneous along the myofibril, but not across the myofibril, with the extra radial swelling probably appearing as voids between filament-containing regions. This in turn suggests that the rather large force seen under extreme conditions arises not from crossbridge strain but more likely from strain in the cytoskeletal elements which envelop and penetrate the myofibrils (Wang & Ramirez-Mitchell J.C.B. 96(1984), Maruyama et. al. ibid. 99(1984)).

W-PM-G7 EFFECTS OF LOW pH AND HIGH IONIC STRENGTH SOLUTIONS ON THE FILAMENT LATTICE OF VERTEBRATE STRIATED MUSCLE: IMPLICATIONS FOR FILAMENT STRUCTURE. B. M. Millman, T. C. Irving and R. M. J. Blair, Biophysics Interdeptl. Group, Physics Dept., University of Guelph, Guelph, Ont., Canada.

We have used an osmotic stress technique (Millman et al., 1983, Biophys. J. 41:259) to compare the thick filament lattice of skinned muscles from frog and rabbit: relaxed and in rigor. The technique gives a sensitive measure of the effective thick filament charge diameter, i.e. the outermost position on the thick filaments where net charge is found. When correlated with electron density maps of the lattice calculated from the equatorial X-ray diffraction patterns, the charge position can be identified with specific parts of the thick filament structure. In relaxed and rigor muscles near physiological pH and ionic strength (pH = 7; ionic strength = 0.1 M) the effective charge diameter lies somewhere near the centre of the thick filament projections. As the pH of the external solution is lowered, the lattice spacing of both relaxed and rigor muscles reaches a minimum at a pH between 5 and 4. Osmotic stress experiments at pH 5.5, where the lattice spacing is substantially smaller than at pH 7, the effective charge diameter decreases by about 10 nm to a position close to the thick filament backbone. This change appears to result from a combination of charge neutralization in the heavy meromyosin part of myosin and a collapse of the thick filament projections against the filament backbone. In contrast, increasing the ionic strength (to 0.3 M) causes only small changes in lattice spacing or in effective charge diameter at either low or normal pH. Thus, large increases in fibre diameter observed with increased ionic strength by Offer & Trinick (1983, Meat Sci. 8:245) do not appear to originate from changes in the filament lattice spacing.

W-PM-G8 EVIDENCE FOR A RADIAL CROSSBRIDGE COMPLIANCE WITH EQUILIBRIUM POSITION AT 380Å Bernhard Brenner [+*] and Leepo C. Yu [+]. [+]NIADDK, NIH; and [*]University of Tubingen, FRG.

Recently equatorial X-ray diffraction showed that lattice spacing, d_{10}, of single skinned psoas fibers decreased with increasing isometric force at ionic strength μ=170 mM, 5°C and pH 7.0 (Brenner & Yu, Biophys. J., 1982). This suggested that there is a radial component in force generation. The decrease in d_{10} leveled off at 380Å±2Å when force was >80% of the maximal level at 5°C. We have since found that upon increasing isometric force another 30% by raising temperature to 10°C, d_{10} remains at 380Å. Since preliminary X-ray diffraction and stiffness measurements indicate that this increase in force is probably due to an increase in the number of force generating crossbridges, this implies that the lack of further decrease in d_{10} is due to either (a) a non-crossbridge lattice component resisting further change, or (b) the radial force per crossbridge becoming negligible at 380Å. To distinguish these two possibilities, 0-7% of dextran T500 were applied to relaxed fibers at μ=170mM. d_{10} decreased from 440Å to 310Å as a linear function of dextran concentration. Since few crossbridges are probably attached under this condition, this shows that the lattice component exhibits an approximately linear compliance around 380Å, thus ruling out possibility (a). Experiments further show that compressing fibers under relaxing, activating and rigor conditions, d_{10} again decreases linearly as a function of dextran concentration. However, the slopes, hence compliance, appear to be inversely proportional to the number of attached crossbridges. The simplest explanation for the results is that there is a radial compliance in the attached crossbridges. In addition, since fibers under rigor and relaxing (at low μ) conditions approached the same minimum value of 380Å (Brenner, et al., Biophys. J. 1984), the equilibrium position appears to be independent of crossbridge state and axial force. These findings place constraints on models of crossbridge geometry and function.

W-PM-G9 SARCOMERE LENGTH UNIFORMITY DETERMINED FROM THREE DIMENSIONAL RECONSTRUCTIONS OF RESTING ISOLATED HEART CELL STRIATION PATTERNS. Kenneth P. Roos and Allan J. Brady. Department of Physiology, UCLA School of Medicine, Los Angeles, Ca. 90024.

Discrete sarcomere lengths have been obtained and three dimensionally reconstructed by computer from the volumes of resting unattached calcium tolerant isolated cardiac cells. These enzymatically digested adult cells (avg. 120 µm long X 25 µm dia.) manifest clear A- and I-band striation patterns and remain quiescent in physiological levels of $[Ca^{2+}]_o$ unless electrically stimulated. Optically discrete subvolumes (86 µm long X .053 µm wide X 1.6 µm thick) are imaged along the length of a cell with a high resolution (.05 µm) computer coupled optical microscope imaging system (Roos and Brady, Biophys. J. 40:233-244, 1982). Planar striation maps are obtained at a given focal plane from sequential image scans displaced laterally across the width of the cell in controlled steps (.34 µm, .82 µm, or 1.01 µm). Multiple planar maps are obtained from regularly spaced (2.5 µm, or 3.0 µm) focal planes throughout the depth of the cell to provide complete striation position data arrays. These matrix arrays have been reconstructed three dimensionally to illustrate the volumetric sarcomere structural uniformity. Rigorous statistical analysis of volumetric sub-regions of cells indicate a remarkable overall sarcomere length uniformity within a given cell. However, 4 of the 7 cells examined had small regions of statistically different sarcomere lengths which were longitudinally in series with one or both of the cell's nuclei. These data suggest that the uniformity of sarcomere lengths within an unloaded isolated cell is the result of the discrete sarcomere length-tension relationship modified longitudinally in certain regions by non-contractile organelles such as the nuclei. (Supported by USPHS HL29671 and HL30828).

W-PM-G10 LASER LIGHT DIFFRACTION IN SINGLE SKINNED RABBIT PSOAS FIBERS. THE NATURE OF THE SUBSTRUCTURE WITHIN DIFFRACTION LINES. Bernhard Brenner. University of Tübingen, FRG.

Light micrographs of single skeletal muscle fibers show that striation patterns are organized in domains defined by striation tilt and sarcomere length (SL). Since SL can vary significantly from domain to domain, a representative group of domains has to be monitored when using light diffraction to measure SL. A convenient way would be to monitor position and movement of individual substructural lines within the first order diffraction line. Rüdel and Zite-Ferenczy (Nature 1979, Biophys. J. 1984) suggested that the domain organization gives rise to this substructure, with each substructural line representing a single domain. The present results, however, suggest a different origin of the substructure: The 'splitting' of the diffraction lines most likely is the result of interference between various domains. When a fiber segment is illuminated successively by means of a movable slit, illuminating one small fraction of the segment at a time, and then summing the resulting diffraction patterns photographically, substructure within diffraction lines is almost absent. Hence, the substructured diffraction line is not simply the sum of the diffraction lines originating from the subsegments. Rather, interference modulates the diffraction lines. The effect of interference between different fiber areas is demonstrated by illuminating two areas simultaneously. The resulting diffraction pattern when compared to the two individual patterns shows additional meridional splitting of the diffraction lines. The separation of these lines is inversely proportional to the distance between the center of the two illuminated areas. These findings suggest that substructure within the diffraction lines is mostly the result of interference between different domains. Therefore, there is no direct correlation between substructural lines and domains; i.e., the substructure cannot be used to determine the sarcomere length of individual domains. Work is supported by: DFG Br 849/1-1.

W-PM-G11 MICROSTRUCTURE IN NEAR-FIELD AND FAR-FIELD LASER DIFFRACTION PATTERNS OF MUSCLE FIBERS. C. L. Sundell[1] Y. E. Goldman[2], and L. D. Peachey[1]. Departments of Biology[1] and Physiology[2], University of Pennsylvania, Philadelphia, PA 19104.

The source of fine structural lines (microstructure) in the optical diffraction patterns of single muscle fibers was investigated by translating a fiber through a fixed laser beam and by masking the beam to reduce the illuminated area. If the diffracting elements leading to the microstructure are localized, then as the fiber is translated longitudinally, the fine structural lines should move in the near-field pattern but not in the far field. Glycerol-extracted single fibers from rabbit psoas muscle were illuminated with HeNe laser light. During fiber translation, fine structural lines in the near-field pattern (corrected for laser beam divergence) moved in the corresponding direction 99% ± 3% (s.e.m., n=8) of fiber movement. When the pattern was converted to far-field diffraction with a 25 cm lens, movement of the fine structural lines was not significantly different from zero. Masking the laser beam most often caused fine structural lines in the near- and far-field diffraction patterns to decrease in intensity, but sometimes the intensity of peaks increased or troughs in the diffraction patterns disappeared. These results indicate that microstructural features of the diffraction pattern arise from localized regions within the muscle fiber. The results are consistent with these regions being relatively uniform and contiguous domains of myofibrils and striations. Some constructive or destructive cross-interference between light scattered by different domains explains the occasional intensity increases as the illuminated region was successively reduced. Support: GM7229 (C.L.S.), HL15835 (L.D.P. and Y.E.G), MDA (H.M. Watts Research Center (L.D.P)), AM00745, AM26846 (Y.E.G.).

W-PM-H1 THE PSYCHOTOMIMETIC ACTIVITY OF PHENCYCLIDINES MAY BE MEDIATED BY BLOCKADE OF SPECIFIC PRESYNAPTIC K CHANNELS. D.K. Bartschat and M.P. Blaustein, Dept. of Physiol., Univ. Maryland Sch. Med., Baltimore MD 21201.

Phencyclidine (PCP), a drug of abuse, produces schizophrenia-like symptoms in man. While the mechanism of PCP's action is unknown, altered central synaptic transmission secondary to enhanced neurotransmitter release appears to be involved. To assess whether PCP affects presynaptic K channels, Rb efflux from ^{86}Rb-loaded rat brain synaptosomes was used to measure the K permeability of the plasma membrane under "resting" (5 mM $[K]_o$) and depolarized (elevated $[K]_o$) conditions. Four distinct K conductances were observed (J. Physiol., in press): A "resting" K permeability ("R"); a quinine and TEA sensitive Ca-activated K channel ("C"); a TEA and 4-AP sensitive voltage-regulated, inactivating K channel ("T"); and a depolarization-stimulated component of Rb efflux ("S") which receives a contribution from "R" (due to the increased driving force for Rb efflux) and a contribution from a voltage-regulated, non-inactivating K channel ("S_V"). PCP selectively and potently blocked S_V (K_I = 1 - 5 μM); R, T, and C were blocked only by >20-50 fold higher concentrations. The PCP-like analogues TCP (see Fig.), m-NH_2-PCP, and m-NO_2-PCP also selectively blocked S_V with the same rank order of potency as for their behavioral effects. Block of presynaptic K channels should prolong action potentials, increase Ca influx, and enhance transmitter release. Thus, our results provide an explanation for the mechanism of action of PCP, and may give new insight into the pathophysiology of mental disorders such as schizophrenia. Supported by NS-16106.

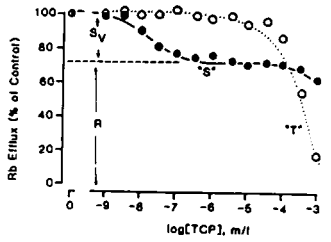

W-PM-H2 THE RAT BRAIN PHENCYCLIDINE RECEPTOR IS A K CHANNEL. R.G. Sorensen & M.P. Blaustein (Spon.: A.S. Hobbs), Dept. of Physiol., Univ. Maryland Sch. Med., Baltimore, MD 21201.

Phencyclidine (PCP, "angel dust") causes schizophrenia-like behavior that may be due to its block of voltage-regulated K channels in the CNS. Here we present biochemical data which support the hypothesis that the rat brain PCP receptor is a K channel. PCP and its analogs, NH_2-PCP and TCP, bind to two sites in synaptic membranes prepared from rat forebrain: A high affinity site (K_D <0.5μM) and a low affinity site (K_D >2μM). The affinities of several PCP analogs for the high affinity binding site, TCP >NH_2-PCP>PCP>PCPY>>NO_2-PCP, correlate well with their behavioral potencies and their ability to block certain K channels in rat brain synaptosomes (preceeding abstract). Substances specific for various receptors were tested for their ability to interact with the brain PCP receptor. No Na or Ca channel or Ca-activated K channel agonist or antagonist tested affected ^{3}H-PCP binding. However, certain K channel blockers, the aminopyridines and tetra alkyl ammonium ions, but not capsaicin, and several non-competitive blockers of the nicotinic acetylcholine receptor (nAChR), amantadine, quinacrine and perhydrohistrionicotoxin, competed with ^{3}H-PCP for the PCP receptor. The rank order of potency and K_I values of the K channel blockers for binding to the PCP receptor were similar to their potency for block of a voltage-regulated, Ca-independent voltage-regulated Rb efflux from $^{86}Rb^+$-loaded synaptosomes (preceeding abstract). PCP and its analogs show no correlation between their affinities for binding to the nAChR and their behavioral potencies. We suggest that, in the CNS, PCP produces its behavioral effects by selective blockade of a voltage-regulated K channel. Supported by NS-16106.

W-PM-H3 POTASSIUM CHANNEL LATERAL MOBILITY AND PHOTODESTRUCTION BY ULTRAVIOLET LIGHT

Richard E. Weiss, William M. Roberts, Walter Stühmer and Wolfhard Almers
Department of Physiology and Biophysics, University of Washington, Seattle, WA 98195

The lateral mobility of delayed rectifier potassium channels in surface membrane of Rana temporaria muscle was studied with the patch clamp technique of Stühmer and Almers (1982, PNAS 79:946). It was found that K currents (I_K) could be destroyed by ultraviolet (UV) irradiation (using the pipette as a light guide) with the same wavelength dependence (range: 280-302 nm) as Na currents (I_{Na}), although with a sensitivity about 1/2-1/3 that of I_{Na}. With constant UV irradiation the time courses of decrease of both I_K and I_{Na} were well fit by single exponentials, suggesting that the destruction of a channel is a one-photon-hit event. The profile of K and Na current density in the region surrounding and including the irradiated spot was also measured. It was found that UV photodestruction of K and Na channels was restricted to the membrane under the patch pipette tip.

K channels were found to be relatively immobile with a diffusion coefficient (D) ≤ 5×10^{-12} cm^2/s in four successful experiments. In two of those experiments Na channel lateral mobility was also measured. Na channels were found to be less mobile, D ≤ 10^{-12} cm^2/s, in agreement with earlier findings (Stühmer and Almers, 1982). Both K and Na channels are significantly less mobile than receptors of a lectin (wheat germ agglutinin) in the same preparation for which D = 5×10^{-11} cm^2/s. The lateral mobility of the lectin receptors was not affected by high doses of UV irradiation which suggests that the relative immobility of K and Na channels is an intrinsic property and not the result of UV irradiation.

Supported by grants from the NIH (AM17803 and AM06915 to REW) and the Muscular Dystrophy Assoc.

W-PM-H4 WHY IS A CHANNEL BOTH HIGHLY SELECTIVE AND HIGHLY PERMEABLE? THE EFFECT OF PORE MOUTH CHARGE DISTRIBUTIONS. Peter C. Jordan, Department of Chemistry, Brandeis University, Waltham, MA 02254

The K channel from sarcoplasmic reticulum (SR) and the Ca activated channel from transverse tubule (TT) both exhibit high selectivity and high conductivity, properties which are apparently contradictory. The interpretation of convergence conductance measurements (Latorre and Miller, J. Membr. Biol., 71:11, 1983) suggests that the constriction radii in these channels must be roughly .25 nm (SR) and .34 nm (TT), properties inconsistent with ion specificity. I will present electrostatic model calculations assessing the consequence of various charge distributions which may be present in those parts of channel proteins that form the pore mouth. They show that reasonable charge distributions produce significant aqueous phase electrical potentials in the vicinity of the entrance to the constriction. These potentials substantially increase cation concentration in this region; three to ten-fold enrichment factors are quite plausible. If such a mechanism is operative estimates of the constriction radii in the SR and TT channels can be lowered dramatically; models can be constructed which accommodate both high selectivity and high permeability.

W-PM-H5 SINGLE CHANNEL ANALYSIS OF Ia CURRENTS FROM MAMMALIAN SENSORY NEURONS. Alvin Shrier and Ellis Cooper. Department of Physiology, McGill University, 3655 Drummond Street, Montreal, Quebec H3G 1Y6.

The objective of these experiments was to measure inactivation of Ia (fast transient K^+) current at the level of single channels. The single channels were recorded, using the intact patch clamp technique, from sensory neurons at room temperature. These neurons were dissociated from the nodose ganglia of newborn rats, and were grown in cell culture for 5 - 33 days. Ia channels could be distinguished from other K^+ channels because: (1) Ia channels are inactivated at rest; (2) they require hyperpolarization to remove inactivation; (3) a depolarizing step from a hyperpolarizing level activates the channels; (4) channels appear transiently within 100 msec after the step. The open channel conductance was ~22 pS, and was constant over most of the physiological voltage range; single channels did show inward rectification at more depolarized levels. Summing single channel currents, evoked by repeated steps to a given depolarized potential, resulted in an average current whose kinetics were similar to macroscopic Ia currents; the inactivation time course was fit with a single exponential with a time constant of ~30 msec. For the currents evoked by the large depolarizing steps to + 30 mV, the mean channel open time equals the inactivation time constant. For currents elicited at less depolarized levels, - 10 mV, the mean open time equals approximately half the inactivation time constant; this discrepancy can be explained by an increased latency to activate the channels at this level. Supported by the Medical Research Council of Canada.

W-PM-H6 SINGLE ION CHANNELS IN CULTURED HIPPOCAMPUS SHOW INWARD RECTIFICATION. J.M. Sullivan and S.A. Cohen, (Intr. by J. Wojtczak), Depts. of Physiol./Biophys. and Anesthes., Mt. Sinai Med. Ctr., New York, N.Y. 10029.

Hippocampal pyramidal neurons are known to possess a macroscopic inward rectifying potassium conductance. To probe for single ion channels responsible for this behavior, the patch clamp technique was used on neurons grown in primary dissociated cell cultures derived from 14-16 day fetal mouse hippocampus. The pyramidal-shaped neurons in this study showed mature electrophysiological properties: resting membrane potentials (RMP) 51.8±9.8mV (mean±SD) and spontaneous and stimulus evoked synaptic and action potentials. Fire-polished pipettes were filled with (mM): 140 KCl, 1 $MgCl_2$, 0.135 $CaCl_2$, 2.2 EGTA-K, 4 HEPES-K(pH 7.2). GOhm seals were obtained from the somal membranes and the cell-attached patch mode was used. Cells were bathed in (mM): 137 Tris-HCl, 1 $MgCl_2$, 1 $CaCl_2$, 10 glucose, 4 HEPES-K (pH 7.2). With no applied potential, inward currents of 4-5 pA were seen in most of the cells (>75%). The channel showed inward rectification upon applying prolonged voltage steps to the pipette. The linear region of the I-V curve was used to estimate channel conductance at ~200 pS. Conductance decreased with decreased K^+ in the pipette while holding Cl^- constant, and currents were never observed with isotonic Cs^+ replacing K^+. The steady-state probability of opening (P(o)) progressively decreased by hyperpolarizing the patch, whereas P(o) increased by depolarizing the patch. It was not possible to reverse current through the channel. Near RMP the channel exhibited complex kinetics with unitary events (10-20msec) grouped into bursts with an estimated mean duration of 250msec, consistent with macroscopic activation kinetics of inward rectification. Within single bursts a maximum of four unequal current levels was noted possibly indicating substates of conductance. This inward rectifying channel shows gating behavior and voltage dependence and is similar to one found recently in ventricular muscle but has a much higher conductance. JMS is an MSTP trainee on GM-07280.

W-PM-H7 SENSITIVITY OF A-CURRENTS IN PERFUSED APLYSIA NEURONS TO EXTRACELLULAR CALCIUM. Douglas Junge, School of Dentistry and Department of Physiology and Brain Research Institute, University of California, Los Angeles 90024.

The intracellular perfusion technique of Lee et al. (J. gen. Physiol. 71, 489-507, 1978) was used to study transient outward currents in neurons in the visceral ganglion of Aplysia californica. The A-currents in response to depolarizations from holding potentials near -90 mV were activated in the range -60 to -20 mV, below the threshold for the delayed outward current. The rising phase half-time was about 17 ms and the falling phase half-time was about 130 ms. The A-currents were abolished by external application of 4 mM 4-aminopyridine. It was also found that external application of 30 mM $CoCl_2$ in Ca-free solution reduced or blocked the currents. This probably was not due to an effect on the Ca-dependent outward current, or C-current, since this rises much more slowly than the A-current and is only activated above 0 mV (Thompson, S., J. Physiol. 265, 465-488, 1977; Eckert, R. and Tillotson, D., Science 200, 437-439, 1978). The Co-effect on the A-currents could have been caused by divalent screening of membrane fixed negative charges, shifting the activation and inactivation parameters positively along the voltage axis. If that were the case, however, increasing external calcium should have the same effect as cobalt, since all divalents should be equally effective. It was found that increasing external Ca-concentration to 30 mM increased the A-currents about 30%. Further, application of 10^{-4} M verapamil hydrochloride reduced the currents about 25%. These results suggest that A-currents in Aplysia neurons are dependent on Ca-ions entering from the external solution. Supported by USPHS grant RR05304.

W-PM-H8 PHORBOL ESTERS REDUCE VOLTAGE-DEPENDENT AND CALCIUM-ACTIVATED K^+ CURRENTS IN HERMISSENDA TYPE B PHOTORECEPTORS. J. Farley, S. Auerbach, Princeton, NJ 08544.

Hermissenda Type B photoreceptors exhibit enhanced depolarizing generator potentials and decreased membrane conductances for days following associative training of the animal. These persistent changes in B cell excitability result from training produced reductions in two K^+ currents in B cells (I_A, $I_{K\text{-}Ca}$), and enhancement of a calcium current (I_{Ca}) (Farley et al., 1984, Soc. Neur. Abstr., 10:270). Similar changes in light response and ionic currents are produced by the endogenous neurotransmitter 5-HT (Wu & Farley, 1984, Soc. Neur. Abstr., 10:620) as well as by increases in intracellular Ca^{2+} levels. We are examining the possibility that 5-HT's effects, as well as those of associative training, are initiated by the turnover of inositol phospholipids and protein kinase C activation. 1-10 nM bath applied concentrations of the tumor promotor 4β-phorbol 12β, 13α - dibutyrate (PDB), an activator of protein kinase C, produced an irreversible enhancement of the Type B cell's steady-state depolarizing light response (n=9; mean increase = 32%), and a decrease in net membrane conductance (n=8; mean increase = 41%). PDB-solvent application was without effect (n=5).

Voltage clamp analysis revealed 30-50% reductions by PDB of the fast, 4-AP-sensitive K^+ current (I_A) of B cells (n=5), and a hyperpolarizing shift of 4-6 mV in the voltage-dependence of inactivation. Isolation of the Ca^{2+}-activated K^+ current by the addition of 5-10 mM 4-AP and 100 mM TEA revealed a reduction by PDB of 20-33% (n=4) in $I_{K\text{-}Ca}$, with no obvious changes in kinetics or voltage-dependence. These results suggest that PDB, substituting for diacylglycerol, may induce protein kinase C activation effecting a reduction in I_A and $I_{K\text{-}Ca}$. (NSF BNS-8316707).

W-PM-H9 CATION SELECTIVITY AND Cs^+ BLOCKADE IN A Ca^{2+}-ACTIVATED K^+ CHANNEL FROM RABBIT INTESTINAL SMOOTH MUSCLE. D. Wolff, X. Cecchi, D. Naranjo, O. Alvarez and R. Latorre. Dept. Biology, Fac. Sciences, University of Chile, Santiago, Chile.

The conductance and selectivity of a large conductance Ca^{2+}-activated K^+ channel (CaK) was studied in planar lipid bilayer membranes. The channel was incorporated into the bilayer by fusing smooth muscle membrane vesicles. In phosphatidylethanolamine (PE) bilayers, channel conductance is a non-linear function of K^+ concentration. The conductance of the channel is 230 pS in 0.1M KCl. Furthermore conductance departs from a single-site saturation curve. Na^+, Li^+, Cs^+ do not pass through the channel and Rb^+ permeability is 60% that for K^+. Na^+, Li^+, Rb^+ block the channel. Cs^+ blocks the channel from both sides. From the cis, Ca^{2+} site side, Cs^+ blockade can be described in terms of a single-blocking site with an effective valence of 0.65 and an apparent dissociation constant of 57 mM. From the trans side the voltage dependence of the blockade is a function of Cs^+ concentration. It increases as the Cs^+ concentration increases. The effective valence is 0.4 at 0.01mM Cs^+ and 1.6 at 10mM Cs^+. The Cs^+ blockade is reinforced if the potassium concentration in the trans side is raised from 100 to 200 mM. The conductance and the blocking experiments indicate that the large CaK channel behaves as a multi-ion channel.

Supported by Univ. of Chile Grant B-1985-8523 and Fondo Nac. Investigación 1299

W-PM-H10 VOLTAGE DEPENDENT BARIUM BLOCK OF CA^{++}-ACTIVATED K^+ CHANNELS IN CULTURED RABBIT KIDNEY MEDULLARY THICK ASCENDING LIMB CELLS (MTAL). S.E. Guggino, B.A. Suarez-Isla, W. B. Guggino, N. Green, and B. Sacktor. LMA, LNS, NIA and Dept. of Physiology, Johns Hopkins University, Baltimore, MD., and LKEM, NHLBI, Bethesda, MD.

We studied the effect of Ba^{++} on the Ca^{++}-activated K^+ channel in the apical membrane of cultured MTAL cells, using the cell-attached patch clamp technique (bath and patch pipets contained in mM: 135 NaCl, 5 KCl, 1 $CaCl_2$, 1 $MgCl_2$, 25 NaHepes at pH 7.4, 22°C). This channel has a single channel conductance of 133 ± 24 pS, is active at the resting membrane potential and depolarization increases mean and fractional open time. Bath application of 5 mM Ba^{++} causes an increase in the amplitude of single channel fluctuations at constant pipet voltages that corresponds to a shift in the depolarizing direction of the current-voltage relationship, with no change in single channel conductance. In addition, Ba^{++} blocks the channels from the intracellular face of the patch in a voltage dependent manner. This is seen as a decrease in mean burst length and as an increase in the number of long closures with depolarization of the patch as shown in the figure. We conclude that Ba^{++} causes a depolarization of the apical membrane potential and gains access to the intracellular face of the cell membrane producing a voltage-dependent block of the K^+ channel.

W-PM-H11 SPIKE AFTERHYPERPOLARIZATIONS (AHPs) IN BULLFROG SYMPATHETIC GANGLION "B" CELLS. P.R. Adams, P.Pennefather & B.Lancaster, Dept. Neurobiology, SUNY, Stony Brook, NY 11794.

Following a spike the membrane potential of these cells always rapidly increases to about -75mV, but the subsequent AHP patterns show great variability. An important factor contributing to this variability is the shunting effect of the impalement leak. Thus as sealing improves one can see (1) a simple rapid passive decay of the AHP (2) a rapid AHP decay followed by a brief afterdepolarization (3) a rapidly decaying AHP merging into a slowly decaying component (4) an almost purely slowly decaying AHP and (5) a further rapid increase in membrane potential to nearly -90mV, followed by a slow decay back to rest. At least 4 active potassium conductances contribute to these patterns. The 2 most important are Ca-activated G_K's. One, which we term G_C, is large, fast and voltage dependent (Nature,296,746). The other, G_{AHP}, is small, slow and voltage independent (P.N.A.S., in press). We model these as a current waveform injected into a passive RC circuit. The waveform is the sum of a delta function (charge Q_f) representing the I_C component and an exponentially (τ_S) decaying component representing I_{AHP} (charge Q_S). This treatment assumes $V_m >> E_K$. The predicted AHP rises instantaneously and then decays as $(a\text{-}Q_f/C)\exp\text{-}t/RC\text{-}a.\exp\text{-}t/\tau_S$ where $a = Q_S R/(\tau_S\text{-}RC)$. As R is increased the sign of the first exponential changes, explaining patterns 3 through 5. Pattern 2 is observed when R is low enough to depolarize the cell into the M-current range. I_M turns off during the early AHP, and then reactivates. In very leaky cells the effect of the small currents I_M and I_{AHP} is not visible and a simple passive decay is seen. When G_C and G_{AHP} are blocked by cadmium or removing calcium, the spike repolarization slows enough that delayed rectifier current becomes the main contributor to afterhyperpolarization. Supported by NS 15986.

W-PM-H12 TWO TYPES OF K CHANNELS IN T LYMPHOCYTES FROM MRL MICE. T.E. DeCoursey*, K.G. Chandy#, M. Fischbach**, N. Talal**, S. Gupta#, M.D. Cahalan*. *Depts. of Physiology & Biophysics, & #Medicine, Univ. California, Irvine, CA 92717; **Dept. of Medicine, Univ. Texas, San Antonio, TX 78284.

MRL-l and MRL-n mice, which differ by the single gene locus, lpr (lymphoproliferation), develop a disease resembling human systemic lupus erythematosus, MRL-n late in life, MRL-l early in life. MRL-l mice also express severe lymphoproliferation of functionally abnormal T-cells. We studied T lymphocytes from the two congenic strains, using giga-ohm seal recording (Ringer/KF, 22° C). Lymph node or splenic T cells from both strains express K channels, but the maximum K conductance is twenty-fold larger in MRL-l (median 3.9 nS, n=31) than in MRL-n (median 0.16 nS, n=37). One day after activation by Con A, the K conductance in 5 of 6 MRL-n T cells increased to 1.0-2.3 nS. Several types of evidence indicate that two types of K channel behavior (here called 'l' & 'n') can be expressed by MRL T lymphocytes. The gating kinetics and pharmacology of type 'n' channels in the mouse resemble K channels in human T-cells more closely than type 'l' channels. Type 'l' channels, compared with type 'n', activate at 20-40 mV more positive potentials, have 10-fold more rapid tail current kinetics, inactivate more slowly and less completely, are 100-fold more sensitive to block by external TEA (half block of 'l' channels at 50-80 uM), and are at least 10-fold less sensitive to block by external Co^{++} (half block of 'n' channels at 2-5mM Co^{++}). The predominant channel in MRL-l T cells is type 'l'; non-stimulated MRL-n T cells may express either type of channel. Con A-activated MRL-n T cells express predominantly type 'n' channels. MRL-l T cells do not respond in culture to the mitogen Con A; MRL-n T cells divide in response to Con A, and this response was inhibited by K channel blockers. The dose-response curve for inhibition of Con A-induced mitogesesis in MRL-n T cells by TEA suggests a requirement for type 'n', but not type 'l' channels. Supported by NIH grants #NS14609, AI-20717 & AG-04361.

W-Pos1 A THEORETICAL ANALYSIS OF THE FOOTPRINTING EXPERIMENT. J. Goodisman and J. C. Dabrowiak, Department of Chemistry, Syracuse University, Syracuse, New York 13210.

Footprinting analysis is widely used for studying ligand-DNA interactions.[1-3] In a typical footprinting experiment, an end-labeled segment of DNA is partially digested with an endonuclease in the presence and absence of a DNA binding ligand. If the bound ligand is capable of altering the enzymatic cleavage rate, the sites of ligand binding can be identified by analyzing the digest-produced oligonucleotides using polyacrylamide gel electrophoresis. Despite the fact that footprinting data have been used to determine the strength of ligand-DNA contact, a detailed analysis of the kinetic events taking place in the footprinting experiment has not appeared. Using coupled kinetic expressions we analyze the footprinting experiment in terms of the on and off rates of the ligand and the cleavage rate of the endonuclease. We further examine the ability of the endonuclease to accurately report the fraction of site bound present on a segment of DNA and discuss the conditions under which footprinting analysis can be used to determine binding constants for ligand-DNA contacts. The support of the National Institutes of Health, GM 31895, is gratefully acknowledged (J.C.D).

1. Dabrowiak, J. C. Life Sci. **1983**, 32, 2915.
2. Lane, M. J.; Dabrowiak J. C.; Vournakis, J. N. Proc. Natl. Acad. Sci. USA **1983**, 80, 3260.
3. Lane, M. J.; Vournakis, J. N.; Dabrowiak, J. C. in Molecular Basis of Cancer: Part B, Macromolecular Recognition, Chemotherapy and Immunology, R. Rein ed. Alan R. Liss Pub. New York, 1984, P 145.

W-Pos2 COMPARISON OF QUANTITATIVE DNase FOOTPRINT AND FILTERBINDING TITRATION METHODS FOR RESOLVING THE ENERGETICS OF PROTEIN-DNA INTERACTIONS AT MULTIPLE,SPECIFIC SITES ON DNA. D. F. Senear, M. Brenowitz, M. A. Shea, and G. K. Ackers, Dept. of Biology, The Johns Hopkins University, Baltimore, MD 21218.

Two experimental techniques for studying the interactions of genome regulatory proteins with multiple, specific sites on DNA are compared. We find that the individual-site binding information resolved by the method of Quantitative DNase Footprint Titration is necessary for understanding the energetics of cooperative interactions such as those known to be responsible for genome regulation in many systems. This information is not obtainable from the filterbinding technique of Riggs et al. (1970, J. Mol. Biol. 67, 48). We have recently developed DNase Footprint Titration to be a rigorous method which yields thermodynamically valid binding and cooperativity constants (M. Brenowitz, D. F. Senear, M. A. Shea, & G. K. Ackers (1985) Meth. Enz.,in press). This technique resolves isotherms that separately represent the fractional saturation of each site of a multi-site system. We have studied the binding of the cI repressor protein to the three-site right and left operators of phage lambda, and to mutant and synthetic DNA sequences in which the valency of the operator is reduced. These studies yielded both the local-site binding constants and the free energies of cooperative interactions between sites. By contrast, standard techniques for monitoring the interactions of regulatory proteins with specific DNA sites are incapable of monitoring interactions at the individual sites. Only macroscopic constants, which are composite averages of the various local-site and cooperativity constants, are resolved by these methods. The filterbinding technique is an example. Moreover, high precision filterbinding data are insensitive even to the presence of the third site of either lambda phage operator. (Supported by NIH grant GM 24486).

W-Pos3 FOOTPRINT TITRATIONS YIELD VALID THERMODYNAMIC CONSTANTS FOR PROTEIN-DNA INTERACTIONS. M. Brenowitz, D. F. Senear, M. A. Shea, G. K. Ackers, Dept. of Biology, The Johns Hopkins University, Baltimore, MD 21218.

Experiments are presented which demonstrate that the individual-site binding isotherms (Ackers et al. (1983) J. Mol. Biol. 170, 223-242) resolved by quantitative DNase footprint titration studies are thermodynamically valid. Determination of the individual-site isotherm for each protein binding site in a multi-site system effectively decouples the microscopic interaction constants, allowing their resolution. In a footprint titration, a series of equilibrium mixtures of radio-labelled DNA fragments (that contain specific binding sites) and binding protein at different concentrations are exposed to DNase I under conditions such that each molecule is, on the average, nicked only once. The DNase cleavage products are separated electrophoretically and autoradiographed. Bands corresponding to binding sites are diminished in density when the bound protein prevents DNase nicking at those sites. We show that the density of the bands within each binding site can be unambiguously related to the fractional saturation of that site. Although the technique of DNase protection mapping (or footprinting) was originally developed as a qualitative technique to locate the specific binding sites of DNA-binding proteins, our studies show that it is possible to obtain thermodynamically valid intrinsic binding constants and cooperative interaction constants. The interaction of lambda phage cI repressor with its three-site operators was used as a model system in these studies. (Supported by NIH grant GM 24486).

W-Pos4 EFFECTS OF THE POSITION OF SPECIFIC SITES IN DNA MOLECULES ON THE KINETICS OF THEIR REACTIONS WITH PROTEINS: A THEORETICAL DESCRIPTION WITH EXPERIMENTAL OBSERVATIONS FROM THE E. COLI lac REPRESSOR-OPERATOR SYSTEM.

Sharlyn J. Mazur, Sigrid L. Liermo and M. Thomas Record
Departments of Biochemistry and Chemistry, University of Wisconsin-Madison, Madison WI 53706

A simple theoretical model for the kinetics of reactions of nucleic acids with proteins is developed which incorporates complex mechanisms involving nonspecific sites in the association to a specific site. A method for describing the kinetics of nonhomogeneous systems allows diffusion of the protein, competition by nonspecific sites and facilitating mechanisms to be included. In particular, the effect on the kinetics of the position of the specific site in the DNA molecule differs when the facilitating mechanism involves intramolecular transfer as opposed to sliding. Some experimental data from the lac repressor-operator system pertaining to the effect of the position of the site on the rate of association are presented. In addition, when facilitating mechanisms operate, the proximity of an end of the DNA molecule to a specific site can affect the rate of its reaction. Experimental determination of the distribution of the lac repressor between the operator and pseudo-operator sites in various DNA molecules provides insight into the association mechanism.

W-Pos5 NMR STUDIES OF THE INTERACTION OF A RIBONUCLEOTIDE TEMPLATE WITH THE KLENOW FRAGMENT OF DNA POLYMERASE I FROM E. COLI. Lance J. Ferrin and Albert S. Mildvan. Johns Hopkins University, School of Medicine, Baltimore, MD 21205

Measurements of interproton distances by nuclear Overhauser effects in abortive, ternary, enzyme-Mg^{2+}-substrate complexes of pol I and Klenow fragment have revealed B-like conformations of bound dATP and TTP (Ferrin and Mildvan, Fed. Proc. 43, 1539). The binding of the nuclease resistant template $(rU)_{54}$ slightly increased the glycosyl torsional angle (χ) of dATP from 50° to 62° and decreased the exocyclic deoxyribose torsional angle (δ) from 95° to 90°. However, the conformation of bound dATP remained anti, O1'-endo and B-like. The conformation of the bound $(rU)_{54}$ template was also B-like, as revealed by the average conformational angles of the uridyl units (χ = 60 ± 10°, δ = 105 ± 10°). The presence of the $(rU)_{54}$ template did not alter the relative affinities of dATP and dGTP. The possibility of a "wobble" base pair of G with U is suggested by the observation that in absence of $(rU)_{54}$ the conformation of enzyme-bound dGTP is a 2:1 anti:syn mixture, while in the presence of $(rU)_{54}$ only the anti conformation of bound dGTP is detected (χ = 32 ± 10°; δ = 90 ± 10°). Intermolecular NOE's from protons of the protein to those of bound dATP and TTP indicate that the substrates bind in close proximity to at least two hydrophobic residues (ile, leu, val) and one aromatic residue. Large NOE's to H5 of $(rU)_{54}$ seen on irradiation of protein resonances at 1.6, 2.1, and 3.1 ppm, indicate that the template binds in close proximity to cationic (arg, lys) residues.

W-Pos6 REGULATION OF RNA POLYMERASE - PROMOTER INTERACTIONS AND OF OPEN COMPLEX FORMATION.
J.H. Roe and M.T. Record, Jr., Departments of Chemistry and Biochemistry, University of Wisconsin, Madison, Wisconsin 53706

The interaction of E.coli RNA polymerase (R) with the λP_R promoter (P) involves at least two intermediates (I_1,I_2) on the pathway to formation of an open complex (RP_o):

$$R + P \underset{k_{-1}}{\overset{k_1}{\rightleftarrows}} I_1 \underset{k_{-2}}{\overset{k_2}{\rightleftarrows}} I_2 \underset{k_{-3}}{\overset{k_3}{\rightleftarrows}} RP_o$$

Under pseudo first order reaction conditions where the excess concentration of polymerase is R_T, the reaction time constant is τ_{obs}:

$$\tau_{obs} = (k_a R_T)^{-1} + k_2^{-1} + k_3^{-1}$$

where $k_a = k_1$ for a sequential mechanism ($k_{-1}<k_2$) and $k_a = K_1 k_2$ for a binding pre-equilibrium mechanism ($k_{-1}>k_2$). The following factors have important effects on τ_{obs} both in vitro and in vivo, and hence regulate this most fundamental step of gene expression : 1) the concentration of monomeric, active RNA polymerase holoenzyme; 2) the sequence, structure and degree of supercoiling of the promoter site; 3) accessory proteins and effector ligands; and 4) physical and environmental variables, including temperature, ion concentrations, pH and solvent composition (e.g. glycerol).

Evidence in support of the three-step mechanism will be presented, and the sites of action of the factors that regulate open complex formation will be discussed.

W-Pos7 THE EFFECT OF POLYAMINES ON THE RNA POLYMERASE-DNA INTERACTION. Michael G. Fried and Victor Bloomfield, Dept. of Biochemistry, University of Minnesota, St. Paul, MN 55108

Polyamines have long been known to stimulate RNA polymerase II-mediated transcription, although the origin of this effect remains obscure. We have examined the interactions of RNA polymerase II with non-promoter DNA fragments in order to determine whether this effect occurs at the level of DNA binding. The linear binding isotherms obtained in the presence of spermine are consistent with a simple binding mechanism of the type $n\text{RNApol II} + \text{DNA} \rightleftharpoons \text{RNApol II}_n\text{-DNA}$, with $n \sim 1$. Analysis of the change in K_{eq} with [spermine] suggests that approximately one molecule of polyamine is displaced when a polymerase-DNA complex forms. In contrast, isotherms obtained in the absence of spermine, with or without KCl are notably curved, and yield estimates of K_{eq} ($4 \times 10^{-7} M^{-1}$) that are surprisingly insensitive to changes in salt concentration. This counterintuitive result may stem from compensating effects in a complex binding mechanism. These results show that spermine not only causes quantitative changes in binding, but also has a fundamental effect on the mechanism of the process.

W-Pos8 IDENTIFICATION OF A LAC REPRESSOR-INDUCED CONFORMATIONAL CHANGE IN OPERATOR AND NON-OPERATOR DNA. Michael G. Fried, Department of Biochemistry, University of Minnesota, St. Paul, MN 55108

The interaction of lac repressor with short operator and non-operator DNA fragments has been studied by transient electric dichroism. At low densities, lac repressor binding decreases the base tilt angle, α, of both types of sequences. I estimate that formation of the 1:1 complex reduces α(non-operator) by 10±2 degrees and α(operator) by 14±2 degrees. In principle this reduction might be due to either i) bending or kinking of the duplex, or ii) increase in the base-pair propeller twist or roll. Experiments in which repressor is preferentially bound near one end of the DNA molecule, minimizing the potential effect of bending on measured values of α, strongly favor the second model. These results are compatible with, and help to explain, the B to "A-like" circular dichroism change induced in the lac operator by repressor binding (F. Culard and J. Maurizot (1981) Nucl. Acids Res. 9, 5175-5184).

W-Pos9 THE CATABOLITE ACTIVATOR PROTEIN STABILIZES ITS PRIMARY BINDING SITE IN THE LAC OPERON PROMOTER. by H. DeGrazia, S. Abhiraman, and R.M. Wartell, School of Physics, Georgia Institute of Technology, Atlanta, GA 30332 (Intr. by D. Dusenbery)

The effect of the catabolite activator protein, CAP, on the thermal stability of DNA was examined. The site specific effect was studied with a 62 bp DNA restriction fragment containing the major CAP binding site of the E. coli lactose, lac, operon promoter. A 234 bp DNA from pBR322 provided a comparable non-specific CAP binding region (gift of A.S. Benight). Thermal denaturation and binding studies were carried out in 1mM NACl + 40% DMSO. Polyacrylamide gel electrophoresis (PAGE) showed that CAP requires cAMP for site specific binding in this solvent. Saturation of binding occurs at the same molar CAP/DNA ratio (4:1) observed in 0.1 M KCl. UV absorbance was employed to obtain differential melting curves. The 62 bp DNA alone shows a melting temperature Tm of 31.7°C. The width of the melting curve is about 1.3°C at 0.5 maximum amplitude. Saturating amounts of CAP with 10uM cAMP increases the Tm by 16.4°C. The melting curve is monophasic with a width of 4°C at 0.5 maximum amplitude. Melting curves of the 62 bp DNA showed some biphasic character at lower CAP to DNA ratios. The 234 bp DNA has a single melting transition with a Tm of 40°C without CAP. Saturating amounts of CAP-cAMP increases the Tm by 5.4°C. The stability of CAP for site specific binding was monitored in these experiments by PAGE. When complexed with DNA (specific or nonspecific) CAP maintained its ability for site specific binding up to the DNA melting region. CAP alone denatured at 41°C in 1mM NaCl-40% DMSO. The above results show that CAP with cAMP stabilizes DNA. Site specific binding to its primary lac promoter site produces a much larger increase in stability than non-specific binding. (Supported by N.I.H.)

W-Pos10 SEQUENCE-SPECIFIC RECOGNITION OF DNA: ^{13}C AND ^{1}H TWO-DIMENSIONAL NMR OF THE λ REPRESSOR-OPERATOR COMPLEX. Michael A. Weiss. Department of Chemistry, Harvard University, Cambridge, Massachusetts 02138. λ repressor (cI) regulates gene expression by recognizing operator DNA sequences in the phage genome. We are studying the structural basis of this protein-DNA interaction by heteronuclear one- and two-dimensional NMR. Resonances have been assigned in the active site through the study of mutant repressors containing single amino-acid substitutions and through the biosynthetic incorporation of specific ^{2}H and ^{13}C labels. Extensive assignments have been made in the synthetic operator oligonucleotide O_L1; in addition, mutant operators containing single base-pair substitutions are under study. Our strategy is thus to use site-specific changes in both the repressor and operator to probe structure-function relationships. We conclude that (1) the N-terminal arm of repressor is flexible and becomes immobilized in the complex; (2) helix 5 forms a dimer site that is responsible for the cooperative binding of monomer domains to operator; and (3) single amino-acid substitutions in the arm or dimer helix perturb these interactions.

W-Pos11 SPECIFICITY IN THE RECOGNITION OF DNA OPERATOR SEQUENCES BY REPRESSOR PROTEINS. A. Sarai and R.L. Jernigan. Laboratory of Mathematical Biology, DCBD, NCI, NIH, Bethesda, MD.

To understand the mechanism of sequence-specific recognition of DNA by proteins we have studied the interaction between DNA operator region and repressor molecules with the following strategy: (1) First, model the interaction between protein side chains and DNA bases with CPK molecular model, and tabulate possible numbers of interactions (H-bonding, hydrophobic interactions and steric hindrances). (2) According to this interaction table, scan the DNA sequence to see how the interaction is specific to the binding region relative to the rest of DNA. (3) Finally, estimate the relative strength of the interactions for each site to evaluate the relative affinity of the specific binding. So far, we have performed the first two analyses for cro, cI and lac repressors, for which the mode of interaction has been modeled. The results obtained so far are: In the case of cro-operator interaction proposed by Ohlendorf et al., the α-helix arms of cro bind to the operator OR3 uniquely out of 48500 binding sites of λ phage; whereas its bindings to the other five operators are less specific, giving about 50 binding sites with similar interaction strengths. In the case of cI repressor, the interactions of the corresponding α-helix arms to the operators are much less specific. The bridging interactions of side chains to the neighboring base pairs increase the specificity. But the interaction is still less specific than cro, with more than 100 sites to which cI can binds with similar affinity to the operators. If we take account of the fact that the interactions of cI to the operators are cooperative, the cooperative binding of cI to OR1 and OR2 can become unique. In the model of lac repressor-operator interaction, the interaction is much less specific than were λ repressors. Probably additional interactions which were not considered in this analysis are necessary to explain such specificity.

W-Pos12 THERMODYNAMIC ORIGINS OF SPECIFICITY IN THE lac REPRESSOR-OPERATOR INTERACTION Michael C. Mossing and M. Thomas Record Jr. Department of Chemistry, University of Wisconsin, Madison Wi 53706.

The thermodynamic consequences of operator-constitutive mutations on the lac repressor-operator interaction have been investigated. O^c mutations have been cloned onto identical 300 bp fragments free from competing operator sites, and the temperature and salt dependences of the interaction have been studied by nitrocellulose filter binding. From measurements of the equilibrium retention levels of complexes of lac repressor with operators differing by a single base pair we can derive quantitative information about the thermodynamic basis of specificity. Our results show much more drastic effects for point mutations than were previously observed (three orders of magnitude in the equilibrium constant for a single base pair change). These results are being correlated with those of Caruthers et al. (Acct. Chem. Res. 13, 155, 1980) on synthetic operator fragments. Preliminary results indicate that interaction-free energies aren't simply additive on a base-pair by base-pair level.

W-Pos13 CONTROL OF INITIATION OF TRANSCRIPTION AT THE E. coli LACTOSE OPERON. Donald D. Lorimer and Arnold Revzin, Department of Biochemistry, Michigan State U., East Lansing, MI 48824

We are studying regulation of gene expression by applying a variety of techniques to solutions of purified proteins and DNA fragments embracing the E. coli lac promoter. Initiation of transcription at this promoter in vitro can occur from either of two overlapping sites. In the presence of the catabolite activator protein (CAP) and cyclic AMP, transcription from the P1 promoter begins at nucleotide +1. In the absence of CAP transcription starts at P2, 22 bp upstream of the P1 start site. The addition of RNA polymerase (RP) to solutions containing the wild-type lac promoter leads to formation of heparin-insensitive complexes only at P2 as judged by protection from exonuclease III digestion. Adding CAP before RP results in protection at P1 only. If CAP is added after RP, exo III protection is seen at both P1 and P2 in approximately equal proportion; in this case there occurs a steady increase in P1 transcripts over time without any decrease in initiation from the P2 promoter. When truncated DNA fragments cut at -59 are used, no heparin-insensitive complexes are observed (and the number of transcripts is nil). Thus, on this fragment binding at P2 has been eliminated (as has the CAP site, which normally extends from -55 to -70). However exo III digestions performed in the absence of heparin show binding at P1. We conclude that CAP plays a dual role at the lac operon. It can stimulate transcription both by excluding RP from P2 (so that more polymerase can bind at P1), and also by enhancing the conversion of the RP-promoter "closed" complex (formed at P1 in the absence of CAP) to a stable, transcriptionally competent configuration.

W-Pos14 PHYSICAL STUDIES OF A MONOCLONAL ANTIBODY - ALKYLATED NUCLEOSIDE INTERACTION AS A MODEL FOR EPITOPE RECOGNITION ON NUCLEIC ACIDS. Stacieann C. Yuhasz, Lou-sing Kan, Robert Chou, P.O.P. Ts'o, Gary K. Ackers, Manifred Rajewsky, and Jurgen Adamkiewicz. Biophysics Division, SHPH, The Johns Hopkins University, Baltimore, MD. 21205 and The Institute of Cell Biology, West Germany.

The objective of this study is to examine the forces that govern the affinity and the specificity of the interaction between the rat monoclonal antibodies (ER-6 and ER-3) directed against O^6-ethyl-2'-deoxyguanosine (O^6EtG). Thermodynamic data was evaulated from both the affinity constant (K_a) and microcalorimetric measurements. The K_a values were monitored via a nitrocellulose affinity filter assay (NAFA) (Huang et.al., submitted to J. of Immunol. Meth.) as a function of temperature, ionic strength, pH, and surface tension parameters, as well as for a series of non-specific antigens such as O^6-methyl-2'-deoxyguanosine (O^6MeG) and 2'-deoxyguanosine (G). In the assay the tritiated nucleoside/ monoclonal antibody complex is retained on the filter and the amount of complex measured directly. The K_a for O^6EtG/ER-6 was found to be in the range of $1\text{-}3\times10^8$ M^{-1}, 10 fold higher than the K_a of O^6MeG/ER-6. The K_a was slightly affected by ionic strength (0.1 to 1.0M NaCL), pH variation (pH= 6-10), and temperature. The temperature effects are currently being evaluated in terms of the enthalpy of interaction and will be compared with Batch microcalorimetry results. (NIH 5T32)

W-Pos15 TRYPSINIZATION STUDIES OF HYPERACETYLATED CHROMATIN. M. R. Riehm and R. E. Harrington, Dept. of Biochemistry, University of Nevada at Reno, 89557.

We have investigated the role of the N-terminal regions of histones in the maintanance of nucleosome core structure integrity in the 10nm fiber of chromatin. Our studies included isolation of hyperacetylated nucleohistone from butyrate treated HeLa cells. The N-terminal regions were selectively removed using trypsin. Characterization of the degree of DNA condensation in our preparations with circular dichroism suggests that at 0.2mM EDTA hyperacetylated chromatin is less condensed than the nonacetylated control. This difference disappears at 5mM sodium. A broad transition occurs for both preparations upon the removal of H1. Tryptic removal of all N-terminal regions of the histones resulted in a dramatic decrease in nucleosomal core stability as determined by DNA thermal denaturation. The differential tryptic cleavage of the N-termini from, first H3/H4, then H2a/H2b resulted in a stepwise transfer of DNA melting between the three resolved transitions. These observations suggest that the N-termini from H3/H4 play a role in stabilizing the flanking DNA while the N-termini from H2a/H2b can stabilize the central core loop of DNA. Partial removal of the H3/H4 termini from H1 stripped control chromatin resulted in a DNA melting profile identical to that of intact H1 stripped hyperacetylated chromatin. Hyperchromicity changes are consistent with a symmetric redistribution between DNA melting in the flanking region and the linker region of the nucleosome in control chromatin. The same type of redistribution is seen for hyperacetylated material, but between the central loop of DNA and the flanking DNA. This suggests that hyperacetylation induces a fundamental change in nucleosome dynamics in the 10nm fiber.

W-Pos16 STRUCTURE OF INTACT TOBACCO MOSAIC VIRUS AT 3.6 Å RESOLUTION. Gerald Stubbs and Keiichi Namba, Dept. of Molecular Biology, Vanderbilt University, Nashville, TN 37235

Intact tobacco mosaic virus has been studied by fiber diffraction methods. The structure has been determined at a resolution of 3.6 A, using a number of new techniques to deal with the special problems of phase determination in fiber diffraction, caused by the cylindrical averaging of the diffraction pattern. The map and model are substantially improved from those described in 1977 by Stubbs, Warren and Holmes, although the nominal resolution has improved only from 4A to 3.6A. The data are better, particularly at high resolution, because Makowski's angular deconvolution procedure enabled us to make better estimates of intensities and backgrounds in the regions of substantial overlap of layer lines. The map is improved, particularly near the outer surface of the particle, because all five contributing Bessel terms were able to be considered, instead of only three. The map was further improved by various refinement procedures, including solvent flattening and the simultaneous refinement of the isomorphous replacement phases and the model. The map clearly shows the entire main chain of the protein and RNA. Many side-chains are extremely well-resolved for this resolution, including a number taking part in inter-subunit contacts. Refinement and extension of resolution are continuing, using an adaptation of the Hendrickson-Konnert restrained least-squares procedure to fiber diffraction data.

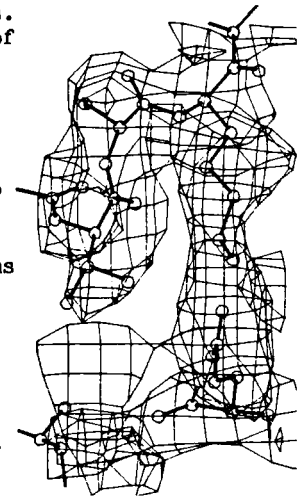

W-Pos17 ORIENTATION DISTRIBUTION IN MAGNETICALLY ALIGNED TMV LIQUID CRYSTALS MEASURED BY X-RAY SCATTERING. R. Oldenbourg, R.B. Meyer and D.L.D. Caspar, Physics Department and Rosenstiel Center, Brandeis Univ., Waltham, MA 02254.

Rod shaped particles like the Tobacco Mosaic Virus (TMV) form at moderate concentration a liquid crystalline phase, where the particles tend to be parallel to a common axis in the solution. In order to determine the orientation distribution of TMV particles in the anisotropic phase we collected X-ray patterns from solutions with TMV concentrations between 8 and 15%. During the measurements the samples were kept in a steady magnetic field of 1.6 Tesla to orient the common axis of allignment perpendicular to the X-ray beam throughout the sample volume. We derived a simple relationship between the spread of the scattered intensity perpendicular to the equator in the X-ray pattern and the orientational distribution of the rods in solution. Our results show that the orientation distribution function can be modeled by a Gaussian distribution, which becomes broader with decreasing TMV concentration. For the most dilute sample we observed the formation of an isotropic and an anisotropic phase. The angular spread of particle orientation is 41 degree in the anisotropic bottom phase, a value larger than seen in any of the single phase samples. This degree of disorientation is 15% larger than expected from the "athermal" theory published by Onsager in 1949. Thermal orientation fluctuations will possibly account for the discrepancy. Our results may clarify the association of rodlike particles into biological assemblies.

W-Pos18 X-RAY DIFFRACTION STUDIES OF PROTEIN STRUCTURE IN THE FILAMENTOUS BACTERIOPHAGE M13 Marc J. Glucksman and Lee Makowski
Dept.of Biochemistry & Molecular Biophysics, Columbia University P & S. NY, NY 10032

The class I filamentous bacteriophages are rod-like, flexible cylinders, with dimensions of 60Å in diameter and about 9000Å in length. M13 and the very similar f1 and fd are made up of many copies of a small α-helical(>80%), 50 a.a. polypeptide that encase the viruses' single-stranded, circular DNA. Due to their large anisotropy in magnetic susceptibility, highly oriented fiber specimens for X-ray analysis can be formed in a high strength, homogeneous magnetic field. These viruses align with their long axis parallel to the magnetic field. The structure of the major coat protein of M13 is currently being determined using high resolution X-ray diffraction methods. These studies are directed toward an understanding of the structural organization of the viral particle.

The half width of disorientation of our M13 specimens is $< 2°$. Using methods of angular deconvolution and layer line splitting by non-overlapping Bessel functions, structural information is being processed. The current model as determined by diffraction, shows the coat protein symmetry as $C_5S_{2.0}$, in other words, the proteins are related by a 5-fold rotation axis and a 2-fold screw axis (Makowski & Caspar JMB 145,611 (1981)). The axial repeat of the helical array is about 32Å. The protein subunits must interact with the DNA in numerous ways, since the DNA can not conform to the symmetry of the protein coat. These studies are aimed at determining the structure to high resolution and will ultimately enable us to model a detailed system of protein-protein and protein-DNA interactions.

W-Pos19 A NEW APPROACH TO THE ARCHITECTURE OF MAMMALIAN VIRUSES. Roger M. Burnett. Department of Biochemistry & Molecular Biophysics, Columbia University, New York, New York 10032.

The morphology of many mammalian viruses was originally explained by Caspar & Klug in 1962. The morphological features were thought to arise from clustering of identical polypeptides about the local symmetry elements of hexagonal lattices. For adenovirus, the triangulation number (T) of 25 associated 1500 polypeptides within 240 hexameric and 12 pentameric groups. However, since 240 trimeric hexons and 12 pentons are found, the theory cannot apply to adenovirus. For polyoma, the pentamers at the local 6-folds of the supposedly T=7d shell also appear to be distinct molecules.

A model for the overall arrangement of hexons in adenovirus has been derived. A quartet of hexons repeats with exact 532 symmetry to form the icosahedral shell, leaving holes at the vertices into which pentons may be inserted. The packing in the four topologically distinct locations of hexon is such that its pseudo-hexagonal symmetry permits the conservation of no less than 2/3 of the inter-hexon chemical bonds. Since each facet of adenovirus is a small crystalline array, only one additional topologically related location is necessary to achieve a capsid of infinite size. A similar simplification may be achieved for polyoma by dividing the pentamers into two classes: 60 arranged with exact icosahedral symmetry, and 12 at the vertices. Accurate assembly of large capsids is explained by the small number of differently bonded structure units required by this method of construction. The earlier approach failed to explain sharp capsid facets and led to a myriad of different bonding states for structure units. Accurate assembly of the "complex" structure units, which must be highly stable to act as building blocks, requires relatively weak interactions. The final capsid strength is achieved by the addition of further components, such as polypeptide IX in adenovirus. (Supported by NIH Grant AI 17270).

W-Pos20 THE STRUCTURE OF THE ADENOVIRUS CAPSID. Jan van Oostrum and Roger M. Burnett. Dept. of Biochemistry and Molecular Biophysics, Columbia University, New York, New York 10032.

Dissociation of the icosahedral adenovirus under mild conditions results in the loss of the 12 pentons, located at each of the vertices, with their 5 surrounding peripentonal hexons. The remaining 180 hexons, forming the major part of each facet, dissociate together as 20 groups-of-nine (GON). The 6 Å crystallographic model of the hexon trimer, determined in our laboratory, has facilitated the interpretation of high resolution electron micrographs of various capsid fragments, and has led to a model for the location of hexon and polypeptide IX within the capsid. The disruption behaviour of the virion depends not only on the hexon bonding, but also on the presence of polypeptide IX, Mr 14,300, which has long been suspected to act as a capsid cement. A temperature sensitive mutant which lacks protein IX is known to produce thermolabile virus capsids which do not produce GONs upon disruption. A stoichiometric analysis of the proteins within the virion and the GON has provided the absolute number of polypeptides in the two assemblies. This information, combined with the determination of the spatial orientation of the peripentonal hexons by image analysis of electron micrographs of novel capsid fragments, gives experimental proof for the capsid model. Recent neutron scattering experiments on penton have indicated a trimeric penton base and a dimeric fibre (Devaux, C. et al., (1982;84) J.Mol.Biol. 156, 927; 174, 729). This would result not only in a symmetry mismatch between the fibre and base, but also between the base and the peripentonal hexons at the 5-fold vertex. However, our results from the chemical analysis indicate a pentameric penton base in association with a trimeric fibre. Moreover, the existence of two slightly different penton base polypeptides suggests a mechanism by which the single symmetry mismatch, between fibre and penton base, can be overcome. (Supported by NIH Grant AI 17270).

W-Pos21 TRIFLUOPERAZINE INHIBITS FUSION PROTEIN OF SENDAI VIRUS. Ruby I. MacDonald, Dept. of Biochem., Mol. Biol. and Cell Biol., Northwestern University, Evanston, IL 60201.

The well-known tranquilizer and probe of protein conformation, trifluoperazine (TFP), inhibited hemolysis by Sendai virus under conditions distinguishable from the effects of TFP on red cells. TFP did not disrupt the virus, which sedimented slightly faster than and with all viral proteins in the same proportions as untreated virus in TFP-containing sucrose gradients. Trifluoperazine did not affect the envelope hemagglutinin, HN, insofar as TFP did not inhibit viral hemagglutination. Thus, inactivation of viral hemolysis by TFP appeared to involve the fusion protein, F.

Concentrations of trifluoperazine required to inhibit 50% of viral hemolytic activity were an order of magnitude greater per membrane lipid than concentrations of trifluoperazine required to directly lyse 50% of a red cell population. Based on these data and hence, derived indirectly, the partition coefficient of TFP between red cells and the aqueous medium was about 8000 and an order of magnitude greater than that between Sendai virus and the aqueous medium. When directly determined by centrifugation of the TFP-treated virus and spectrophotometric measurement of free TFP in the supernatant, the partition coefficient of TFP between Sendai virus and the aqueous medium was about 2000. The uptake of TFP by Sendai virus was also demonstrated by the fluorescence energy transfer from viral protein tryptophan to trifluoperazine. Finally, the temperature dependence of the inhibition of Sendai virus hemolysis by TFP was several-fold greater than that of hemolysis by TFP itself. These data are compatible with the findings of others that the Sendai virus envelope is much more rigid and/or tightly packed than other cholesterol-containing viral membranes and that this structural feature is temperature dependent.

W-Pos22 LOCALIZED SWITCHING IN STRESSED ASSEMBLIES: HELICAL FLAGELLA, SUPERCOILED DNA, AND THE RIGOR-STATE MYOFIBRIL. C.J. Ritz-Gold, Dept. of Chemistry, San Francisco State Univ., San Francisco, CA 94132.

Localized switching of identical subunits is now recognized to occur within certain protein assemblies, including the polyoma virus capsid and the supercoiled bacterial flagellum, (Caspar, 1982, Biophys. J. 37, 5a). In the flagellum, this has been associated with the ability of the deformed helical polymer to relieve strain energy by switching a strand of monomers into a conformation with a different unstrained (rest) length (Asakura, 1970, Adv. Biophys. 1, 99). In supercoiled DNA, switching of a segment into an alternative conformation with a smaller unstressed twist value (e.g., a locally melted region), has been similarly associated with relief of torsional stress in the molecule as a whole (Benham, 1979, PNAS 76, 3870). In the rigor-state myofibril, a certain fraction of the rigor-complex crossbridges are known to suffer mechanical deformation due to the incommensurate periodicities of the actin and myosin filaments. Current EPR studies on spin-labled psoas fibers also appear to be consistent with the switching of rigor-state myofibril segments into localized regions in which crossbridges exist in a detached "melted" state. The origin of localized switching in stressed biological assemblies will also be discussed in relationship to certain condensed matter physical systems in which the creation of localized conformational defects and excitations is associated with the presence of "frustration" arising from conflicting interactions of various types (Bishop, 1979, Phys. Scripta 20, 409). (Supported by NSF Grant RII-8310749).

W-Pos23 MICROTUBULE STRUCTURE AT 18Å RESOLUTION BY X-RAY DIFFRACTION. Lorena Beese*, Gerald Stubbs+ and Carolyn Cohen*. *Rosenstiel Center, Brandeis University, Waltham, MA 02254; +Department of Molecular Biology, Vanderbilt University, Nashville, TN 37235.

A model for hydrated calf brain microtubules has been derived by analysis of X-ray fiber diffraction patterns to a resolution of 18Å. The diffraction patterns were obtained from oriented gels of reassembled microtubules prepared as described by Mandelkow, Thomas and Cohen (PNAS 74, 3370-3374; 1977), and diffracted intensities were determined using Makowski's angular deconvolution procedure. The data extend to a resolution of better than 5Å, but the analysis was limited to 18Å because of the increasing difficulty of phase determination at high resolution in fiber diffraction.

Starting phases were obtained from a model based on that of Mandelkow et al. (1977), which had a crystallographic R-factor of 0.30. These phases were refined against the observed X-ray intensities by applying the "box function" constraint that the structure lie within physically plausible radial boundaries. The refined model has an R-factor of 0.077.

The microtubule wall extends from about 70Å to 150Å in radius, and on the outer surface the subunits appear to be elongated and tilted in the same direction as in the Mandelkow, Thomas and Cohen model. Longitudinal splitting of the subunit on the outer surface is, however, not observed. The inner surface shows low density features in more detail than does the previous model. The interior of the microtubule wall appears to be divided into two high-density regions, separated by a region of low density. Taken together, these features are beginning to define the major domains of the tubulin monomer.

Supported by NIH grants AM17346 and GM33265.

W-Pos24 LIGHT SCATTERING STUDY ON THE STRUCTURE OF NATIVE PROTEOGLYCAN AGGREGATES EXTRACTED FROM DAY 8 CHICK LIMB BUD CHONDROCYTE CELL CULTURES by Hiroyuki Ohno*, John Blackwell*, Alexander M. Jamieson*, David Pechak**, David A. Carrino** and Arnold I. Caplan**, Department of Macromolecular Science* and Biology**, Case Western Reserve University, Cleveland, Ohio 44106

Laser light scattering has been used to investigate the size of native proteoglycan aggregates (PGA-aA1) isolated from day 8 chick limb bud chondrocyte cell cultures under associative conditions in 0.4M guanidinium chloride (GdnHCl) solution. Dynamic measurements yield a hydrodynamic radius, R_S, of 244 ± 10 nm and a molecular weight, $\overline{M}_w$, of 150 ± 50 x 10^6 is obtained from a Zimm plot for PGA-aA1 in 0.4M GdnHCl. Disaggregation in 4M GdnHCl yields subunits (PGS) with R_S = 39 ± 2 nm, $\overline{M}_w$ = 1.6 ± 0.3 x 10^6 which reassemble in 0.4M GdnHCl solution to form reconstituted native aggregates (PGA-raA1) with R_S = 121 ± 6 nm, $\overline{M}_w$ = 17 ± 3 x 10^6. These data are compared with those for reconstituted aggregates (PGA-A1) extracted under dissociative conditions and reaggregated in 0.4M GdnHCl solution, for which R_S = 138 ± 9 nm, $\overline{M}_w$ = 45 ± 8 x 10^6. From these figures we can calculate approximately weight average number of subunits per aggregate. These are 93 for PGA-aA1 and 10 for raA1 as compared to 27 for PGA-A1 aggregates. The numbers of subunits per aggregate are also determined from electron micrographs of spread specimens. The results obtained compare well with those from light scattering, but those obtained by microscopy are generally smaller, probably due to disaggregation during sample preparation. Thus our data point to a more compact aggregation of subunits along the hyaluronic acid chains in native as compared to reconstituted aggregates. The fact that PGA-raA1 is smaller than PGA-A1 indicates that the former contains relatively shorter hyaluronic acid chains.

W-Pos25 STRUCTURAL STUDIES OF FISH EYE LENS, L. Aha, A. Howard, D. Eisenberg

The packing of proteins in successive layers of the spherical fish lens was studied using x-ray diffraction, electron microscopy, and biochemical analysis. Preliminary results indicate domains of liquid crystalline character in the dense packing of lens proteins, with some directional anisotropy. Small angle x-ray scattering patterns from oriented slices of white fish lens lack radial symmetry: when the incident x-ray beam is parallel to the lens optical axis, we observe a periodic variation of intensity in the scattered rings. This suggests a prefered orientation of protein molecules in the lens, possibly with respect to fiber cell direction. Consistent with this, electron micrographs from thin lens sections reveal aligned particles along cell membranes.

X-ray scattering patterns from slices of lens cortex show a broad reflection at $1/170\ A^{-1}$. It varies slightly in scattering angle and breadth as a function of radial distance of the diffracting region from the lens center. In preliminary studies of lens nucleus, the broad peak is split into several overlapping reflections which demonstrate a quasicrystalline, short-range order.

Biochemical analysis of the soluble proteins in successive lens layers show that the only change in the distribution of soluble protein sizes is the addition of a a few large ($2\text{-}5\times10^6$ Dalton) aggregates in the nucleus. However, much of the nuclear protein is insoluble. Hence, changes in scattering from successive layers of cortex may be attributed to increasing protein concentration and not to a difference in proportions of different size scatterers. The sharper x-ray reflections from nucleus arise from increased quasi-crystalline order. This order may result simply from the higher protein concentration, or may result from the organization of the insoluble fractions.

Models of lens organization are being formulated consistent with this data.

W-Pos26 THE CONDENSATION-LIKE BEHAVIOR OF REVERSIBLY POLYMERIZING PROTEINS. Judith Herzfeld, Department of Physiology and Biophysics, Harvard Medical School, Boston, MA 02115.

Polymerizing proteins produce long rod-shaped particles that align spontaneously due to packing constraints. The lattice theory for the coupling between polymerization and alignment, developed originally for systems forming thin polymers by end-to-end associations between monomers, has recently been extended to systems forming thick polymers with additional side-to-side contacts between monomers. Assuming that the polymers are rigid and that long-range interactions are negligible, we can calculate the dependence of the monomer concentration, polymer length and orientation distributions, and solute and solvent chemical potentials on the total protein concentration and the strength of the associations between monomers. The theory predicts that, whereas for thin polymers the strength of polymerization primarily influences the concentration at which the alignment transition occurs, for thick polymers the qualitative phase behavior at the alignment transition is also markedly affected. In particular, when polymerization is strong, an extremely wide two-phase region exists, such that a very dense anisotropic phase separates from a dilute isotropic phase at the alignment transition. This result may be applicable to normal polymerizing proteins such as tubulin, as well as to deoxy sickle cell hemoglobin at high inorganic phosphate concentrations. In contrast, when polymerization is weak, there is no phase separation at the alignment transition at all. This result may be applicable to sickle cell hemoglobin at ordinary inorganic phosphate concentrations. An intermediate degree of phase separation, such as is seen generally for thin polymers, occurs only over a limited range of conditions for thick polymers. (Supported by NIH grant HL-30632).

W-Pos27 HYDROSTATIC PRESSURE EFFECTS ON SYNTHETIC THICK FILAMENT DISAGGREGATION Santa J. Tumminia, Jane F. Koretz, and Joseph V. Landau, Biology Dept., Rensselaer Polytechnic Institute, Troy, NY 12181

Many soluble proteins, such as actin, show an increase in volume upon aggregation. Thus, the application of hydrostatic pressure to such systems will result in partial or complete dis-aggregation, while the release of pressure will allow reaggregation to occur. This technique is currently being used by us for the study of the myosin aggregation mechanism, since myosin has been reported to show a large volume increase upon aggregation. Pressure was applied to separate samples at multiples of 2000 psi up to 10,000 psi, held there for 2 minutes, then rapidly released (less than 10 msec); populations were then characterized by electron microscopy. Our preliminary results indicate: (A) Average filament length decreases with increasing pressure; (B) The post-pressure populations consist of two separate sub-populations which can be distinguished by clear differences in filament diameter and negative stain retention; (C) Statistical analysis of each of these sub-populations indicates that they also differ significantly in average length and length distribution, with the thinner filaments exhibiting the shorter length and sharper distribution; (D) If the filaments are cycled several times between 15 and 10,000 psi, the "fat" filament average length decreases, while "thin" filament characteristics remain unchanged. These results suggest that the "thin" filaments go through the complete aggregation process upon pressure release (i.e., nucleation and elongation), while the "fat" filaments do not.

W-Pos28 NON-ENZYMATIC GLYCOSYLATION OF COLLAGEN ALTERS FIBRIL STRUCTURE. Shizuko Tanaka, Gad Avigad, Barbara Brodsky, Eric Eikenberry. UMDNJ-Rutgers Medical School, Piscataway, NJ 08854.

Non-enzymatic glycosylation of various proteins throughout the body occurs when glucose in its open-chain form reacts with lysyl residues to form a Schiff base which spontaneously rearranges to give a stable adduct. Increased amounts of such glycosylation may be the molecular basis of the wide range of clinical manifestations associated with diabetes, where the concentration of glucose in the serum is elevated. Using an in vitro system, incubation of rat tail tendon in various sugar solutions resulted in non-enzymatic glycosylation of collagen. The degree of glycosylation increased with time and depended on the sugar used, being proportional to the aldehyde available for reaction for a given sugar. Ribose was chosen for further studies because it gave the most convenient time course. X-ray studies indicated that the attachment of ribose to lysine and hydroxylysine residues altered the crystalline packing of collagen in rat tail tendon, and the degree of structural change was correlated with the degree of non-enzymatic glycosylation. At low levels of glycosylation, the molecular packing remained crystalline but the unit cell dimensions increased, suggesting the molecules have moved apart. At higher levels of glycosylation, the crystalline structure was disrupted as the distance between the molecules became larger. The axial meridional D period remained unchanged in all cases, but the intensities of the 14th, 16th and 18th meridional orders increased with increasing glycosylation, suggesting that specific changes occurred in the axial electron density distribution. Analysis of these structural alterations and their correlation with chemical localization of the ribose attachment sites may clarify the molecular interactions stabilizing collagen fibrils and the molecular basis of connective tissue abnormalities in diabetes.

W-Pos29 K^+, NA^+ AND MG^{++} IN HUMAN LYMPHOCYTES PERMEABILIZED BY BRIJ DETERGENT. W. Negendank, Department of Medicine, Wayne State University, Detroit, MI 48201.

Considerable evidence suggests that K^+, Na and Mg^{++} control protein-nucleic acid and protein-protein interactions within the nucleus. We adopted a "mild" detergent technique for the preparation of isolated nuclei that retain a large fraction of their proteins. Peripheral blood lymphocytes were placed into 250 mM sucrose with 10 mM tris, 3 mM $MgCl_2$, and 0.2% Brij-58 (pH 7.2, 37°C.). Within 5 min., all surface, nuclear and organelle membranes were removed, as documented by EM. 99-100% of cells were permeable to trypan blue. At 5 min. the cells retain cytoplasm surrounding the large intact nucleus. Cells were packed at 6000 g; water content was determined by drying and ions by atomic absorption. Trapped medium in the pellet was between 10 and 20% of wet pellet weight, but not directly measured since the cells are permeable to probe molecules. Permeabilized cells retain near-normal levels of K^+ (115 mmoles/kg wet weight), Na^+ (28 mmoles/kg) and Mg^{++} (12 mmoles/kg) for 20 min. They then lose 80% of their K^+, with a half-time of 5 min., but retain most of their Na^{++} and all of their Mg^{++}. After 35-40 min., K^+ (30 mmoles/kg), Na^+ (19 mmoles/kg) and Mg^{++} (14 mmoles/kg) are constant, with medium ions of 0.1 mM K^+, 0.7 mM Na^+ and 2.9 mM Mg^{++}. The loss of K^+ occurs much too slowly to be simple diffusion. It could be explained by collapse of a Donnan equilibrium, desorption of bound K^+, or loss of proteins that bind K^+. Studies of permeabilized cells in media of various concentrations of K^+ and Na^+ suggested that Donnan equilibria were not occurring. In view of this, and results of prior studies in intact lymphocytes (BBA 694:123, 1982), we suggest that K^+ retained for 20 min. in permeabilized cells, as well as most Na^+ and Mg^{++}, are in fact bound to proteins, primarily in the nucleus.

W-Pos30 RAMAN SPECTROSCOPY OF INTACT LYMPHOID CELLS T.J. O'Leary, E.S. Jaffe, T.J. Triche and I.W. Levin, National Institutes of Health, Bethesda, Maryland

We have acquired and analyzed Raman spectra of lymphocytes from four well-characterized cell lines (Raji, Cem, Molt and Daudi). Cells were cultured in RPMI 1640 culture medium at 37°C, harvested under steady state growth conditions and concentrated by centrifugation. Lymphocytes were maintained at 0°C during acquisition of the spectra. Each lymphocyte cell line exhibited spectral features which were reproducible and unique to that line. Spectral features in the 700 - 1700 cm^{-1} region were due primarily to cellular proteins, amino acids and nucleic acids, while features in the 2800 - 3100 cm^{-1} C-H stretching mode region reflected cellular proteins and lipids. B-lymphocytes derived from Burkitt's lymphoma (Raji, Daudi) had lower cellular carotenoid contents, reflected in the intensity of resonance-enhanced vibrational modes at 1157 and 1525 cm^{-1} than did T-lymphocytes derived from acute lymphocytic leukemia (Cem, Molt). Since membrane-associated carotenoids may play a role in protecting cellular contents from oxidation, this difference may reflect differences in the metabolic characteristics of B- and T- lymphocytes. Alternatively, it may reflect differences in the total membrane lipid contents of the cells.

W-Pos31 PHYSICAL BIOCHEMISTRY OF DEFORMATION OF BOVINE RETICULAR DERMIS.

Paul L. Kronick, Bohdan Artymyshyn, and Peter Buechler. (Intr. by Eric Murer)
Eastern Regional Research Center, U. S. Department of Agriculture, Philadelphia, PA 19118.

The resistance of fibrous tissue to deformation depends on the changing configuration of the fibers, their chemical structures, and the osmotic properties of the interfibrillar matrix. In bovine reticular dermis, the fibers form a three-dimensional network with a preferred fiber orientation about 45° to the hide surface. We measured the storage and loss components of the dynamic modulus $E^* = E' + iE''$ at small, non-perturbing deformations ($\Delta L/L=10^{-3}$) and related them to the biochemical environment and to the configurations of the fibers determined by X-ray diffraction and laser light scattering. Both the storage modulus E' and the loss modulus E" increase by as much as two orders of magnitude as the tissue is stretched by only 15%. The behavior was modelled as an assembly of slack fibers with distributed contour lengths imbedded in an isotropic, osmotically active matrix. We find that the second model, in which crimped fibers are made taut and so are recruited into contributing to the small-deformation incremental modulus as an affine transformation is applied to the tissue geometry, completely explains the changes in E* that are observed. Both components of modulus decrease by an order of magnitude at extremes of pH (<5 or >9), but only if the water content is permitted to increase. The changes are smaller, but are not eliminated, if the matrix proteoglycans are removed or if the water content is held constant. The dynamic mechanical properties of this tissue under various chemical and physical conditions then are quantitatively described by osmosis and by fiber recruitment.

W-Pos32 CATIONIC DYE BINDING BY OLIGOSACCHARIDES OF SODIUM HYALURONATE.

R. E. Turner and M. K. Cowman, Chem. Dept., Polytechnic Institute of N.Y., 11201

Oligosaccharides were obtained from sodium hyaluronate by enzymatic digestion with bovine testicular hyaluronidase. The enzymatically digested material was chromatographed on a BioGel P-30 column. By this method oligosaccharides containing up to approximately 25 disaccharide units are separated, allowing the molecular weight distribution of the digest mixture to be determined. Digest mixture samples were also subjected to analysis by polyacrylamide gel electrophoresis. The anionic hyaluronic fragments (of constant charge to mass ratio) are separated in a manner similar to that observed for DNA fragments. The electrophoretic pattern is visualized by staining with any of a number of cationic dyes. The chromatographic and electrophoretic profiles differ as a result of a marked chain length dependence in dye binding. Oligomers smaller than 7 disaccharide units did not bind any dye tested, whereas species larger than 12-30 disaccharides bind dye in approximate proportion to their concentrations. There may be a requirement for dye binding to hyaluronate oligomers which is not fulfilled by the smaller oligomers. The higher molecular weight oligomers may be capable of chain-chain association leading to an increase in linear charge density necessary for effective dye binding. Alternatively, this chain length dependent phenomenon may represent a change from simple electrolyte to polyelectrolyte behavior. Oligomers of sufficient size to mimic polymer behavior may serve as useful models for the study of hyaluronate in solution. (Supported by NIH Grant EY 04804).

W-Pos33 VIRAL PROTEIN STRUCTURE ELUCIDATED BY SOLID STATE NMR.

D. M. Schneider, K. M. Valentine, and S. J. Opella. "(Intr. by P. Lu)".

The structure of the fd coat protein backbone is being determined by solid state NMR methods. The viral filament containing 2700 copies of this molecule orients along an applied magnetic field allowing extraction of angular information from anisotropic spin interactions. Defined sites can be probed through biosynthetic incorporation of labeled amino acids containing a variety of spectroscopically interesting nuclei.

The 15N chemical shift anisotropy(CSA) as well as 15N - 1H and 15N - 13C dipolar couplings have been measured in one and two dimensional experiments. These experiments yield the angular orientations of CSA tensor elements and bond vectors with respect to the viral filament. A set of angles is generated which can orient individual peptide bond planes with respect to a common axis system mapping out a three dimensional structure.

The NMR data show that the coat protein in the virus is almost entirely α-helix with segments that vary somewhat in their orientation with respect to the viral filament. Residues 25 - 33 for example are tilted at a 20° angle, residues 34 - 38 are parallel, and residues 39 - 45 are oriented at an angle of 8°.

W-Pos34 MOLECULAR DYNAMICS SIMULATION OF PARVALBUMIN WITH A MULTIPLE TIME STEP METHOD

O. Teleman, P. Ahlström and B. Jönsson (Intr. by S. Forsén), Physical Chemistry 2, Chemical Centre, University of Lund, P.O.Box 124, 221 00 LUND, Sweden.

The dynamic behaviour of the carp muscle calcium binding regulatory protein parvalbumin (homologous to calmodulin and troponin C) has been simulated in vacuo and in aqueous solution. The simulations were made using a multiple time step method (Teleman & Jönsson, to be submitted) in which bond forces were evaluated every 0.2 fs ($1fs=10^{-15}s$) while angular and nonbonded interactions were evaluated every 1.0 fs. Semiempirical Lennard-Jones and bond parameters were used and the electrostatic interactions were taken into account by assigning partial charges to each atom.

The first in vacuo simulation was made with the two calcium binding sites occupied whereas the second was made with both sites unoccupied. Both of these simulations covered a period of 110 ps. The simulation in aqueous environment was made with the two calcium binding sites occupied and counterions present so as to achieve electroneutrality. In all cases the X-ray structure of the protein was used as starting configuration.

W-Pos35 ELECTRO-ACOUSTICAL PROPERTIES OF MICROTUBULES CAN EXPLAIN THE GEOMETRY OF PERICENTRIOLAR STRUCTURES (PCS) AND DYNAMIC ACTIVITIES.

Djuro L. Koruga,Ph.D. and Stuart R. Hameroff,M.D. Dept. of Anesthesiology, Univ. of Arizona HSC, Tucson, AZ 85724

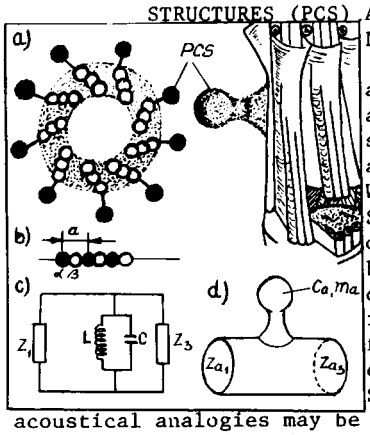

Microtubules (MT) are polymers of subunit dimers of equal weight α and β tubulin. MT possess crystal characteristics since the subunits are arranged on a cylindrical surface by sphere packing of the Oh ($\bar{6}/4$) symmetry group law. Because tubulin subunits contain more acidic amino acids than basic, surplus electrons can lead to capacitance behavior. With available thermal energy, α and β tubulin subunits should oscillate. Since the masses of α and β tubulin are approximately equal, the photon-optical and phonon-acoustical frequency (ω^+ and ω^-) characteristics will be equal when the frequency wave vector ($q/2\pi$) is $\frac{1}{2}a$ (where a is the distance between α and β tubulin centers - fig.b). Interactions among ions (Mg^{++}, Ca^{++}...), and MT subunits may result in functional electric fields in MT which may be induced in other proteins or structures (dynein, actin...). In figure c, these are viewed as an LC parallel circuit. Since α and β tubulin masses are equivalent and for $q/2\pi=\frac{1}{2}a$ electro-acoustical analogies may be used. Thus the electrical circuit [$1/Z_2=1/j\omega L + j\omega c$] has an analogous acoustic form [$1/Za=1/j\omega Ma+j\omega Ca$] with a physical component as in fig.d. Electro-acoustic analogy can explain perpendicular geometries such as local thickenings of ciliae and pericentriolar structures. Electro-acoustic properties of MT can also explain dynamic organization and information processing.

W-Pos36 CHANGES IN MEMBRANE STEADY STATE POLARIZATION AND OTHER PROPERTIES IN RESPONSE TO FREE RADICAL-INDUCED INJURY.

B.F. Dickens, I.T. Mak, J.H. Kramer and W.B. Weglicki, Cardiovascular Research Program, Oklahoma Medical Research Foundation, Oklahoma City, Okla., 73104.

The interaction of exogenous free radical generating systems with membrane physical properties was investigated in vitro. The fluorescent probe 1,6-diphenyl-1,3,5-hexatriene was used in steady state fluorescence polarization experiments to determine the effects of exogenously supplied free radicals on biological membranes. We used the following free radical generating systems in these experiments; 1) Dihydroxyfumarate (DHF) and 2) Fe^{3+}-ADP + DHF. We found that the fluorescence polarization increased in mammalian cardiocyte microsomes and sarcolemma, as well as in mammalian hepatic lysosomes in response to these free radical systems. The time course and extent of the increase in fluorescence polarization in response to these exogenously provided free radical systems appear to correlate with the extent of lipid peroxidation, as measured by malondialdehyde formation and with the loss of membrane function. The free radical generating systems also induce an apparent increase in lysosomal size as measured by a Coulter Sub-micron Particle Analyzer. Plots of the polarization versus temperature for all three membranes displayed thermotropic inflection points in the range of 9-14°C and 20-25°C. Preliminary results with sarcolemma suggest that exposure to exogenously supplied free radicals results in significant smoothing of these inflection points. These results suggest that free radical induced membrane injury may be mediated in part through effects on membrane physical properties.

Supported by NIH grants HL-32776 and HL-28985.

W-Pos37 SUBSTRATE DEPENDENCE OF METABOLIC STATE AND CORONARY FLOW IN PERFUSED RAT HEART. Joseph W. Starnes, David F. Wilson, and Maria Erecińska, Dept. of Biochemistry and Biophysics and Dept. of Pharmacology, Univ. of Pennsylvania, Philadelphia, PA 19104.

The effect of substrate source on the regulation of energy metabolism and coronary flow was studied in isolated perfused rat hearts. Compared to glucose-perfused hearts, those perfused at the same work load with palmitate or acetate demonstrated increases ($P<0.01$) in oxygen consumption of 16% and 18%, respectively, and increases ($P<0.01$) in coronary flow of 30% and 32%, respectively. Parallel substrate-related changes occurred in the levels of high energy phosphate compounds: tissue creatine, ADP_{free}, and inorganic phosphate (Pi) were significantly decreased, leading to increases ($P<0.01$) in the [creatine phosphate]/[creatine] and $[ATP]_{free}/[ADP]_{free}[Pi]$ ratios. These changes were accompanied by increased reduction of intramitochondrial pyridine nucleotides. To allow comparison of our measurements of metabolites in freeze clamped hearts with related studies that employed NMR methodology we perfused some hearts with phosphate-free media. Omitting orthophosphate from the perfusate lowered intracellular Pi and modified cardiac function, but the substrate-related differences were similar to those in media containing Pi. Substrate-dependent differences were observed in intracellular pH which may contribute, in some instances, to differences in energy metabolism and coronary flow. When work load was altered in glucose- and acetate-perfused hearts, both oxygen consumption and coronary flow were linearly related to cytosolic $[ATP]_{free}/[ADP]_{free}[Pi]$ and the slopes of the regression lines were similar for both substrates. These correlations support the view that $[ATP]_{free}/[ADP]_{free}[Pi]$ is a major determinant of oxygen consumption by cardiac cells and of coronary flow.

Supported by NIH Grant GM 21524

W-Pos38 IONIC CONDUCTANCE OF PHOTORECEPTOR MEMBRANES AND PHOSPHOLIPID VESICLES MEASURED WITH A PHOSPHONIUM SPIN-LABEL. David M. Ojcius and Wayne L. Hubbell, Jules Stein Eye Institute, UCLA School of Medicine, Los Angeles, CA 90024.

Spin labeled hydrophobic ions have previously been used to measure the proton resistance of phospholipid vesicles (Cafiso and Hubbell, Biophys. J. 44:49, 1983). Since the EPR spectra of membrane-permeable phosphonium spin labels are a function of the equilibrium transmembrane potential, the H+ current and hence the current-voltage curve is obtained by quickly creating a transmembrane pH gradient and measuring the time-dependent potential that develops. The current-voltage curve is linear with a resistance of 3 X 109 ohm-cm2.

In an extension of this approach, we have recently measured the conductance of alkali cations and halide anions in photoreceptor membranes and phospholipid vesicles. These conductances can be determined by establishing a pH gradient and observing the effect of the ion of interest on the time-course with which the H+ diffusion potential develops. It was found that the Cl- resistance of phosphatidylcholine vesicles is 5 X 108 ohm-cm2 (50 mM Cl-) and its conductance is proportional to its concentration at low concentrations. Br- is twice as permeable as Cl-, and the Na+ and K+ conductance is too low to be discerned with our method.

The proton resistance of photoreceptor membranes is 1 X 107 ohm-cm2, and its current-voltage curve is also ohmic. There is very little difference between 150 mM Na+, K+, or Li+, with a resistance of 5 X 107 ohm-cm2. Cl- is twice as permeable as the alkali cations, and Br- four times as much. No light or c-GMP effects were observed for any of these ions. These results will be compared with the anomalous behavior of reconstituted rhodopsin/phospholipid membranes.

W-Pos39 THE PERMEABILITY OF RED CELLS TO AMINE SPIN PROBES

A. Paul Todd, Robert I. Macey, and Rolf J. Mehlhorn
Department of Physiology-Anatomy, U.C. Berkeley, CA 94720

Models for the permeability of cell membrane lipid bilayers to nonelectrolytes remain largely untested because of the difficulty of measuring all the relevant parameters for a particular solute. Water soluble ESR spin probes are useful as model solutes because their membrane partitioning and permeability may be measured by fairly straightforward methods. In addition, spin probes yield information about where in the membrane they partition.

We have measured the red cell permeabilities for a homologous series of amine nitroxides: Tempamine, Methyltempamine and Dimethyl tempamine. Cells were suspended in an impermeable paramagnetic line broadening agent such as ferricyanide. Upon rapid mixing of the probe, the kinetics of emergence of the internal protected signal allowed calculation of the permeability of the neutral amine. These permeabilities correlate well with probe partitioning in hydrophobic solvents such as hexadecane, but not with average partition coefficients in red cell membranes. This suggests that diffusion through the hydrocarbon interior is the principal energy barrier in permeation.

The membrane hyperfine splittings indicate a uniformly polar environment for all three probes, suggesting that they partition primarily to the region of the polar headgroups. To determine more precisely the depth of partitioning of these probes in the membrane one can utilize the through-space dipolar interaction of paramagnetic transition metal ions with nitroxides. The extent of dipolar line broadening is proportional to proximity of the probe to the membrane/water interface. The results of these measurements will be reported. (Supported by Grants NIH18819, AG04819).

W-Pos40 HIGH RESOLUTION ^{23}Na NMR STUDIES OF HUMAN ERYTHROCYTES: ^{23}Na NMR-INVISIBILITY.

Jane K. Schreiber, John R. Sachs, and Charles S. Springer, Jr., Department of Chemistry and Hematology Division, School of Medicine, State University of New York at Stony Brook, NY 11794

The ^{23}Na NMR spectrum of washed, packed human erythrocytes suspended at different hematocrits was investigated under high resolution conditions at 79.4 MHz. The erythrocyte suspensions contained a membrane impermeable, aqueous shift reagent in the extracellular space which allowed us to discriminate between the intra- and extracellular ^{23}Na NMR signals. At a constant shift reagent concentration, the chemical shift difference between the intracellular and extracellular Na resonances is decreased and the extracellular Na resonance broadened with increasing hematocrit. The measurements of the areas under the peaks (after curve resolution) were used along with NMR calibration curves and the measured hematocrits to determine the NMR-visible intra- and extracellular Na^+ concentrations. Complete separation of the intra- and extracellular phases using repeated centrifugations and subsequent analyses by atomic absorption and flame photometric methods showed that extracellular Na became progressively NMR-invisible with increasing hematocrit (up to 98%) while intracellular Na remained essentially 100% NMR-visible. It may be that, at increased hematocrits (>80%), the ^{23}Na NMR-invisibility is due to an increased fraction of Na^+ binding to sites on the outer surface of the erythrocyte membrane as the volume of the extracellular space is decreased.

W-Pos41 **^{1}H – AND ^{13}C – NMR STUDIES OF DRUG (CETIEDIL)-ERYTHROCYTE MEMBRANE INTERACTION**

C. Narasimhan and L. W.-M. Fung, Department of Chemistry, Loyola University of Chicago, Chicago, IL 60626

Cetiedil is a membrane drug that exhibits antisickling effects on deoxygenated sickle red blood cells. Its effectiveness in antisickling is believed to be due to its ability to cause hemoglobin dilution in red blood cells. We have measured the ^{1}H NMR relaxation times (T_2) of water to study the effect of cetiedil on the diffusional water permeability of human red blood cells. The water exchange time is monitored as a function of cetiedil concentration at 20 and 37C in order to understand the effect of cetiedil on water transport in erythrocytes. We have also investigated the cetiedil-membrane interaction using high-resolution ^{13}C – NMR. NMR spectra of cetiedil in the presence and absence of membrane ghosts at 20 and 32C were obtained. The resonances in the spectra of cetiedil in the presence of membrane are generally broadened when they are compared with those in the spectra of cetiedil in buffer or in glycerol solution which has viscosity higher than that of membrane samples. The carbonyl and aromatic resonances of cetiedil are more affected by membrane addition than the resonances in the aliphatic region. These broadenings are likely due to motional restriction of selective moieties in the cetiedil molecule by membrane components. The mode(s) of cetiedil action on erythrocyte membranes will be discussed based on these NMR results and our earlier studies of cetiedil by EPR and UV spectroscopy.

(Supported in part by grants from NIH (HL-01190 and HL-31145.)

W-Pos42 SLOW AND RAPID PASSAGE PARAMAGNETIC RESONANCE FROM SINGLE-COMPONENT LIPOXYGENASE SPECIES.

D. V. Mavrophilipos and B. J. Gaffney. Johns Hopkins University, Baltimore, MD 21218.

Lipoxygenases are non-heme, non iron-sulfur proteins that oxidize unsaturated fatty acids to hydroperoxides. Soybean lipoxygenase is the most studied, but lipoxygenases have also been isolated from other sources such as rabbit reticulocytes. We have used EPR to examine the multiple iron environments in oxidized soybean lipoxygenase. Samples exhibiting single-component EPR spectra of several types have been prepared. Oxidation with highly purified linoleate hydroperoxide and gel filtration gives an active, ferric lipoxygenase in which >90% of the EPR visible iron has a single spectrum which may be computer simulated with g-values for high spin iron with $\lambda = 0.047$ ($g_{xx} = 4.9$; $g_{yy} = 7.1$; $g_{zz} = 1.0$). Another well-defined state of lipoxygenase occurs in the oxidized enzyme complex with the alcohol decomposition product of linoleate hydroperoxide. Here a sharp signal indicative of an axial, ferric environment is seen, as reported earlier by Slappendel et al. (BBA, 708, 259 (1982)). Because multicomponent-EPR spectra are seen for many biochemically important samples of lipoxygenase, we have studied ways in which conditions of rapid, adiabatic passage allow components of the EPR spectra to be examined separately. Sensitivity of the passage spectra is >10 times that of the slow-passage ones. Due to different T_1's for the multiple components, the phase angles by which the adiabatic, rapid passage spectrum lags the slow passage one differ among the components. For instance, detection of the second, harmonic, 90° out-of-phase spectrum at 10 mW of power enhances the ratio of signal from the axial (g = 6.0) component to that giving g = 7.1 by a factor of 6 compared to the ratio in the first harmonic in phase spectrum.

Supported by NSF, PCM 83-03948.

W-Pos43 ENDOR OF IMIDAZOLE-LIGATED LOW SPIN FERRIC HEME SYSTEMS. C. P. Scholes and K. M. Falkowski, Dept. of Physics, SUNYA, Albany, NY 12222; C. T. Martin and S. I. Chan, Dept. of Chem., Caltech, Pasadena, CA 91125.

ENDOR of these systems has yielded evidence for previously unseen nitrogen hyperfine couplings to axially-liganded imidazole. Bis-imidazole complexes were prepared either with model porphyrins or as the imidazole adduct of metmyoglobin, and these had either naturally abundant ^{14}N-imidazole or isotopically-enriched ^{15}N-imidazole. It is clear from the accompanying figure that we have observed ENDOR from ^{15}N on imidazole. We have also obtained ENDOR from cytochrome a of yeast cytochrome c oxidase which was grown on ^{15}N-histidine and have unambiguously identified histidine as a ligand of cytochrome a.

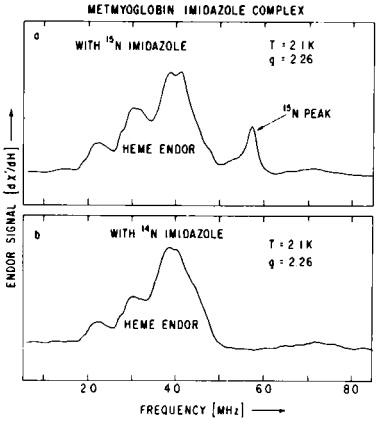

Using selective deuteration, we have assigned protons on the porphyrin periphery and have noted at the porphyrin periphery of bis-imidazole ferric tetraphenyl porphyrin a surprising loss of 4-fold electronic symmetry. In bis-imidazole porphyrin models, myoglobin imidazole, cytochrome b_5, or cytochrome a, the best resolution of imidazole proton ENDOR occurs at characteristically different electronic g-values for the respective systems. We intend to link this characteristically different resolution with an imidazole orientation that differs from one system to the next.

W-Pos44 REDOX ACTIVE COMPONENTS OF FORMATE DEHYDROGENASE FROM CLOSTRIDIUM PASTEURIANUM Roger C. Prince, Chi-Li Liu, T. Vance Morgan and Leonard E. Mortenson, Exxon Research and Engineering, Route 22 East, Annandale, NJ 08801

Formate dehydrogenase from C. pasteurianum catalyzes the reversible interconversion of CO_2 and formate, although in vivo it functions to fix CO_2. It has two subunits of 76 and 34 KD, and contains pterin, 2Mo, 24 non-heme Fe and 28 acid labile S. Twenty of the Fe can be extruded as Fe_4S_4 clusters (Liu and Mortenson, 1984, J. Bact. 159, 375). Redox titrations reveal three epr active species in the native, functional enzyme. Two have properties appropriate for "ferredoxin like" iron sulfur clusters: one has apparent g values of 1.87, 1.95 and 2.05, E_{m8} - 318 mV, the other is more axial with apparent g values of 2.05 and 1.92, E_{m8} -372 mV. Enzyme stability seems to require that the former center be maintained in the reduced form. The lower potential component is reducible by the substrate formate. In four preparations, the maximal amount of each signal integrated to 0.3 spin per enzyme. An additional signal near g2 was also visible in the reduced form. This component, with E_{m8} -150 mV, integrated to 0.8 spins per enzyme, and was isotropic at low temperature (apparent g = 2.005, ΔH = 1.25 mT). On warming, the zero crossing shifted slightly upfield, and additional structure appeared on the wings of the central feature. This species did not change on addition of substrate. Formate dehydrogenase from C. pasteurianum thus has rather different potentiometric and epr properties from other molybdo-pterin enzymes.

W-Pos45 NMR STUDIES OF THE E. COLI cAMP RECEPTOR PROTEIN

J. M. Karohl and W. R. McClure, Dept. Biological Sciences, Carnegie-Mellon University, Pittsburgh, PA 15213.

CRP (cyclic AMP receptor protein), with its cofactor cAMP, mediates the transcriptional regulation of a number of genes in E. coli. The CRP-cAMP complex acts by binding specifically to sites near promoters, and in particular activates the transcription of catabolite sensitive genes. The focus of our work is the basis of the specificity of the CRP-cAMP and CRP-DNA interactions. We have taken advantage of the phosphorous atom of cAMP and ^{31}P NMR to probe the ligand binding site. We have used ^{1}H NMR to assess the extent of conformational change induced by ligand binding, and to investigate hydrogen bonded protons. The relationship between the fractional saturation of the dimeric protein by cAMP, and the extent of the resulting conformation change will be discussed. Some characterization of CRP mutants with altered ligand-binding specificities will also be presented.

W-Pos46 MULTINUCLEAR NMR STUDIES OF PROTEOGLYCAN-CATION INTERACTIONS by LAURA LERNER intr. by DENNIS TORCHIA

We have used NMR spectroscopy of quadrupolar nuclei (^{23}Na, ^{39}K, ^{25}Mg, and ^{43}Ca) to study the nature of the interactions between cations and cartilage proteoglycans, in solution and in intact tissue. T_1, T_2, and lineshape for quadrupolar nuclei depend on the electric field gradient at the nuclei and the average correlation time of the nuclei. In addition to shortening relaxation times, an increase in correlation time may push the nuclei out of the extreme narrowing limit. Neither sodium nor potassium interact strongly with bovine nasal proteoglycan aggregates or their substituent GAG's in solution. The observed decreases in T_1 and T_2 depend on the concentration of polymer. Spectral parameters of sodium are affected to the same extent whether the polymer is charged or neutral. Sodium does interact strongly with heparin, which has a higher charged density than chondroitin sulfate. In intact bovine nasal and articular cartilage, ^{23}Na lineshapes are best fit by two superimposed Lorentzians. Possibly sodium exists in two environments with different average concentrations of GAG's. The relaxation times for ^{25}Mg and ^{43}Ca depend on polymer concentration, but GAG's are more effective at enhancing relaxation than is Ficoll, a neutral polymer, indicating an electrostatic contribution to the interaction. Also, T_2 is always significantly shorter than T_1 for these divalent cations in the presence of polymer; whereas they are equal, within experimental error, for sodium even when sodium is chelated to an organic molecule.

W-Pos47 TOTAL SOLVENT PEAK SUPPRESSION IN HIGH RESOLUTION NMR

T. M. Eads, M. Nath & R. G. Bryant, Radiology Department, Box 648, University of Rochester Medical Center, Rochester, New York 14642

The magnetic field dependence of paramagnetically induced solvent proton relaxation is not widely appreciated, but suggests a simple method for achieving total suppression of water proton signals, thus solving the dynamic range problem and providing the opportunity for exploring the solute spectrum under the solvent peak. In the presence of low concentrations of certain paramagnetic complexes, application of the CPMG pulse sequence $90\text{-}(\tau\text{-}180\text{-}\tau)_n\text{-ACQ}$ where τ is a few ms and n sufficient for the solvent contribution to dephase completely in the transverse plane, yields excellent suppression of the solvent resonance without selective irradiation methods and with retention of the usual high resolution appearance of the spectrum. Results using two fundamentally different types of paramagnetic reagent at low concentration will be presented. This method appears to have wide application to the study of aqueous solutions including in vivo investigations.
This work was supported by the National Institutes of Health, GM-29428 and GM-34541, and the National Science Foundation PCM-8106054.

W-Pos48 ^1H NMR STUDY OF HEME POCKET MOBILITY IN HEMOGLOBIN. Kyouhoon Han and Gerd N. La Mar, Department of Chemistry, University of California, Davis.

The exchange characteristics of proximal histidyl (F8) N_1H protons have been examined by the ^1H NMR hydrogen exchange technique to investigate dynamic mobility of the heme pocket in Hb A as well as in several modified and mutant Hbs. For all Hbs studied, the kinetic inequivalence of two different heme pockets is clearly manifested in such a way that the proximal side of the alpha heme pocket shows a higher mobility than that of the beta. Heme pocket mobility is higher in oxy or R-state than in deoxy or T-state. An interesting correlation exists between the oxygen affinity of Hb and the heme pocket mobility, reflected in the hydrogen exchange rate constants. From the pH dependence study of exchange rates, mechanisms of exchange for F8 N_1H were obtained. The exchange in the beta subunit can be described by a simple EX_2 mechanism with a first-order pH dependence while that in the alpha subunit follows the same mechanism but shows a non-first order pH dependence. The equilibrium constants as well as free energy changes corresponding to exposure of F8 N_1H to solvent were calculated.

W-Pos49 ^{1}H NMR STUDY OF THE EFFECT OF ISOCITRATE ON NUCLEOTIDE BINDING TO NADP^{+}-DEPENDENT ISOCITRATE DEHYDROGENASE. Robert S. Ehrlich and Roberta F. Colman. Department of Chemistry, University of Delaware, Newark, DE 19716.

The substrate manganese-isocitrate enhances the binding of nucleotide fragments to pig heart NADP^{+}-dependent isocitrate dehydrogenase and substantially weakens the binding of NADPH. Line broadening of the resonances of adenine ring protons, the 1'-adenine ribose proton and nicotinamide ring protons (of NADPH) was used to determine dissociation rates. Substrate increases the dissociation rate of NADPH from < 7 sec^{-1} to 60 sec^{-1}. In contrast, the dissociation rates of 2'-phosphoadenosine 5'-diphosphoribose and adenosine 2',5'-bisphosphate are reduced tenfold. Possible changes in the conformations of bound nucleotides were explored using transfer of nuclear Overhauser effect (NOE) between free and bound molecules. Distance determinations based upon NOE are consistent with a syn conformation of the adenine-ribose glycosidic bond with or without isocitrate present. Likewise, the nicotinamide-ribose conformation is anti with or without substrate. Selective irradiation of protons in the enzyme indicate proximity of methyl groups and either a non-titrating histidine or aromatic residue to the adenine ring without any substantial changes produced by isocitrate. Alterations in enzyme-nucleotide conformation produced by substrate must involve either small shifts in the positions of the amino acid side chains or changes in groups not visible in the proton NMR spectrum. (Supported by USPHS and Delaware Heart Association)

W-Pos50 THE USE OF NMR SCANNING TO STUDY THE EVOLUTION OF THE BONE CALLUS. J.T. Ruszkowski, R. Damadian. Program in Biophysics, Downstate Medical Center, Brooklyn, New York 11203

Volunteers have been examined by nuclear magnetic resonance scanning. Appropriate imaging parameters as well as scanning techniques have been developed which demonstrate the capability of NMR imaging to differentiate between bone and soft tissues. In addition, a unique determination of the spin-lattice relaxation time, T_1, of a localized volume has been developed which enables quantitative measurement of T_1 rather than estimation through computed T_1 images. The use of NMR scanning coupled with precise T_1 measurements holds promise in the evaluation of the repair of bone fractures. NMR scanning may be used to: 1) non-invasively monitor the healing process of fractures while the limb is encased in plaster, and 2) predict fracture union.

W-Pos51 PROTON NMR INVESTIGATION OF HEMOGLOBIN IN H_2O: BROADBAND NON-SATURATING SOLVENT SUPPRESSION USING SOFT PULSES, by C. Yao, A. K.-L. C. Lin, and C. Ho, Department of Biological Sciences, Carnegie-Mellon University, Pittsburgh, PA 15213, U.S.A.

Two downfield, well-resolved exchangeable resonances (~70 ppm downfield from H_2O) in the proton nuclear magnetic resonance (NMR) spectra of human normal adult hemoglobin (Hb A) have previously been assigned to the NH protons of the proximal histidyl residues of the α and β chains. These residues are directly bonded to the heme iron and the two resonances are seen only when the heme iron is in the paramagnetic ferrous state. They offer a unique opportunity for examining by NMR chain-specified oxygen binding. Measurement of the exchangeable resonances should be carried out in H_2O which causes severe dynamic range problems. Currently known pulse techniques for solvent suppression suffer from one of the following three aspects: (i) high rf power is required; (ii) the effective bandwidth of suppression is too small; or (iii) the solvent line is saturated, with possible saturation transfer to the exchangeable resonances. We report a fast, non-saturating, low-power pulse sequence that achieves very broadband solvent suppression and simultaneously broadband maximal excitation of target resonances. The sequence has been optimized specially, based on the Bloch equations, to observe these two resonances. Only minimal rf power ($\gamma B_1/2\pi \sim 7$KHz) is required to cover the resonances at more than 20 KHz downfield from solvent water peak. The pulse repetition rate is limited by the T_2 of water and can be higher than 10 scans per second. 300 MHz ^{1}H NMR spectra of purified hemoglobin solutions and of whole blood are obtained. Preliminary results of saturation-recovery T_1 measurements and oxygen saturation studies are shown as examples of the application of the pulse sequence. [This work is supported by a research grant from the NIH (HL-24525)].

W-Pos52 KINETICS OF THE NEUTROPHIL METABOLIC BURST VIA ESR. F. W. Kleinhans and S. T. Barefoot, Dept. of Medical Research, Methodist Hospital, Indianapolis, IN 46202 and Dept. of Physics, IUPUI, Indianapolis, IN 46223.

Hydroxyl radicals produced during the metabolic burst of stimulated neutrophils may be readily detected by trapping the OH· with DMPO to produce a moderately stable spin adduct which is detectable via ESR. A curve of ESR signal strength, A, vs. time, t, is readily obtained but there are problems of interpretation. The metabolic burst lasts 5' to 10' with typical stimuli, e.g. opsonized zymosan. If the spin adduct lifetime were long compared with this time, >10', the ESR signal would be the net OH· production and if the spin adduct lifetime were short, ∿ seconds, the ESR signal would reflect the rate of OH· production. The actual situation is intermediate and greatly complicates the analysis. The tail end of A vs. t exhibits simple exponential decay with a time constant, tc, of 300 to 500 S. If this tc is assumed constant during the metabolic burst, A vs. t is readily deconvoluted to yield the true OH· production rate vs t. The results obtained yield very non physical rates for early times, suggesting tc varies and is shorter during the peak of metabolic activity. If ascorbic acid is added (∿ 0.1 to 1 mM), the decay time may be shortened according to (1/tc)obs. = (1/tc)natural + (1/tc)ascorbic acid. By varying the ascorbic acid concentration and measuring the reduction in ESR amplitude and shift of the A vs t peak to earlier times, an estimate of tc during the peak of metabolic activity may be obtained. We find a preliminary value of 30 to 60 S.

W-Pos53 31-P NMR OBSERVATIONS ON ISOLATED LENSES AND OF LENSES IN INTACT EYES C. Tyler Burt, H-M Cheng, P. Barnett, G. Gonzalez and L. T. Chylack, Jr. Tufts New England School of Veterinary Medicine, FrancisBitter National Magnet Laboratory, Mass. Institute of Technology, and Howe Laboratory of Ophthamology, Harvard Medical School, Boston, Massachusetts.

The 31-P NMR response of lenticular tissue to stress in isolated lenses bathed in either low oxygen, low glucose saline or low glucose "hypoglycemic" media and of lenses in enucleated eyes were followed as a function of time after introduction of the solution or of enucleation. The isolated lenses could be examined in conventional NMR tubes while the enucleated eyes were subjected to surface coil analysis. Several general trends could be documented: 1-ATP falls in all systems as a function of time of stress; 2-ADP can be seen most clearly in enucleated eyes and in the simple saline; 3-pH changes little or becomes more alkaline as has been reported by others; and 4-most interestingly the chemical shifts of ATP and ADP (where present) indicate that free magnesium decreased during the metabolic challenge. The last point is demonstrated by an increase in frequency between the beta and alpha resonances of ATP and a difference of at least 1 ppm between the beta phosphate of ADP and the gamma phosphate of ATP. In lenses incubated with "hypoglycemic" media these differences are less profound that with the other two systems but could be seen in some cases. This change in regulation of intracellular divalent metal ion concentration with metabolic stress represents a new aspect of lenticular biophysics that may have clinical as well as biochemical consequences.

W-Pos54 C-13 NMR ISOTOPE SHIFTS AND TETRAHEDRAL INTERMEDIATES FOR PEPTIDES BINDING TO PORCINE PEPSIN. Paul G. Schmidt, Mark W. Holladay, Francesco G. Salituro and Daniel H. Rich; Vestar Research Inc., Pasadena, CA 91106 (PGS) and School of Pharmacy, University of Wisconsin - Madison, Madison, WI 53106 (MWH, FGS, DHR).

The synthetic ketone peptide analogue of pepstatin, isovaleryl-L-valyl-[3-^{13}C]-(3-oxo-4S)-amino-6-methylheptanoyl-L-alanyl-isoamylamide is a strong inhibitor of aspartyl proteases. When the peptide is added to porcine pepsin in H_2O at pH 5.1, the ^{13}C NMR chemical shift of the ketone carbon moves from 208 ppm for the inhibitor in solution to 99.07 ppm when bound to the enzyme active site. In ^2H_2O the bound shift is 98.71 ppm, 0.36 ppm upfield. For the analogous experiment contrasting $H_2{}^{16}O$ and $H_2{}^{18}O$, the ^{13}C chemical shift was 0.05 ppm to higher field for the heavier isotope. These data show that water, and not an enzyme nucleophile, adds to the peptide carbonyl to yield a tetrahedral diol intermediate in the enzyme-catalyzed reaction. The above peptide is not isosteric with substrates; the (3-oxo-4S-amino-6-methylheptanoyl (statone) moiety is too large for one peptide bond and too small for a dipeptide. We incorporated the dipeptide isostere [4-^{13}C]-(2 R,5S)-5-amino-2,7-dimethyl-4-oxo-octanoic acid in place of statone and tested the ^{13}C NMR isotope shifts. For the change H_2O to ^2H_2O the bound shift is 0.30 ppm upfield and for $H_2{}^{16}O$ to $H_2{}^{18}O$ the shift was 0.04 ppm. These data again point to water as the nucleophile in forming a tetrahedral adduct for an isosteric ketone analog of pepsin substrates.

W-Pos55 IN-VIVO DETERMINATION OF LEAD IN THE TIBIA BY X-RAY FLUORESCENCE.* K. W. Jones, H. W. Kraner, and G. Schidlovsky, Brookhaven National Laboratory, Upton, NY 11973, and R. P. Wedeen, VA Medical Center, East Orange, NJ 07019 (Introduced by Jane K. Setlow)

The design parameters for an x-ray fluorescence apparatus for the in-vivo determination of bone lead in the tibia are presented. The method is based on the use of gamma rays from the decay of ^{109}Cd or ^{57}Co to fluoresce the characteristic K-x rays from lead. Calibration is accomplished by using the ratio of x rays to Rayleigh-scattered full energy gamma rays. The Rayleigh scattering is dominated by contributions from Ca and P so that the ratio is a direct measurement of the atomic ratio of Pb/(Ca + P). The ratio is also insensitive to positioning of the tibia since the detector solid angle does not enter into the ratio. Estimates of detection sensitivity were made by use of several types of phantoms. Minimum concentrations around 10 ppm can be determined with reasonable source strengths (25-100 mCi) and counting times. Results of the present investigation will be compared with the parameters of a similar device already reported by Somervaille, et al.[1] and other workers using similar devices.

1. L. J. Somervaille, E. E. Laird, D. R. Chettle, and M. C. Scott, Proc. Intern. Conf. on Heavy Metals in the Environment 1, 521 (1983), Heidelberg, July 1983.

*Supported by the Processes and Techniques Branch, Division of Chemical Sciences, Office of Basic Energy Sciences, US Department of Energy, Contract No. DE-AC02-76CH00016, and the Veterans Administration under Contract No. V561(134)S-81025.

W-Pos56 RAPID RELEASE OF PROTONS BY PHOTOLYSIS OF A BIOLOGICALLY INERT PRECURSOR, 2-HYDROXY-PHENYL 1-(2-NITRO)PHENYLETHYL PHOSPHATE, A 'CAGED-PROTON'. J.A. McCray, Dept. of Physics, Drexel University, Philadelphia, PA 19104, and D.R. Trentham, National Institute for Medical Research, The Ridgeway, Mill Hill, London NW7 1AA, U.K.

Many biological energy transducing processes are mediated by proton gradients across membranes. Mechanistic studies of these and other proton dependent biological processes would be facilitated by the availability of a rapid pulse of protons released photochemically at specific sites. We describe here the properties of a phosphate diester mono-anion that on photolysis generates a phosphate monoester dianion with concomitant release of a proton.

2-Hydroxyphenyl 1-(2-nitro)phenylethyl phosphate, 'caged-proton', was synthesized from o-phenylene phosphorochloridate and 1-(2-nitro)phenylethyl alcohol. When partitioned between chloroform and water caged-proton partitions into the aqueous phase, suggesting that it will not readily diffuse across biological membranes. Following a pulse of 300-350nm irradiation from a Chadwick Helmuth Strobex Model 238 Xenon arc flashlamp protons were released. The aqueous solution in a 4mm pathlength cell contained 0.4mM caged-proton, 1mM EDTA, 0.1mM tris, 1mM dithiothreitol and phenol red at pH 8.0. The quantum yield for the photochemical reaction was 0.4 ± 0.1. Proton release was analyzed spectrophotometrically at 565nm. At pH 8 protons were released in a biphasic manner; first a rapid phase (<1ms) within the time resolution of the apparatus followed by uptake of protons (corresponding to 20% of the rapid phase) at $20s^{-1}$. This slower process matched the rate of decay of the presumed aci-nitro intermediate characteristic of the photolysis of 2-nitrobenzyl compounds (McCray et al., Proc. Nat. Acad. Sci. 77 7237-7241, 1980). At pH 7 only the rapid release of protons could be detected. Support: NIH grant HL 15835, MDA, and MRC, U.K. J.A.M is a Fogarty Fellow.

W-Pos57 DYNAMIC MECHANICAL PROPERTIES OF HUMAN DERMAL FIBROBLASTS, Peter L. Dorogi and Leon M. Wilkins, Gillette Research Institute, Rockville, MD 20850

Propagation characteristics of low-amplitude mechanical (shear) waves have been previously used to measure the rigidity modulus and shear viscosity of living human tissue (Potts et al., J. Biomechanics, 16, 365-372). The method has been adapted for monolayer cultures of fibroblast cells, and provides reproducible measurements of the cell layer's mechanical constants over the frequency range 8-500 Hz. Normal human dermal fibroblast cultures were seeded at sufficient cell density to reach confluency within 3 days incubation. During the final 18 hrs, cells were exposed to either 0.02% ethylenediaminetetraacetic acid (EDTA), 3% ethanol, or growth medium only (control). Both modulus and viscosity vary dramatically with frequency, suggesting that different components and molecular interactions are measured at different wave frequencies. Presence of EDTA in the growth medium for 18 hrs results in a large decrease in measured modulus between 200-300 Hz, but no decrease in viscosity, which suggests a weakening of long range (amorphous) bonds without any net structure-breaking effects. Exposure to 3% ethanol for 18 hrs produces decreases in modulus and viscosity at low frequencies, but increases these mechanical constants in the high-frequency range. Decreases in modulus and viscosity are consistent with membrane destabilization and increased fluidity due to ethanol; the observed increase in modulus and viscosity may reflect membrane fusion phenomena and resulting cell aggregation. Such dynamic mechanical in vitro tests may also provide useful insight to both short- and long-range interactions in other types of monolayer cell cultures.

W-Pos58 NEAR FIELD SCANNING OPTICAL MICROSCOPY (NSOM): INVESTIGATION OF RADIATION TRANSMITTED THROUGH SUB-WAVELENGTH APERTURES. E. Betzig, A. Harootunian, A. Lewis and M. Isaacson, Department of Applied Physics, Cornell University, Ithaca, NY 14853.[SUPP.AFOSR,NSF(NRRFSS)]

The transmission of light through sub-wavelength apertures is investigated both theoretically and experimentally. Several methods are described for the production of these apertures, including the electron beam fabrication of aperture arrays and the production of metallized pipettes smaller than 1000 Å. The merits of these various techniques are considered. The properties and applications of such apertures are then discussed. First, both incandescent and fluorescent sources are used to determine the far field distribution and intensity of radiation transmitted through small apertures. Second, the progress made since our initial report [Biophys.Soc.Abs.(1983)405a] on the construction of a super resolution scanning optical microscope is described. This microscope consists of an illuminated aperture which is placed in the near field relative to an object to define a light source considerably smaller than the wavelength of the incident radiation. Sample scans are provided demonstrating a resolution well beyond that of convential diffraction limited systems. The feasiblity of NSOM is also studied from a theoretical point of view by calculating the near field energy flux and electromagnetic field transmitted through a slit. A Green's function technique is used to find solutions of broad validity. It is found that the collimation is indeed limited by the slit width rather than the wavelength of the radiation in the near field and calculations are provided showing the spread of the collimation with distance. Furthermore, the transmission through the slit is found to vary periodically with the screen thickness, although the thickness has little effect on the near field collimation. Finally, the potentials and limitations of NSOM are discussed in terms of specific biological problems.

W-Pos59 DIFFUSION-ENHANCED ENERGY TRANSFER: DISTANCES FROM NON-EXPONENTIAL FLUORESCENCE DECAY Richard O. Leder and David D. Thomas, Univ. of Minnesota Medical School, Mpls. MN 55455

Diffusion imposes two limiting cases on Förster energy transfer (1). In the static limit, the average energy transfer efficiency is a minimum, and fluorescence decay is non-exponential. In the rapid-diffusion limit (RDL), E is maximized and decay kinetics are monoexponential with $k_T(RDL) = \langle k_T(STATIC) \rangle = (1/\tau) - (1/\tau_o)$. $\langle k_T(STATIC) \rangle$ is the static limit ensemble average energy transfer rate; τ and τ_o are observed lifetimes with and without acceptors present. $\langle k_T(STATIC) \rangle$ depends on a^{-3} and is easily measured in the RDL; a is the closest approach distance between donors and acceptors in solution. It has not been appreciated previously that $\langle k_T(STATIC) \rangle$ is easily measured even when non-exponential decay occurs due to incomplete spatial averaging around donors.

We present new evidence here that a can be measured when the RDL is not attained. First, we show that the initial slope of fluorescence decay is independent of the diffusion coefficient (D), and can be used to determine $\langle k_T(STATIC) \rangle$ directly. This yields a. The finite difference equation which couples diffusion and energy transfer (2) is then solved numerically (1) to generate fluorescence decays for model systems with R_o=20 to 50Å and a=5 to 50Å. The time-resolution needed for distance measurements depends on acceptor concentration and donor lifetime as will be shown. We have verified the theory by varying D from static to RDL conditions in terbium-rhodamine solutions. We conclude that a can be measured outside the rapid-diffusion limit, when decays are non-exponential.

(1) Thomas, Carlsen and Stryer, PNAS USA 75(1978):5746-5750.
(2) Steinberg and Katchalski, J. Chem. Phys. 48(1968):2404-2410.
We gratefully acknowledge Professor Kazuhiko Kinosita for helpful discussions.

W-Pos60 CONTACT X-RAY MICROSCOPY. Lorena Beese, Ralph Feder, and David Sayre. IBM Thomas J. Watson Research Center, Yorktown Heights, NY 10598.

In recent years, imaging biological specimens with soft X-rays (10 Å to 100 Å) has provided a bridge between light and electron microscopy. In contact X-ray microscopy, long wavelength X-rays pass through a biological specimen and expose an underlying X-ray sensitive material (resist), producing an image that reflects the photon absorbance within the specimen. The technique is capable of resolution of the order of 100 Å, far beyond that of light microscopy, and without many of the disadvantages of electron microscopy. Staining of biological specimens is unnecessary as adequate contrast is produced by the differential absorption of photons. Furthermore, the high penetrating power of X-rays enables images to be obtained from specimens up to several microns thick.

An important application of this technique stems from the use of tuneable synchrotron radiation to determine the distribution of elements within a sample. For example, the inorganic calcium phosphate phase of bone can be specifically studied by making use of the calcium absorption edges at wavelengths of 35.3 Å and 35.5 Å. The contrast due to the calcium varies among the images recorded above and below these absorption edges. Similarly, the carbon absorption edge at 44 Å can be used to study the organic collagen phase.

Another application of major potential importance is the use of a single, high intensity pulse of X-rays to record an image of a living cell. The X-ray source (Maxwell Laboratories, Inc.) produces a 100 nanosecond burst of radiation with wavelengths between 23 Å and 43 Å from an imploding gas jet plasma. The technique should permit the direct visualization of cell morphology during processes occuring over sub-millisecond times, such as phagocytosis, pseudopod formation, and axonal transport.

W-Pos61 DETERMINATION OF PARAMAGNETIC ION CONCENTRATIONS AT THE MEMBRANE-WATER INTERFACE BY FLUORESCENCE QUENCHING: INTRINSIC AND X537A-MEDIATED COBALT FLUXES. R. Homan and M. Eisenberg, Departments of Biochemistry and Pharmacology, SUNY at Stony Brook, N.Y. 11794

Techniques which measure bulk aqueous phase ion concentrations are not suitable for quantifying the concentration of ions at the surface of a charged membrane. We used fluorescence quenching of the fluorescent phospholipid N-4-nitrobenzo-2-oxa-1,3-diazole egg-phosphatidylethanolamine (NBD-PE) to measure the concentration of Co^{2+} at the membrane-solution interface. NBD-PE was incorporated at 0.1 mole percent into large unilamellar vesicles of egg-phosphatidylcholine and was found to be distributed at essentially equal surface densities in both monolayers. The NBD fluorophore is covalently linked to the headgroup amine of PE and thus located at the membrane surface where it is readily accessible to quenching by the paramagnetic cobaltous ion. We obtained a quenching constant of 59 M^{-1}. We demonstrate one use of this fluorescence quenching technique by measuring the intrinsic and X537A-mediated transmembrane Co^{2+} flux. The addition of Co^{2+} to one side of the bilayer results in the quenching of only those NBD moeities located in that monolayer. Permeability-dependent changes in the concentration of Co^{2+} at the site of NBD in either monolayer were calculated from time dependent changes in fluorescence quenching of NBD-PE. The intrinsic rate constant for Co^{2+} flux was $3 \cdot 10^{-6}$ s^{-1}. We also confirmed that the neutral Co-$(X537A)_2$ complex is the main component of the X537A-mediated cobalt flux. Since this method measures the concentration of Co^{2+} at the site of the fluorophore, it is generally applicable to the measurement of paramagnetic ion concentrations at the membrane-solution interface.

W-Pos62 AN AUTOMATIC SYSTEM TO CALIBRATE ION SELECTIVE MICROELECTRODES. L. Tillem, S. Levy and D. Tillotson. Dept. of Physiol., B.U. Sch. Med., Boston, MA 02118 (Intro. by W. Lehman)

Calibration of ion selective microelectrodes involves delivering and measuring the potential of several different solutions both before and after intracellular measurement. A system is described which completely automates that tedious process. It is composed of an electrometer, an AIM 65 computer, a stepping pneumatic actuator, a 6-way rotary valve, and a calibration chamber. The actuator consists of a double-acting cylinder coupled to a crank arm to produce the required rotary motion of the valve. The actuator is controlled by 2 electropneumatic valves. A program, written in the assembly language of the AIM 65 (6502 microprocessor) controls the order of delivery of the different solutions. With an ion selective electrode in the calibration chamber, the program "reads"(samples) the digital voltmeter output of the electrometer at 1 Hz for 20 seconds, and stores the readings in an internal table; it then averages the 20 readings and compares the average to each reading. If the average value is within the desired tolerance (usually 0.5mV) of each reading, it is stored and printed along with the solution number. It then causes the rotary valve to switch to the next solution. After delivering the six solutions in a given order, the program is designed to deliver them again in the reverse order; this checks the electrode for hysteresis. The rotary valve is coupled to a 6 position rotary switch connected to 6 LEDs to show remotely the actual position of the valve. This system is being used daily to calibrate Ca selective microelectrodes. A second program plots the calibration curve and translates intracellularly recorded Ca signals into Ca concentration. Supported by NIH grant NS18813.

W-Pos63 DEVELOPMENT OF PHOSPHOROUS - SPECIFIC HPLC DETECTOR FOR QUANTITATIVE ANALYSIS OF PHOSPHOLIPIDS - Margaret V. Merritt, Tamra J. Fader, Hilary A. Gleekman, Iris H. Kopeloff, Elizabeth A. Phelan, Ann E. Remmers, and Angela M. Schmidt, Chemistry Department, Wellesley College, Wellesley, MA 02181

An HPLC detection scheme based on the post-column reaction between phospholipids (PL's) and a molybdenum reagent has been developed and illustrated below.

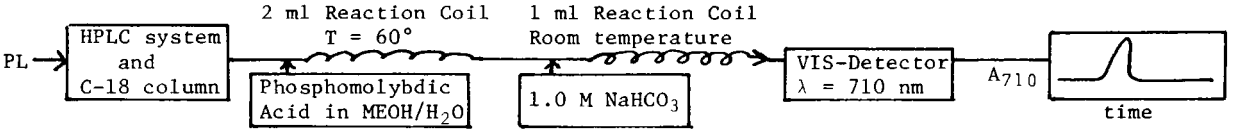

Test-tube experiments have been used to optimize the reaction between phosphatidylcholine (PC) and various molybdenum reagents to produce a product where absorbance at 710 nm is proportional to PC concentration. Similar results have been obtained for phosphatidylethanolamine and sphingomyelin. Inorganic phosphate does not interfere with this assay. The response of the HPLC visible detector (λ = 710 nm) is proportional to the amount of PC injected on a reverse phase column using a methanol/water mobile phase. A comparison of this detection scheme with conventional HPLC analysis of PL's with uv detection at 205 nm suggest that the former is proportional to the phosphorous content of the PL's rather than to the degree of unsaturation of the fatty acid substituents.